Sediment transport through the Eastern Scheldt storm surge barrier

TU Delft
Delft University of Technology

EcoShape
Building with Nature

Van Oord

Deltares
Enabling Delta Life

Report title	Sediment transport through the Eastern Scheldt storm surge barrier
Report type	MSc. thesis
Author	L. Hoogduin
Student number	1272462
Date	May 2009
Institute	Delft University of Technology Faculty of Civil Engineering and Geosciences Department of Hydraulic Engineering
Exam committee	Prof. dr. ir. M.J.F. Stive Prof. dr. ir. W.S.J. Uijttewaal Dr. ir. Z.B. Wang Dr. ir. A. Hibma Ir. M. Eelkema

Photo cover page: *www.BeeldbankVenW.nl, Rijkswaterstaat*

Client	Delft University of Technology
Title	Sediment transport through the Eastern Scheldt storm surge barrier

Abstract

The aim of this research is to determine to what extend the scour holes limit the sediment transport through the Eastern Scheldt storm surge barrier and whether or not human adaptations, like sand-nourishments in the scour holes, can have a positive effect on the sediment import. To investigate these scenarios a numerical model (Delft3D) is used to study the tide-induced flow and sediment transport in and around the scour holes and the storm surge barrier. First a theoretical analysis of the scour holes and their possible sand-trapping function is made after which a numerical 2DV model is constructed to analyze the vertical processes that are taking place inside the scour holes. To include also the influence of asymmetrical ebb- and flood flow from the shoals through the barrier, a depth-average (2DH) numerical model of the Roompot inlet is constructed. With this model an analysis of the main sediment transport patterns in the vicinity of the scour holes is made. With the same 2DH model, a scenario analysis is made where different human adaptations to the scour holes are examined on their effectiveness to increase the sediment import to the Eastern Scheldt.

The two most important conclusions resulting from the analysis on the vertical processes in the scour holes are: (1) A vertical flow recirculation develops behind the barrier-sill, but no vertical flow recirculation inside the scour hole is expected and (2) The hydrostatic model with a σ-coordinate layer distribution in Delft3D shows significantly higher flow velocities at the bottom of the scour hole than the model with a (hydrostatic and non-hydrostatic) Z-coordinate layer distribution. Due to a lack of field-measurements it is difficult to determine the accuracy of both models, but the differences can be of importance when a 3-dimensional model is constructed in the future.

In the analysis on the horizontal transport patterns around the Roompot inlet, the 2DH model results show mainly import of sediment from the south-western channel during flood and large seaward-directed transports through the northern part of the inlet during ebb. In this way the seaward scour hole forms a blockage of the sediment transport from the ebb-tidal delta towards the storm surge barrier. At the eastern side of the storm surge barrier, much smaller net sediment transport rates are found compared to the seaward side.

In the scenario analysis, all model runs show a trend where the adaptations mainly increase the net sediment transport in the direction of the ebb-tidal delta, rather than transport towards the basin. Also, the absolute net yearly transport rates are very small compared to the total sand demand of the Eastern Scheldt to reach a new equilibrium. Although the model results contain some uncertainties and improvements have to be made, one conclusion from the present study is that the studied scenarios do not seem to be very efficient measures in order to significantly decrease the sand demand of the Eastern Scheldt on a short time scale.

References

Ver	Author	Date	Remarks	Review	Approved by
1.0	L. Hoogduin	May 25, 2009		Z.B. Wang	T. Schilperoort

Project number	1002334
Keywords	Eastern Scheldt, storm surge barrier, sediment transport, scour hole, process-based modeling, Delft3D
Number of pages	104
Classification	
Status	Final

Preface

This M.Sc. thesis is written as final part of my master in Coastal Engineering at the Faculty of Civil Engineering and Geosciences of Delft University of Technology. The study concerns the influence of local scour holes near the Eastern Scheldt storm surge barrier on the sediment transport from the ebb-tidal delta to the Eastern Scheldt tidal basin. This study is part of the Dutch national program Building with Nature, which is an innovation program managed and administered by the foundation EcoShape, Building with Nature. This programme, funded jointly by a consortium of private companies, knowledge and academic institutes and the Netherlands government, aims at creating innovations enabling sustainable development of hydraulic infrastructure: building with nature. Activities include the realization of pilot projects and development of practical tools as well as applied and fundamental research. As part of this program, I got the opportunity to work in the different working environments at TU Delft, Research institute Deltares and Van Oord dredging and marine contractors.

I am grateful to all the people who are involved in my master thesis and especially my supervisors who gave me great support and guidance through my graduation project. First of all, I would like to thank professor Stive, for his involvement during the meetings and being the chairman of my graduation committee, Ms. Hibma for getting me involved the topic and in the Building with Nature program, Mr. Wang for his support at Deltares, Mr. Uijttewaal for his input on the complicated hydrodynamic topics and Mr. Eelkema for his involvement in my research and his advise on the practical questions of writing a thesis. I would also like to thank my temporary colleagues at Deltares for their input during many meetings, special thanks goes out to Mr. Luijendijk for his help during my modeling work.

At Deltares and Van Oord, I had the privilege to work with a lot of other students with whom I had a great time; John, Thijs, Marten, Chris, Arend, Roald, Wouter, Carola, Sepehr, Reynald, Komla, Steven, Claire and Dennis you all helped me a lot during my graduation period and I really enjoyed working and lunching with you!

I hope you will enjoy reading this report.

Lars Hoogduin

Delft, May 2009

Summary

The construction of the Eastern Scheldt storm surge barrier has significantly influenced the tidal characteristics in the Eastern Scheldt. The reductions of the tidal prism and current velocities have disturbed the morphological balance, resulting in a chronic shortage of sand in the estuary. Due to this so-called 'sand-hunger' the tidal flats are eroding, and additional sand is required to reach a new equilibrium.

Studies have been performed to find ways to accomplish a long-term structural increase of sediment transport from the ebb-tidal delta into the Eastern Scheldt. A possible cause for the limited sediment import are the scour holes behind the bottom protection on both sides of the storm surge barrier. These scour holes have developed after the construction of the barrier up to a depth of 60 m below mean sea level. Adaptations to the scour holes, like filling and covering the holes, are mentioned as a possible solution to increase the sediment import to the Eastern Scheldt.

The aim of this research is to determine to what extent the scour holes limit the sediment transport through the storm surge barrier and whether or not adaptations to these scour holes can have a positive effect on the sediment import. Besides a theoretical description, a numerical model (Delft3D) is used to study the flow and tide-induced sediment transport in and around the scour holes. In the theoretical analysis, possible occurrence of different hydrodynamic phenomena is discussed. A very important aspect to take into account when determining the sediment transport near the storm surge barrier, is the asymmetry of flow velocities near the barrier. Ebb- and flood tidal jets are developing as a result of the large water mass that is forced through the storm surge barrier, resulting in much larger flow velocities downstream the barrier compared to the upstream side. Due to the tidal regime this means that at the seaward side of the storm surge barrier larger velocities occur during ebb than during flood and the opposite happens at the landward side. Another hydrodynamic phenomenon that possibly occurs inside the scour hole is a vertical eddy caused by flow separation at the steep slopes. However, a theoretical analysis shows that for these specific scour holes no vertical eddy is expected to develop.

The first numerical model that has been constructed is a 2DV model with a schematized bottom geometry based on the Schaar van Roggenplaat channel. An important conclusion resulting from this model is the development of a vertically recirculating flow behind the barrier-sill and the absence of such a vertically recirculating flow inside the scour hole. In addition to the hydrodynamic results, this model also resulted in a numerical limitation that is important for the construction of a possible future three-dimensional model. In Delft3D different vertical layer distributions are available to apply; the σ-layered coordinate system follows the bottom geometry and is therefore well suited for simulating bottom boundary layer processes. The Z-layered coordinate system consists of horizontal parallel cells where every layer-thickness is constant along the model, an advantage of this Z-layered distribution is the possibility to represent non-hydrostatic flow behavior.

Comparison of model results for different layer-distributions showed significant differences between the models, especially the bed-shear stress near slopes is not represented correctly in the Z-layered model. Also large differences in flow velocities at the bottom of the scour holes are observed, more research and field-measurements has to be done on this topic to determine the trustworthiness of both models.

To determine the horizontal sediment transport patterns near the scour holes, a larger, depth-averaged, numerical model of the Roompot channel is constructed. This model also includes the effect of asymmetric flow due to the ebb- and flood jets as described above. Because a 3D model has no added value as long as non-hydrostatic flow in combination with sediment transport do not give sufficiently reliable results, a depth-averaged (2DH) approach is chosen. The results of this 2DH approach show net yearly sediment transports which are entering the Roompot inlet from the coast of Walcheren (south-western direction) and largely returning in the direction of the ebb tidal delta through the north-western directed channel. Much smaller transports are observed through the barrier and inside the tidal basin. In the vicinity of the seaward scour hole, the net transport is directed to the ebb-tidal delta and near the landward scour hole the net transport is mainly directed towards the Eastern Scheldt basin.

In the scenario analysis different human interventions to the scour holes are examined; the effect of filling the seaward or landward scour hole. Also the effect of an extension of the seaward bottom protection over the filled scour hole is examined. The scenarios on both sides of the barrier show an effect on the seaward and the landward directed net sediment transport, but the similarity between the scenarios is that the added sand is mainly transported in the direction of the ebb-tidal delta rather than towards the Eastern Scheldt basin. Although the first results of this study do not show a very positive effect of the adaptations on the sand-import to the Eastern Scheldt, there are still some uncertainties in the model. Including waves, different sediment fractions and extending the model to three dimensions will give slightly different results, which can be either positive or negative. Furthermore, additional measurements of flow velocities and sediment concentrations near the storm surge barrier are recommended to increase the trustworthiness of the numerical model results.

Overall, this thesis can be seen as a first investigation whether adaptations near the entrance of the Eastern Scheldt can be useful with respect to the sand demand of the Eastern Scheldt. Despite the uncertainties in the numerical model, a good indication is given of the order of magnitude of the sediment transports near the barrier, and the relative influence of different adaptations. Regarding the immense amount of sand (400-600 million m^3) that is needed to reach a new equilibrium in the Eastern Scheldt, this study shows that only filling the scour hole(s) will not result in sediment import rates which can have a significant impact on restoring the dynamic equilibrium of the tidal basin within a period of decades.

Contents

List of symbols

Roman symbols

A_1	coefficient (v. Rijn)
A_2	coefficient (v. Rijn)
A_c	cross-sectional area below mean sea level [m^2]
b	coefficient of quadratic friction term
B	width of the flow [m]
B	length of scour hole [m]
c_{loss}	energy loss coefficient of porous plate [m]
C	Chezy coefficient [$m^{1/2}\ s^{-1}$]
Cr	Courant-Friedrichs-Lewy number [-]
d	depth with respect to some reference level [m]
e	trapping efficiency factor [-]
f	Coriolis parameter [-]
g	gravitational acceleration [m s^{-2}]
h_0	initial flow-depth [m]
h_s	maximum depth in the scour hole [m]
H	maximum water depth [m]
H	total water depth (H=ζ + d)
M_ζ	energy loss coefficient [-]
p	pressure [N m^{-2}]
P	tidal prism [$m^3 \cdot tide^{-1}$]
Q	discharge [$m^3\ s^{-1}$]
t	time [s]
t	coefficient (in velocity-profile equation of van Rijn) [-]
T_α	transport parameter [-]
u_b	flow velocity at z=0.05h above mean bed [m s^{-1}]
u_h	flow velocity near the surface [m s^{-1}]
u_z	flow velocity at level z [m s^{-1}]
u_{*0}	bed shear velocity [m s^{-1}]
$\vec{U}_{m,n}$	velocity in m,n direction [m s^{-1}]
$\overline{u_c}$	depth-averaged critical flow-velocity (Shields) [m s^{-1}]
$\overline{u_p}$	depth-averaged velocity at the end of the bottom protection [m s^{-1}]
$\overline{U_0}$	mean flow-velocity [ms^{-1}]
w_s	particle fall velocity [m s^{-1}]
z_0	zero-velocity level (=0.03 k_s)

Greek symbols

α	turbulence coefficient [-]
α_0	Angle of incident of flow to channel [°]
Δ	relative density [-]
γ	bottom slope [°]
γ_m	maximum scour-depth [m]
κ	Von Kármán constant [-]
υ	kinematic viscosity [$m^2\ s^{-1}$]
ρ	density [kg m^{-3}]
ρ_s	material density [kg m^{-3}]
υ_H	horizontal eddy viscosity [$m^2 s^{-1}$]
ζ	water level with respect to some reference level [m]

Chapter 1

Introduction

1.1 Research background

The Dutch Delta project was initiated in 1959 for the protection of the south-western Netherlands. A major part of this project was the closure of the Eastern Scheldt tidal basin. Initially the plan was to close the basin completely. But after voices raised in favor of maintaining the tidal flow to preserve the original natural environment of the area, the Dutch government ordered to study the feasibility and finally the realization of a storm surge barrier at the Eastern Scheldt inlet. As a part of the Eastern Scheldt project, together with the storm surge barrier, the Oesterdam and Philipsdam were constructed at the landward parts of the Eastern Scheldt basin. These dams have the function to limit the reduction of the tidal range in the Eastern Scheldt for ecological reasons and at the same time creating a tide-free shipping route between Antwerp and the Rhine [Hesselink et al., 2003].

The Eastern Scheldt project caused a disturbance in the dynamic equilibrium of the tidal basin. Due to the reduced tidal volume the channels in the basin tend to silt up until a new equilibrium is reached. Because of the very limited import of sediment through the storm surge barrier, sediment is transported from the tidal shoals into the tidal channels to fulfill this sediment demand. This need of extra sand in the estuary to restore a dynamic equilibrium is called the "sand hunger" and it is a great challenge to find a long-term solution for this problem in order to save the ecological values in the Eastern Scheldt.

1.2 Problem definition

The Eastern Scheldt project has significantly influenced the tidal characteristics in the basin; decrease of the tidal volume, tidal range and tidal currents resulted in geomorphologic changes of the tidal basin. The formerly eroding basin with expanding channels and aggrandizing sandy shoals, has changed into the opposite. Since 1987 the Eastern Scheldt is a sedimentating basin with channels in demand of sediment, and with degrading shoals [Mulder and Louters, 1994]. The equilibrium of inlets and tidal channels within tidal basins is described by a linear relation

(section 2.2.2), which implies that, in order to achieve a new equilibrium, any change in tidal prism must be followed by a proportional adaptation in channel cross-sectional area [Louters et al., 1998]. With this relation it is estimated that an amount of 400 million m^3 of sediment is required to restore the equilibrium. With an actual import estimate of 1 million m^3 slib per year it is clear that it takes centuries to restore the equilibrium [ten Brinke et al., 1994]. Many studies [van Zanten and Adriaanse, 2008] have been performed to develop a solution in order to accomplish a long-term structural increase of sediment transport from the ebb-tidal delta to the tidal channels in the Eastern Scheldt. One possible cause for the limited sediment import is said to be the scour holes on both sides of the barrier. These holes developed after the construction of the barrier and some of them have now reached a depth of about 60 m below mean sea level.

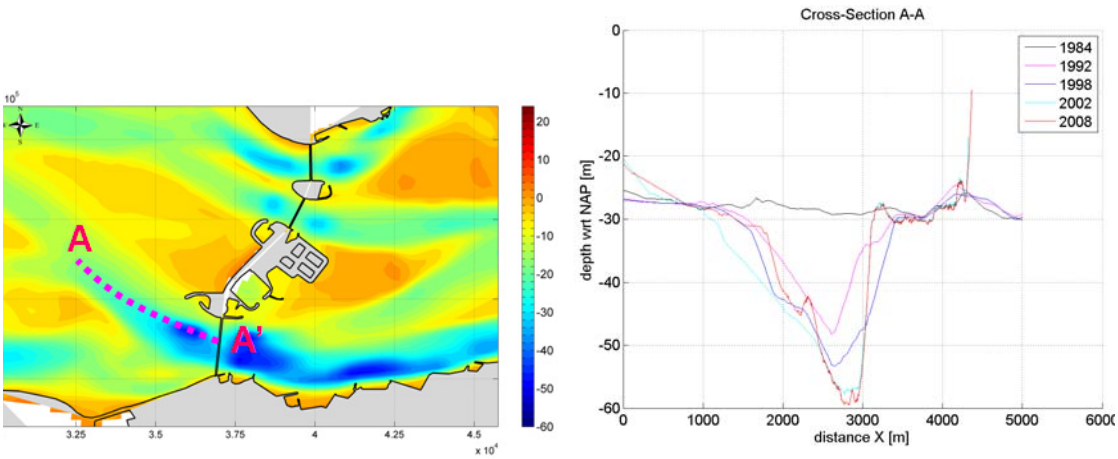

(a) Bathymetry around the Eastern Scheldt storm surge barrier (2004)

(b) Cross-section A-A' over the period 1984-2008

Figure 1.1: Development of the seaward Roompot scour hole

These scour holes possibly block the sediment transport into the Eastern Scheldt. During flood the sediment is trapped in the scour holes and during ebb the sediment is flushed out of the holes in the direction of the North Sea [Maldegem and van Pagee, 2005]. This idea about the sediment-trapping function of the scour holes has not yet been scientifically verified based on field measurements or modeling results. This leads to the problem definition of this MSc Thesis:

It is unknown to what extent the scour holes on both sides of the storm surge barrier contribute to the limitation of sediment transport into the Eastern Scheldt tidal basin.

1.3 Research objectives

To get insight into the influence of the scour holes near the storm surge barrier on the sediment transport, four objectives have been formulated:

1. Obtain more insight in the hydrodynamic and morphodynamic processes that are taking place inside the scour holes.
2. Determine the capabilities of the process-based model Delft3D to reproduce hydrodynamic and morphodynamic behavior around the scour holes correctly.
3. Increase the insight on the influence of scour holes on the sediment transport around the Eastern Scheldt storm surge barrier.
4. Determine the influence of human adaptations to the scour holes near the Eastern Scheldt storm surge barrier on the sediment transport.

1.4 Research approach

To achieve the above mentioned objectives, the following steps will be followed:

1. Analysis of available literature and theories to get insight into the influence of the Eastern Scheldt storm surge barrier and the scour holes around the barrier.
2. Analysis and validation of available data, measurements and existing numerical models.
3. Construct a 2DV numerical model of one single inlet to analyze the important processes in the vertical plane.
4. Construct a 2DH numerical model to analyze the morphodynamics around the Eastern Scheldt storm surge barrier and the scour holes.
5. Run the numerical model for different scenarios with various human adaptations to the scour holes.

1.5 Previous studies

As the Eastern Scheldt barrier is one of the biggest hydraulic interventions in the natural Dutch coast, a lot of research is done on many aspects like morphological and ecological consequences of the barrier. During the design phase of the Eastern Scheldt barrier, extensive model-research has been done to quantify the expected erosion downstream of the bottom protection. But the effect of this erosion on the sediment transport was not described. In the study "Maatregelen ter vergroting van doorstroomcapaciteit en zanddoorvoer stormvloedkering Oosterschelde" [Jongeling, 2007] and the recently published report "Verminderd getij" [van Zanten and Adriaanse, 2008], interventions to the scour holes around the storm surge barrier are mentioned as a possible structural solution to increase the sediment transport into the Eastern Scheldt. However,

no detailed research on the influence of large scour holes on the sediment import has been done yet, and therefore it is unknown whether adaptations to the scour holes can have substantial influence on the sediment import into the Eastern Scheldt.

1.6 EcoShape - Building with Nature

This study is closely related to the PhD research-project "Morphodynamic coupling between estuary and outer delta" by Menno Eelkema [EcoShape, 2008b], which is part of the Building with Nature program. The Dutch national program Building with Nature is an innovative, long-term research program aimed at developing new design concepts for the layout and sustainable exploitation of river, coastal and delta areas. In the new design approach of this program, nature's status will serve as the starting point of the design process [EcoShape, 2008a].

Ambitious plans for rivers, and coastal or delta areas can be best achieved if man treats nature not as an enemy but as an ally, so that nature itself works in support of man's intensions - Building with Nature.

One of the case studies of the program is the South-Western Delta area of the Netherlands. Here the program is challenged to deliver sufficient knowledge about the estuaries in the area to support the efforts related to the potential solutions for problems caused by human intervention in the delta area.

1.7 Thesis committee

The thesis committee consists of four people connected to the Delft University of Technology from whom one is also working for Deltares, and one representative of Van Oord. The structure of the committee is stated below:

Name and titles	Section / company
Prof. dr. ir. M.J.F. Stive	TU Delft, Hydraulic Engineering
Prof. dr. ir. W.S.J. Uijttewaal	TU Delft, Environmental Fluid Mechanics
Dr. ir. Z.B. Wang	TU Delft, Hydraulic Engineering / Deltares
Dr. ir. A. Hibma	Van Oord Dredging and Marine Contractors
Ir. M. Eelkema	TU Delft, Hydraulic Engineering

Table 1.1: Thesis committee

Chapter 2

Description of the project area

2.1 Introduction

The Eastern Scheldt project is part of the Dutch Deltaplan, which has the purpose to ensure the safety of the southwestern part of the Netherlands against flooding and improve the freshwater management in the country. The plan proposed the closure of the main tidal estuaries in the south-western part of the country, with the exception of those giving access to the ports of Rotterdam and Antwerp. After the infamous flood in 1953 it was decided to accelerate the implementation of plans already in existence. After the Delta Act has passed in 1958, the Delta Project was started with the construction of the Storm surge barrier in the Hollandse IJssel.

Figure 2.1: Overview of Delta works

A major part of this project was the closure of the Eastern Scheldt tidal basin. According to the original plans the Eastern Scheldt would be closed, just like the other river mouths. The water enclosed behind the dam would become fresh, like the water in the Haringvliet and the Lake of Veere. It was not long, however, before voices were raised in favor of keeping the Eastern Scheldt open and maintaining the tidal flow to preserve the unique salt water environment. In 1976 the Dutch government agreed to an alternative plan: instead of building a closed dam an open barrier would be built, containing a number of gates that would only be closed during heavy storms and high water levels. The unique saline water environment and the favorable fishery conditions would be maintained. Sixty-two openings, each forty meters wide, would be installed to allow as much salt water through as possible. The Eastern Scheldt storm surge barrier turned out to be one of the biggest structures of the world, and on October 4th, 1986, the Dutch Queen Beatrix officially opened the Eastern Scheldt storm surge barrier.

2.2 The Eastern Scheldt

2.2.1 Hydrodynamic characteristics

Within the framework of the Deltaplan, the Grevelingen dam (1964) and Volkerak dam (1969) were built, which cut off the northern branch of the Easter Scheldt from other estuaries. These construction works caused a gradual increase in tidal volume in the open Eastern Scheldt basin. This increase in tidal volume resulted in a significant increase of the current velocities, which caused erosion and a shift of tidal channels [Vroon, 1994].

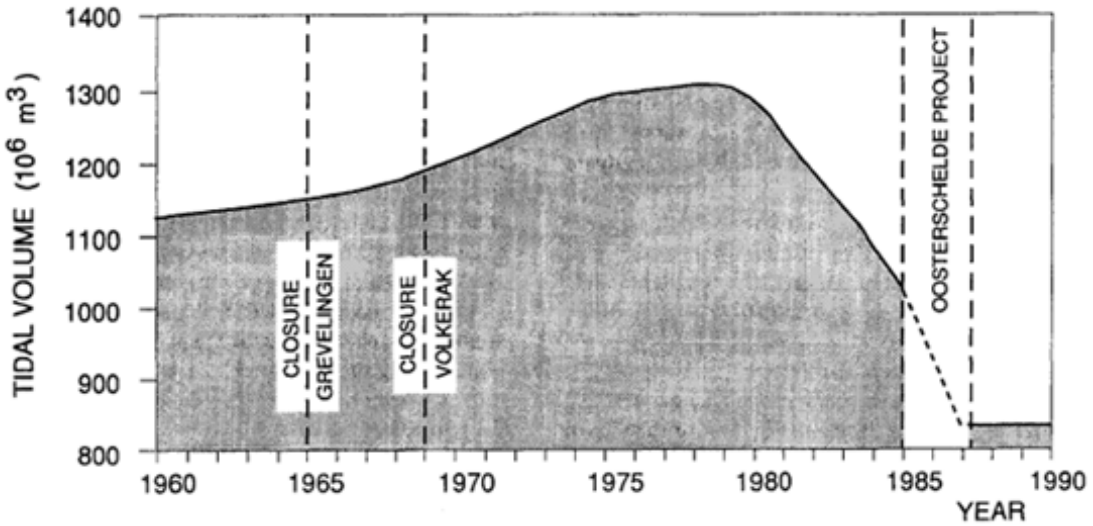

Figure 2.2: Change in tidal volume at the entrance of the Eastern Scheldt in recent decades [Vroon, 1994].

From 1969 to mid-1985 preparations for the Eastern Scheldt storm surge barrier started, including the construction of islands in the mouth of the basin. With these works a start was made with the narrowing of the basin entrance. With the construction of the storm surge barrier, the

effective cross-sectional area at the mouth has been decreased from $80.000m^2$ to $17.900m^2$ (wet cross-sectional area below mean sea level; N.A.P.), this is an effective reduction of about 77%. The resulting reduction of the tidal volume is seen in figure 2.2. It is logical that this has an enormous impact on the hydrodynamics, and thus on the morphology in the tidal estuary.

The decision to build a storm surge barrier also necessitated the construction of two auxiliary dams at the landward site of the Eastern Scheldt; the Philipsdam and the Oesterdam. The construction of these dams was necessary because, although the Eastern Scheldt barrier has an open character, the reduced cross-sectional area caused a reduction of the tidal range. This resulted in salt marches and mud flats came into jeopardy. The Eastern Scheldt storm surge barrier itself would result in a decrease of tidal range at Yerseke of about 25%. With the construction of the Philipsdam and the Oesterdam, the Eastern Scheldt surface area has been reduced from $452km^2$ to $351km^2$. Consequently the total decrease in tidal volume resulted in 30% at the mouth (25% due to the barrier and 5% to compartmentalization). But more important, the reduction in tidal range is only 13% instead of 25% at Yerseke due to the construction of these two dams [Vroon, 1994]. Due to this limitation to the tidal range reduction, the storm surge barrier would have less negative impact on the salt marches, mud flats and the oyster farming in Yerseke. Besides this ecological function, these dams also created a tide-free Scheldt-Rhine Canal, which is an important access channel between the Volkerak and the port of Antwerp. The change in hydrodynamics due to the Eastern Scheldt project is not uniform over the tidal basin, maximum reduction in current velocity was observed in the northern branch of the basin and just behind the storm surge barrier (north of the Hammen channel). The overall consequences of the Eastern Scheldt project are summed up in table 2.1.

	Pre-barrier	Post-barrier	% change
Total surface area $[km^2]$	452	351	-22
Intertidal surface area $[km^2]$	183	118	-36
Tidal volume $[10^6m^3]$	1283	915	-29
Average current velocity [cm s^{-1}]	120	80	-33
Residence time water [days]	50	100	+100
Fresh water input $[m^3s^{-1}]$	70	25	-63
Salinity [‰]	>25	>30	+15
Average depth [m]	8	8	0
Maximum depth [m]	55	55	0
Average tidal range (Yerseke) [m]	3.70	3.25	-12
Average concentration suspended matter [mg l^{-1}]	25	15	-40

Table 2.1: Eastern Scheldt characteristics [ten Brinke et al., 1994]

The consequence of these hydrodynamic changes on the morphodynamics in the basin will be discussed in the next section.

2.2.2 Geomorphological characteristics

As described in the previous section, the Eastern Scheldt project caused a significant change in the hydrodynamic characteristics of the basin. Consequently the geomorphologic characteristics of the basin are influenced by the interventions.

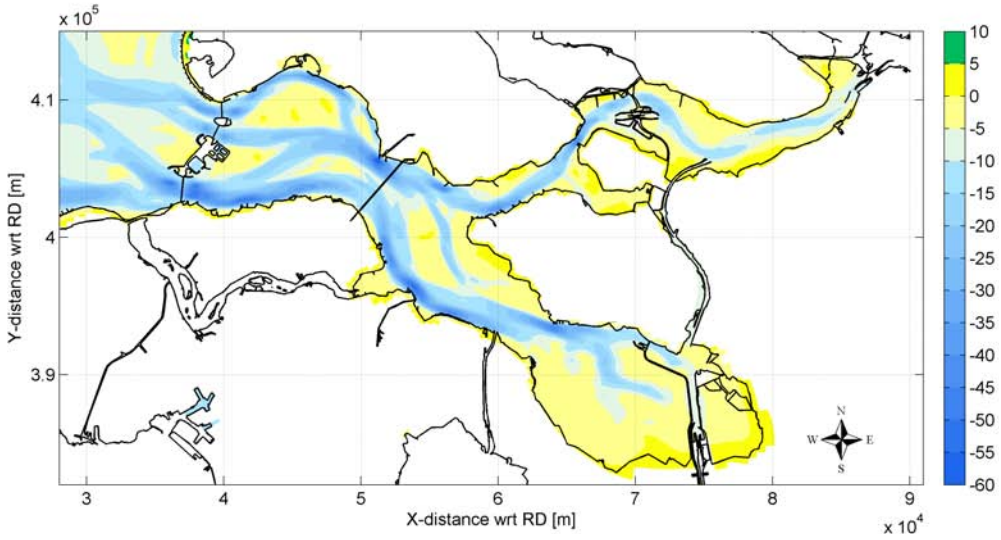

Figure 2.3: Overview of the Eastern Scheldt

At this moment the channels in the Eastern Scheldt are not in equilibrium. It has been observed that under the changed hydrodynamic circumstances after the completion of the Eastern Scheldt project, intertidal areas in the basin are eroding [Geurts van Kessel, 2004]. In the past 20 years the intertidal area has been reduced by 10%. It can be expected that this process will continue in the future. The predictions of the geomorphological changes of a tidal basin can be approximated by linear relationships.

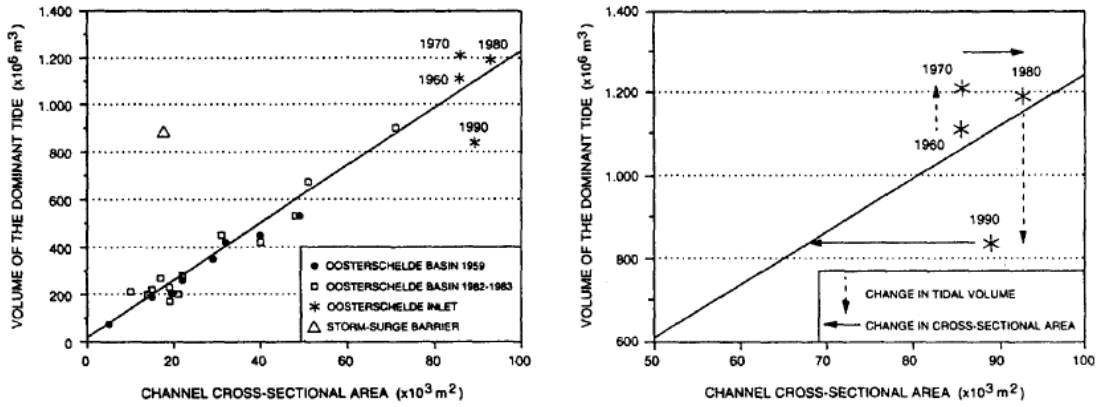

Figure 2.4: Morphodynamic equilibrium relationship between tidal volume and cross sectional area for different tidal inlets (modified after O'Brien, 1969 and van den Berg, 1986), indicating the effects of changes in tidal volume and cross sections [Mulder and Louters, 1994].

The tidal volume of a tidal inlet under conditions of geomorphological equilibrium, generally shows a linear relationship with the cross sectional area of its entrance (figure 2.4 and [van de Kreeke and Haring, 1979]). Others Gerritsen et al. [1990] have shown that such a relationship can also be applied to channels within tidal basins, for instance to individual channels in the Eastern Scheldt. The main implication of this relationship is that, in order to reach a new morphodynamic equilibrium, any significant shift in hydraulic conditions has to result in a proportional adaptation in channel cross section : erosion after a tidal volume increase, sedimentation after a decrease [Louters et al., 1998]. In figure 2.4 it can be seen that the tidal volume increase in the Eastern Scheldt between 1965 and 1970, has induced a disturbance of the equilibrium leading to channel erosion between 1970 and 1980. Since 1985, the decrease in cross section at the Storm-Surge Barrier induces the development of scour pits, while the decrease of tidal volume induces sedimentation in the Oosterschelde channels [Mulder and Louters, 1994].

Given the reduction of the tidal volume from 1230 to 880 million m^3 due to the Eastern Scheldt project, it can be concluded that the average current velocities have decreased, causing more sedimentation in the channels. This process of sedimentation will continue until the current velocities are in equilibrium again with the local geometry. Using the empirical relations it is estimated that there is an amount of 400 million m^3 of sediment required to restore the equilibrium. With an actual import estimate of 1 million m^3 sediment per year it is clear that it takes centuries to restore the equilibrium [ten Brinke et al., 1994]. This lack of sediment supply from the ebb-tidal delta by the tidal currents is often called "sand hunger". However there is a significant amount of sediment available on the tidal flats in Eastern Scheldt. It has been observed that due to the changed hydrodynamics of the basin, these tidal flats are eroding and depositing sediment in the oversized channels. The reason why the shoals are eroding can be addressed to the reduction of the tidal current velocity and the tidal range. Figure 2.5 illustrates the reduction of sediment transport due to the implementation of the Eastern Scheldt project.

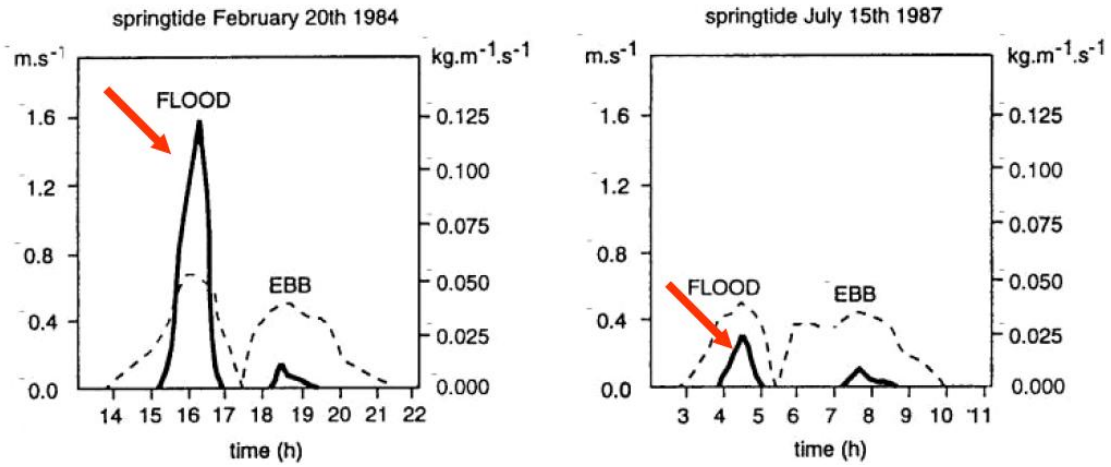

Figure 2.5: Current velocity (left vertical axis; interrupted line) and sand transport (right vertical axis; solid line) in 1984 and 1987, as observed at a station near the North-western edge of the Galgeplaat shoal [Louters et al., 1998]

Model computations have shown that, because of the reduction in tidal range, more wave energy is dissipated near to the edges of the shoal and this results in larger vertical erosion in those areas. Due to the reduced current velocities, there has been an exponential reduction in transport capacities, with the result that the eroded sediments are transported only over small distances. These conditions result in a net vertical erosion of the shoal and a net accretion at the channel 'shoulder', mostly below -5m MSL [Louters et al., 1998].

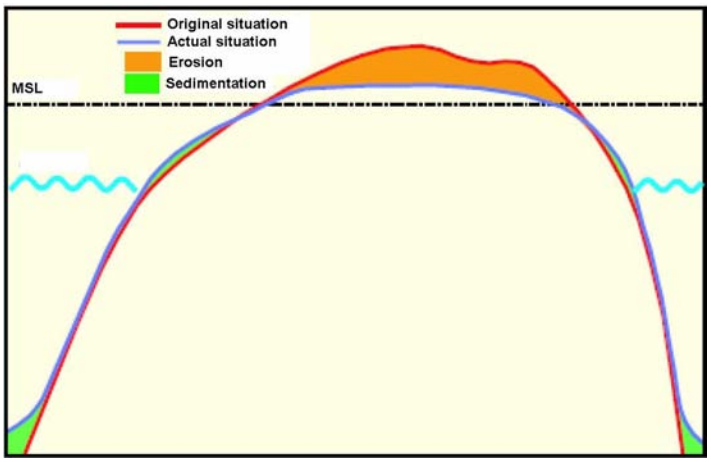

Figure 2.6: Schematized presentation of erosion process of a shoal [Geurts van Kessel, 2004]

The result of the eroding shoals is a reduction of the intertidal area in the Eastern Scheldt and a reduction of the period that the shoals are dry during ebb. This has consequences for the ecological values of the Eastern Scheldt, and as protected nature reserve this is an undesired development. Looking at long-term solutions to increase the sediment import through the Eastern Scheldt storm surge barrier, the scour holes around the barrier are mentioned in different reports as a possible obstacle. In the next section, more detailed characteristics of the area around the storm surge barrier will be discussed.

2.3 The Eastern Scheldt storm surge barrier

The storm surge barrier in the Eastern Scheldt has a length of 3000m and is built across three tidal channels; Hammen, Schaar van Roggenplaat and Roompot (figure 2.7). The barrier consists of 65 prefabricated concrete piers, between which 62 sliding steel gates are installed.

Figure 2.7: Overview of Storm surge barrier

As part of the initial plans to build a dam across the Eastern Scheldt some islands (Roggenplaat and Geul) had already been constructed at shallow locations in the estuary. Additionally Neeltje Jans was turned into a construction island from where operations were conducted. Prefabricated components like the piers, sill beams, upper beams and foundation mattresses were also built here. The piers are one of the main components of the barrier. They have a height between 30 and 39 meters and a maximum weight of 18.000 tons. After the construction in the dock, the piers were floated into place and filled with sand. To ensure the stability of the construction, the piers are protected by high-density rubble-mount with an weight of 6-10 tons. These rocks should prevent erosion around the piers at high current velocities.

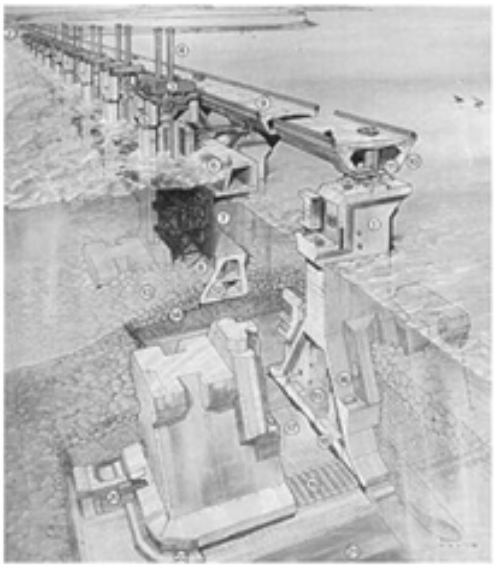

Figure 2.8: Exploded cross-sectional overview of a pier

2.3.1 Bottom protection

At the bottom of the channels, bottom-improvement was needed to create a stable and durable foundation that creates:

- A watertight, but sand-permeable foundation bed underneath and around the piers and sill-construction
- A foundation, where the horizontal and vertical forces from the piers can be transmitted to the subsoil with a minimum of deformation.

To fulfill these requirements, first a cunette was excavated and sand improvement was applied where necessary. This sand was compacted over a distance of 80 meters around the piers to prevent settlement of the piers. After this improvement and leveling of the sand-bed, a prefabricated bottom mattress measuring 200 x 42 x 0.36 meters was laid under each pier. The joints between these filter mattresses, due to a mutual pier-distance of 45m, was sealed with a granular filter of sea gravel and quarry stone. At the positions of the piers smaller mattresses are placed, first a fully gravel-filled second mattress is placed which measures 60 x 29 x 0.36 meters. On some places an extra block mattress was needed to overcome irregularities in the placement of the filter mattresses (see figure 2.9).

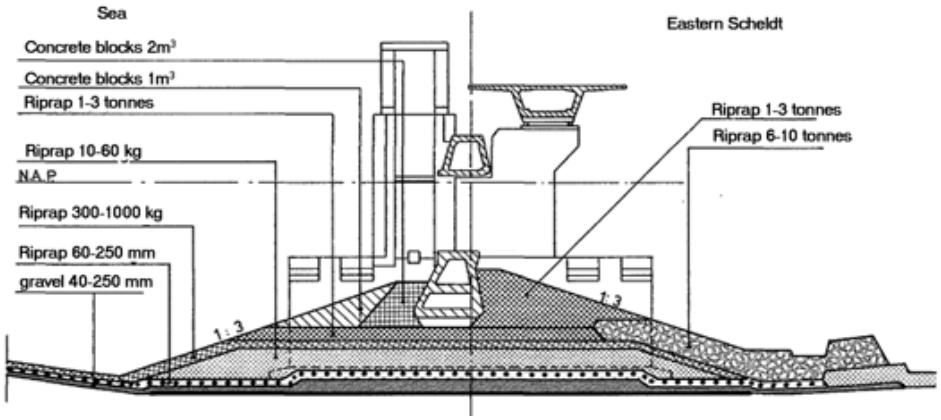

Figure 2.9: Cross-section of a sill

Apart from the bottom improvement underneath the piers, also heavy bottom protection around the inlets was needed. Between the piers, in the axis of the barrier, a sill construction out of graded stones varying from small gravel up to 6-10 tons basalt blocks is constructed. This sill construction increases the stability of the piers and reduces the opening in the Eastern Scheldt with the intention that only that part which can be closed off by the gates during storms, will remain open.

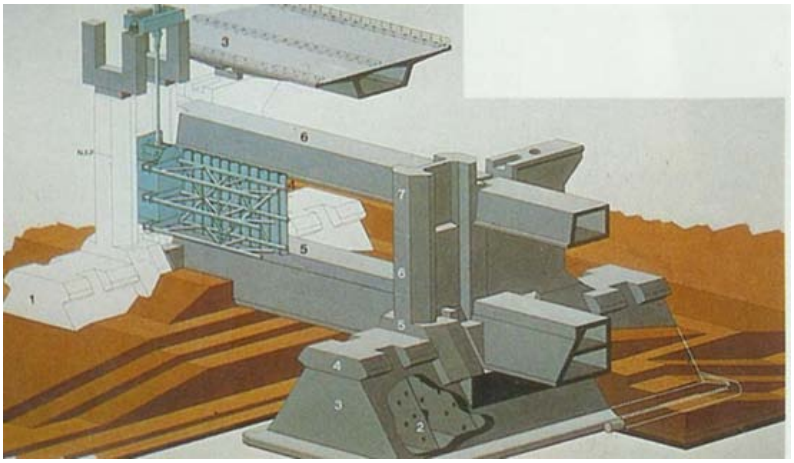

Figure 2.10: Overview of the barrier

On both sides of the sill construction erosion problems might occur due to the increased currents through the openings of the barrier. To prevent excessive erosion on both sides of the axis 550 meter (Schaar van Roggeplaat) and 650 meter (Roompot and Hammen) long bottom protections have been applied. These protections consist of stone-asphalt mattresses or block mattresses. A transition to the bottom protection around the piers has been made by applying mastic asphalt slabs. In spite of this bottom protection it is unavoidable that erosion will take place at the end of the protection. Calculations and modeling has taken place in the design phase of the project to investigate what amount of erosion can be allowed without endangering the stability of the barrier-construction. The design of the border bottom protection was based on the idea that *"an instability at the border of the bottom protection may not endanger the stability of the storm surge barrier and banks"* [Rijkswaterstaat, 1991a]. To satisfy these requirements, a series of experiments and calculations has been performed, which finally resulted in the earlier-mentioned protection lengths of 550-650 meters on both sides of the barrier.

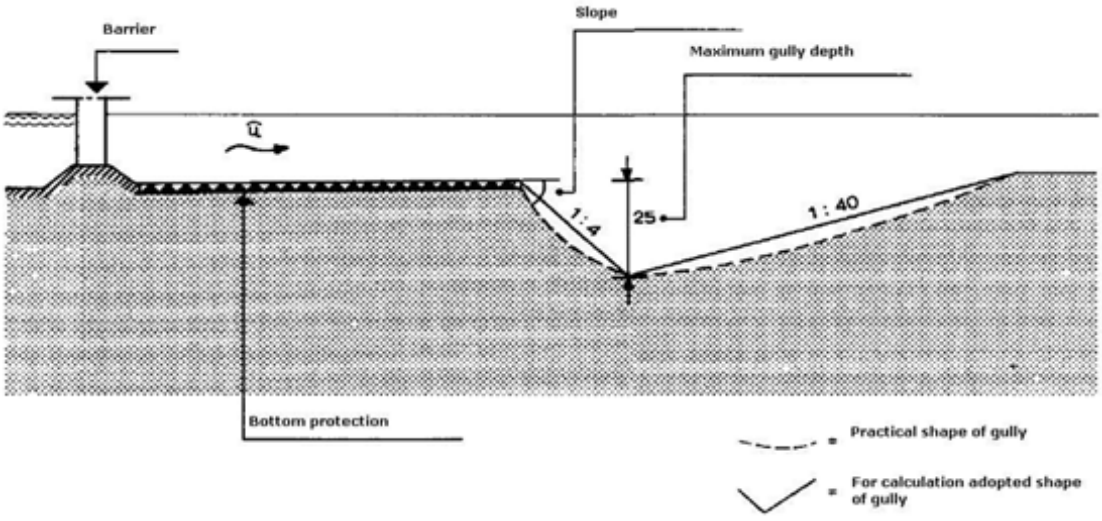

Figure 2.11: Bottom protection and scour hole

The requirement of limiting the maximum slope in the scour hole is based on the stability of the end of the bottom protection (figure 2.11). If the slope becomes too steep, local landslide might occur and the protection will be damaged. In practice this means that regular checks and repairs to the border bottom protection have to be carried out. Besides the limitation to the slope, the maximum allowed erosion depth in the gully was set to 25m; for this depth there is no risk that if, liquefaction takes place, the stability of the barrier will be endangered. This is based on the assumption that the equilibrium slope after liquefaction is 1:15, for a depth of 25m deep a bottom protection of 15x25=375 meters is safe ([Rijkswaterstaat, 1991b], deelnota 9). The depth was also limited by the maximum depth where compression of sand could take place by a ship. This compression of the subsoil under the bottom protection was required to reduce the possibility of liquefaction at the edge of the protection.

Chapter 3

Theoretical scour hole analysis

In this section, theories about the scouring process and scour hole hydrodynamics will be described. Together with the results of the numerical model (chapter 4) conclusions can be drawn on the behavior of the flow in and around the scour holes and storm surge barrier.

3.1 Scouring process

As was predicted and made clear by recent measurements, large scour holes have been formed behind the bottom protection. Scour is the lowering of the sea- or river-bed as a result of non-equilibrium sediment transport conditions. There are many varieties of local scour systems downstream of hydraulic structures, each with its own particular geometry and hence local scour mechanism. Local scour is superimposed on general and constriction scour [Hoffmans, 1993]. The research during the design of the Delta works (from 1961) has played an important role in the development of empirical relations for the prediction of scour behind bottom protections. Many experiments were carried out in order to find the physical background of the scour process. From the results of experiments in flumes (semi-)empirical relations were obtained, which describe the erosion process as a function of time and place [Hoffmans, 1992]. According to Breusers (1966,1967) the development of the scour process in time can be written as: [Jorissen and Stroeve, 1997]

$$\frac{h_s(t)}{h_0} = \left(\frac{t}{t_1}\right)^{\gamma} \tag{3.1}$$

with

$$t_1 = \frac{330 \cdot h_0 \cdot \Delta^{1.7}}{(\alpha \overline{u}_p - \overline{u_c})^{4.3}} \tag{3.2}$$

$h_s(t)$ = maximum depth in the scour hole as a function of time [m]
h_0 = initial flow-depth [m]
$\overline{u}_p$ = vertically averaged velocity at the end of the bottom protection $[ms^{-1}]$
$\overline{u}_c$ = vertically averaged critical velocity $[ms^{-1}]$
t = time [s]

α = turbulence coefficient [-]
Δ = relative density [-]

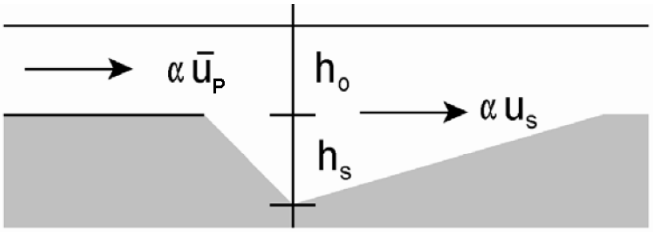

Figure 3.1: Definition sketch for equilibrium scour

In this relation, α is the turbulence coefficient and expresses the disturbance in the flow. The roughness and length of the bottom protection have influence on this coefficient, longer bottom protections give smaller values of α due to the dissipation of turbulence. A maximum value of α=1.5 counts for an infinitely long protection, it can easily be seen from Breusers' relationship such a protection does never prevent scour. According to Hinze (1961) the turbulence coefficient α is related to the relative turbulence intensity r_0 at the transition of the fixed to the erodible bed. When replacing $(\alpha\overline{u}_p - \overline{u_c})^{1.7}$ in equation (3.2) by:

$$\frac{1}{T}\int_0^T (\alpha\overline{u}_p - \overline{u_c})^{1.7}\, dt$$

Breusers' equation can also be used to predict the scour depth for time-varying flow conditions, like the tidal regime in the Eastern Scheldt (equation 3.3, [Schiereck, 2004]).

Systematic scour investigations by using scale models has resulted in values for α in the empirical relation of Breusers and given in different papers, for instance by Hinze (1961), Breusers(1966,1967), Jorissen and Vrijling(1989).

If we take a closer look at the development of the scour holes around the Eastern Scheldt storm surge barrier over the last 20 years, it can be concluded that Breusers' empirical relation was quite accurate in the prediction of the equilibrium scour depth. Although an stable equilibrium of the scour holes as not been reached at the moment, the deepest point of the scour holes is not deepening significantly anymore. This can be seen in figure 3.2, where the depth of the deepest point in the seaward Roompot scour hole has been plotted for the last 20 years.

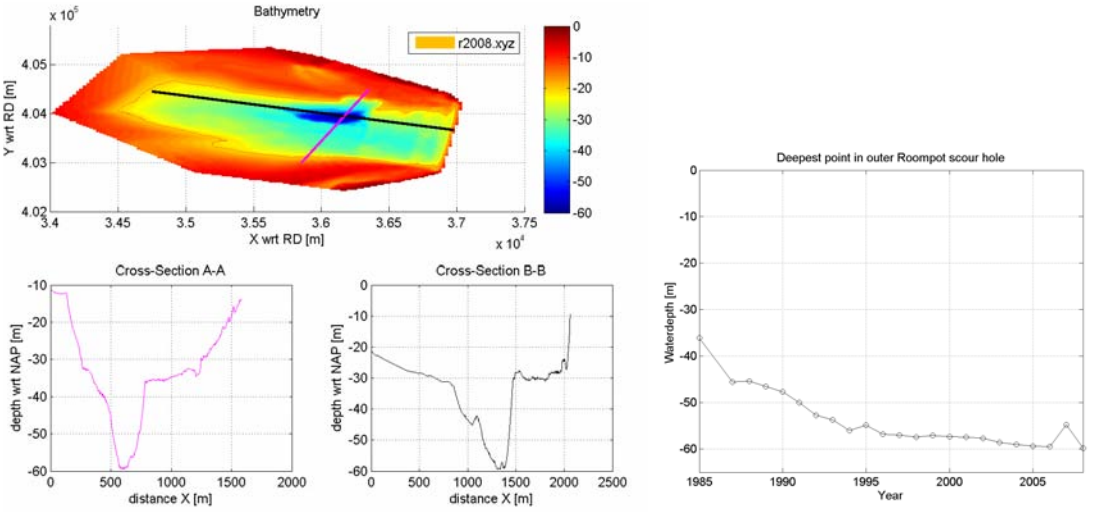

(a) Depth of the seaward scour hole in 2008

(b) Deepest point in the seaward Roompot scour hole over the last 24 years (A landslide in the scour hole was observed in 2007)

Figure 3.2: Overview of the seaward Roompot scour hole

According to the development of the scour holes over the last years, these are not endangering the stability of the storm surge barrier (as was designed for), however regular repair of the border of the bottom protection has taken place. The main question in this report is whether these scour holes act as a limitation for sediment import through the storm surge barrier. Detailed analysis of the hydrodynamics(turbulence) and sediment transport in and around the scour holes will be discussed the next section.

3.2 Hydrodynamics in and around scour holes

Within the Dutch Delta works project, research has been done to get more insight in the hydrodynamics that influences the local scour process behind structures. In the case of the storm surge barrier in the Eastern Scheldt, two 'obstacles' in the flow are distinguished; the scour holes (on both sides of the barrier) and the sill of the barrier. For both situations, different characteristic zones can be distinguished, these are shown in figure 3.3.

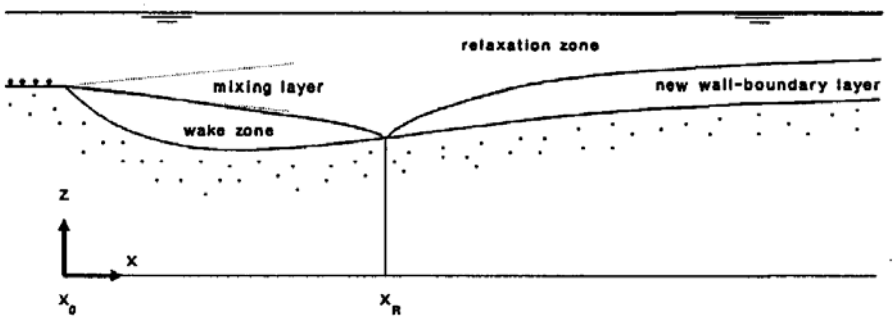

Figure 3.3: Flow regions around a scour hole

Inside a scour hole, the depth-average flow velocity decreases, this can be explained by the depth-average continuity. Over a constant width the discharge in- and outside the scour hole is constant. When the water depth increases the depth-average flow velocity decreases. The influence is most significant in the near-bed layer and the velocities in the near-water surface layers are hardly influenced by the scour hole . If a recirculating flow develops downstream of the sill or bottom protection, the region beneath the mixing layer is defined as the recirculation zone (figure 3.4). If no reverse flow occurs, e.g. if the slope of the scour hole is relatively gentle, this region is defined as a wake zone. According to [van Rijn, 1991] flow separation and reversal will occur for slopes of 1:5 and steeper, resulting in strong reduction of the flow and introducing rather complicated flow patterns. Depending on the initial slope as well as the ratio of the maximum flow-depth and the initial flow-depth, this recirculation zone reaches to a certain reattachment point. According to [Hoffmans, 1992] the new wall-boundary layer starts to grow through the reattached layer, if $x_R/(h_m - h_0) = 6$. Downstream of the reattachment point, a new wall boundary layer develops and the flow tends to reach a new equilibrium situation when the boundary layer thickness equals the local flow-depth. This process is intensified at the up sloping side where the flow accelerates, the velocity profiles become more uniform and the turbulence production is suppressed.

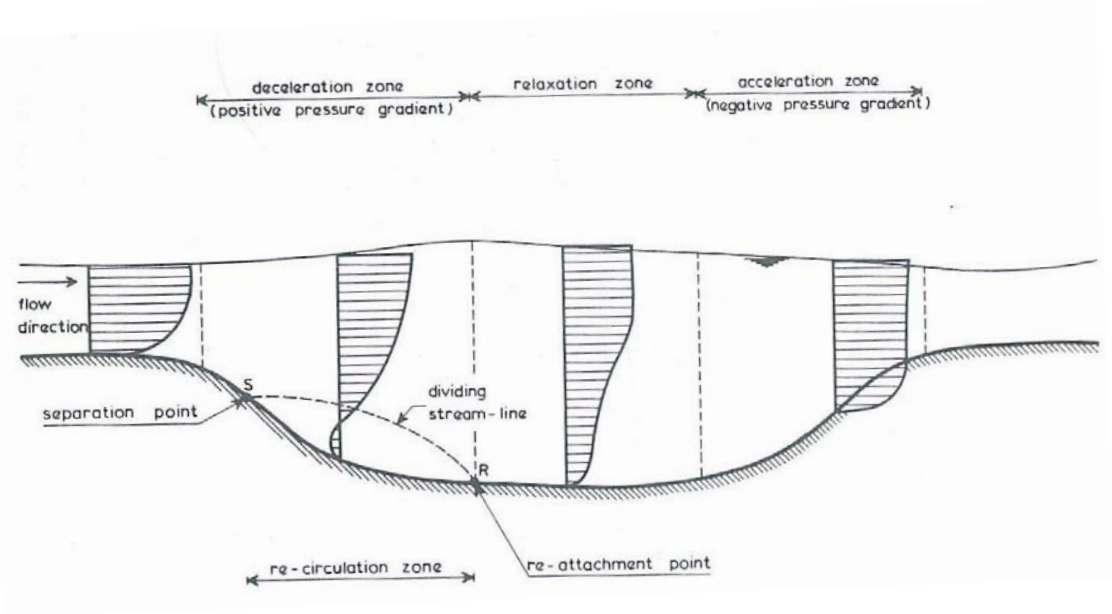

Figure 3.4: Flow profiles around a scour hole [van Rijn, 2005]

Tidal Asymmetry

The principal forcing of the water motion around the storm surge barrier is the astronomical tide which is usually described in terms of a number of harmonic components, of which the frequency is astronomically determined. The combination of these astronomical components allows us to describe a wide variety of tidal curves. In the project area the strongest components are the semi-diurnal lunar tide (M_2) and solar tide (S_2). The declinations of the moon and sun also cause a daily inequality, which is denoted by diurnal components such as K_1 and O_1. Non-linear interactions between tidal components are of paramount importance to the sediment transport, since they give rise to asymmetries in the tidal velocity, which give rise to a net (i.e. tidally averaged) sediment flux, or to a net deposition or erosion of sediment [Wang et al., 1999]. The horizontal tide (flow velocities) around the storm surge barrier is the driving force behind the sediment transport in the area. The tide can cause a residual flow over a tidal period, which can subsequently cause a residual sediment transport. The presence of the storm surge barrier makes the Eastern Scheldt a very complex area, since the tidally induced residual flow is very sensitive for geometry and bathymetry. In figure 3.5 the water level and flow velocity in the Roompot channel are shown, 8km west of the storm surge barrier. In this figure, a slightly longer ebb-period is observed, this results in higher maximum velocities during flood- than during ebb-flow. Closer to the barrier and inside the Eastern Scheldt the tidal wave will also deform due to the bottom geometry and the storm surge barrier. The deformation of the water level and flow velocities from the ebb-tidal delta to the Eastern Scheldt is showed in figure C.3.1 (appendix C). At the seaward side of the storm surge barrier, this figure mainly shows the deformation of the water level curve from the ebb-tidal delta towards the barrier and higher flow maximum velocities closer to the barrier. Inside the Eastern Scheldt the amplitude increases from the barrier towards Stavenisse and the flow velocities decrease in the southern channel inside the basin. The very low flow velocities at Stavenisse are caused by the sheltered location of the measurement point

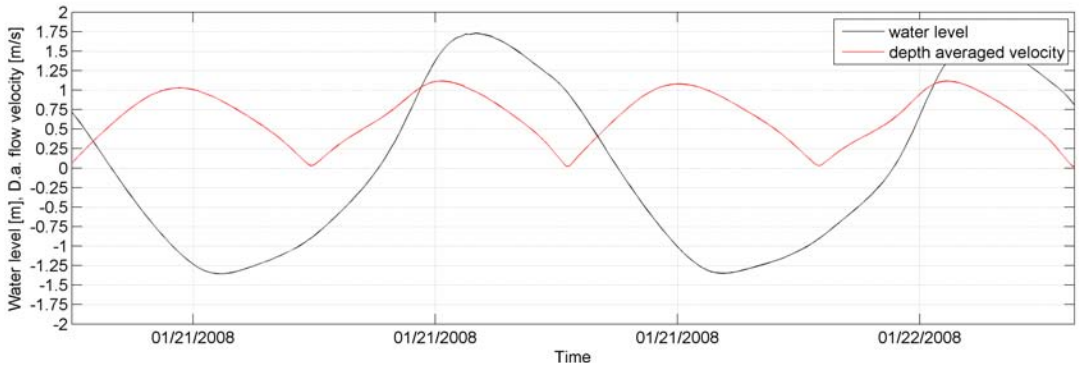

Figure 3.5: Tidal asymmetry in the Roompot channel (1km west of the storm surge barrier)

Flood- and ebb tidal jet

A very important phenomenon caused by the barrier, is the flood- and ebb tidal jet. With the construction of the storm surge barrier the cross-sectional area of the inlet has decreased significantly. During flood the water is contracting from the ebb-tidal delta into the gorge of the inlet, building up so much momentum that it cannot spread out fast enough when leaving

the gorge. The length scale of such an inertial jet is a few hundred times the water depth, so a few kilometers [Stive et al., 2006]. As a result of this jet flow, during flood higher velocities can be expected at the landward side of the barrier, compared to the seaside. During ebb the situation is the other way around, and higher outflow velocities at the seaside of the barrier can be expected. The above described phenomenon is illustrated in figure 3.6

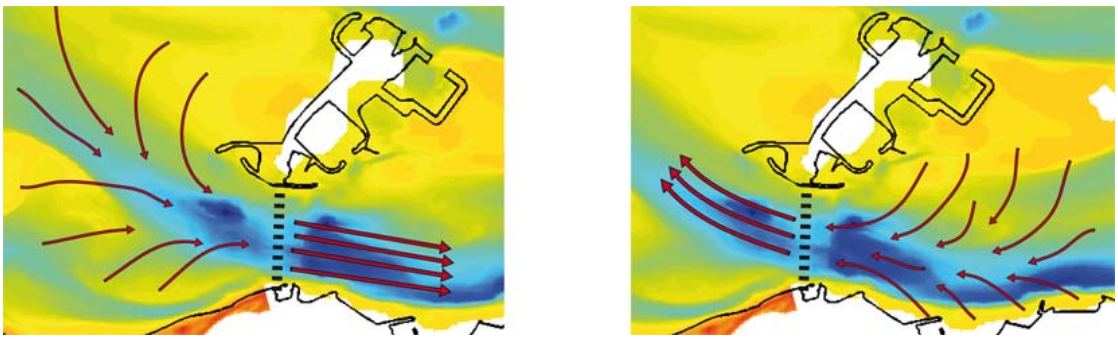

Figure 3.6: flood(left)- and ebb(right) tidal jet at the barrier

This phenomenon supports the hypothesis that sediment particles are settling in the outer scour hole during flood and washed out in seaward direction during ebb. However there are many more complex aspects that are playing a role in the residual sediment transport around the Eastern Scheldt inlet.

Turbulence and slopes

Another aspect that might influence the sediment transport through the barrier, is the turbulent flow caused by the barrier and/or the steep slopes of the scour hole. As illustrated in figure 3.7 it is possible that the outer scour hole sedimentates during flood flow due to a decrease in velocity, steep slopes and the threshold of the barrier-sill. During ebb flow the barrier-sill and steep slope cause large amounts of turbulence that will erode the scour hole again. However, it has to be investigated to what extend this vertical turbulence in the flow is actually present and influencing the sediment transport.

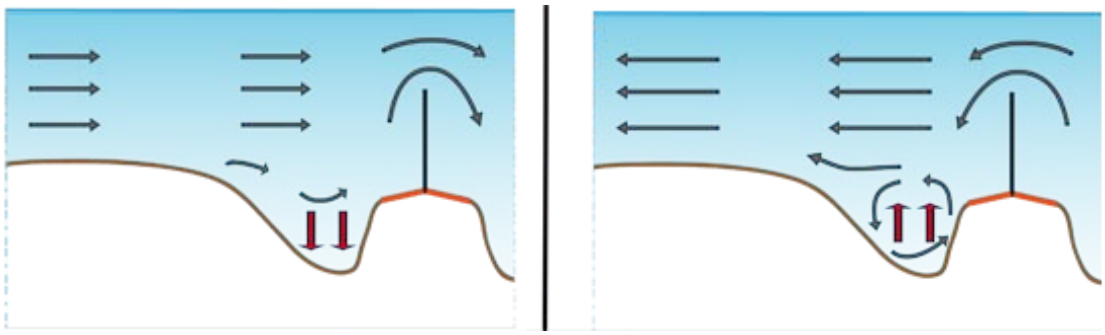

Figure 3.7: Sedimentation during flood(left) and erosion due to turbulence during ebb(right)

In [van Rijn, 1991] it is described that flow separation and reversal will occur for very steep

side slopes of 1:5 and steeper. In the design phase of the Eastern Scheldt project, calculations with slopes of 1:4 have been made to determine the scour depth and the length of the bottom protection. Analysis of recent bathymetry data (2008) has shown maximum slopes of 1:8 behind the bottom protection of the Hammen and Schaar van Roggenplaat channels. Around the bottom protection of the Roompot channel, the slopes are steeper, but still slightly milder than 1:5.

3.3 Sediment trapping

The main phenomenon causing sedimentation in a scour hole is the reduction of bed load and suspended load transport capacities in the scour hole. These transport capacities are decreasing when the current passes the scour hole. As a result the bed-load particles and a certain amount of the suspended sediment particles will be deposited on the bottom. In figure 3.8 the following processes of sedimentation and erosion in a scour hole are shown:

- advection of sediment particles by horizontal and vertical fluid velocities
- mixing of sediment particles by turbulence and orbital motions
- settling of the particles due to gravity
- pickup of the particles from the bed by current and wave-induced bed-shear stresses

In the down sloping (deceleration) area the settling process is dominant, and in the up sloping (acceleration) area the process of sediment picking-up is dominating.

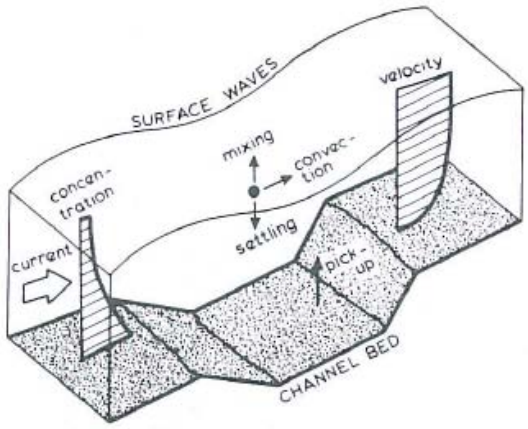

Figure 3.8: Sedimentation and erosion process in a trench [van Rijn, 1991]

The mathematical model SUTRENCH by [van Rijn, 1991] is designed to get an estimate for the trapping efficiency of a dredged trench. This quick method gives a good indication of the sediment trapping function of the scour hole near the Easter Scheldt storm surge barrier. To use this method, the scour hole is schematized as an infinitely wide channel where the flow is entering perpendicular (figure 3.9, with $\alpha = 90$ deg). This assumption of an infinitely wide channel instead of a 'round' scour hole, means that flow and transport variations perpendicular

to the inlet are not taken into account. Aside from this, the method only gives a rough estimate of the sediment trapping efficiency, no absolute transports are calculated with this method.

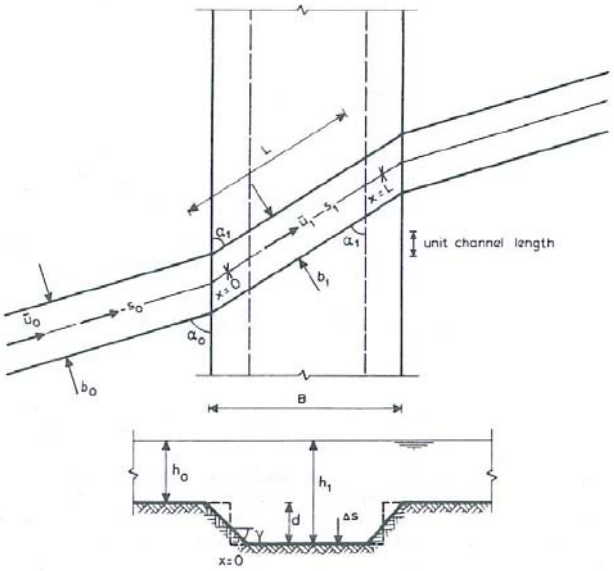

Figure 3.9: Schematization of scour hole in infinitely wide channel [van Rijn, 1991]

The trapping efficiency is defined as the relative difference of the incoming suspended load transport and the minimum suspended load transport in the channel [van Rijn, 1991]:

$$e = \frac{b_0 s_0 - b_1 s_{1,min}}{b_0 s_0} \tag{3.3}$$

where

e = trapping efficiency factor [-]

b_0 = width of approaching stream tube [m]

b_1 = width stream tube in channel [m]

s_0 = incoming suspended load transport per unit width $[m^3 s^{-1} m^{-1}]$

s_1 = suspended load transport in channel per unit width $[m^3 s^{-1} m^{-1}]$

A set of graphs is generated by the SUTRENCH model, from which an estimate of the trapping efficiency is obtained for different approach angles, approach velocities, approach depth/channel depth and channel slopes. The trapping efficiency functional relationship can be described by:

$$e = F\left(\alpha_0, \bar{v}_{r,0}, \frac{w_s}{u_{*0}}, \frac{H}{h_0}, \frac{k_s}{h_0}, \frac{d}{h_0}, \frac{B}{h_0}, tan\gamma\right)$$

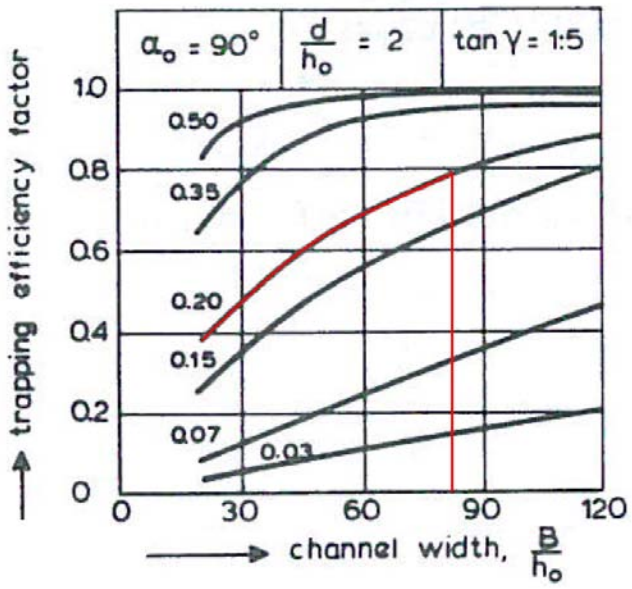

Figure 3.10: trapping efficienct

For this case we consider the following numerical values in the schematization (figure 3.9):

α_0 = 90°; flow perpendicular to channel(scour hole)
$\bar{u}_0$ = 1.25 ms^{-1} ; maximum flood-velocity
h_0 = 20 m ; depth at the seaward border of scour hole
u_{*0} = 0.05 ms^{-1} ; bed shear velocity

$$u_{*0} = \frac{\kappa u_b}{1n\frac{0.05h}{z_0}}$$

d = 40 m ; depth of scour hole, with respect to h_0
$tan\gamma$ = 1:5 ; bottom slope
B = 1250 m ; length of scour hole
w_s = 0.01 ms^{-1} ; particle fall velocity

the dimensionless parameters are

w_s/u_{*0} = 0.2
$\mathbf{d}/h_0$ = 2.0
$\mathbf{B}/h_0$ = 83.3

Above dimensionless parameters and the graph in figure 3.10 result in a trapping efficiency of about 80% for a slope of 1:5. With this trapping coefficient linearly related to the sedimentation rate ($e \cdot s_0 \cdot \alpha_0$), a cautious conclusion can be drawn that the partial sand-trapping of the incoming sediment is likely.

Chapter 4

2DV Scour hole analysis

4.1 Approach

In chapter 3 a theoretical description of the hydrodynamics in the scour holes was given. In this chapter the 2-dimensional hydrodynamic analysis will be extended with the use of a numerical model which is based on the numerical software package DELFT3D. As mentioned in the research approach (section 1.4), first a schematized 2-dimensional vertical-layered model will be set-up. This means that a single inlet of the Eastern Scheldt storm surge barrier is taken, from which a single-cell-wide model is constructed. This model is much more time-efficient than a fully 3-dimensional model and is very useful to analyze the most important processes that are taken place in the vertical plane. This insight is important to draw conclusions on the behavior of sediments around the storm surge barrier. In the Delft3D-FLOW module there are two possible vertical grid compositions, the σ-grid and the Z-grid. To investigate which type of grid is most suitable for this particular case, the model will be executed with both grid compositions and the comparison between them will be given in this chapter.

4.2 The process based model Delft3D

Delft3D is a software package developed by Deltares (former WL|Delft Hydraulics), designed for 2D and 3D computations of coastal, river and estuarine areas. It can carry out simulations of flows, sediment transport, waves, water quality, morphological development and ecology. The Delft3D suite is composed of several modules, grouped around a mutual interface, while being capable to interact with one another. For the first part of this study, only the module Delft3D-FLOW has been used. This is the central module that provides the hydrodynamic basis for the other modules of Delft3D. The module is a multi-dimensional hydrodynamic(and transport) simulation program which is based on a set of mathematical equations based on the first physical principles (conservation of mass, momentum, energy, etc.) and calculates unsteady flow and transport phenomena with a free surface. The model can run in different dimensions, for some cases it is not necessary to calculate in 3D. By simulating a situation in 1D or 2D, costly time-consumption can be saved while the outcome can still be detailed enough. It is expected that a

schematized 2DV model, which is 1 cell wide and has a grid diversion in the vertical direction, can give a good representation of the possible sediment-trapping mechanism of the scour holes near the Eastern Scheldt storm surge barrier. However some remarks must be made by using a 2DV model in this case. The asymmetry of the flow patterns around the storm surge barrier is difficult to represent exactly. Acceleration and deceleration of the flow can be simulated by varying the width of the grid cells. However the asymmetry between the ebb- and flood flow in lateral direction behind the barrier cannot be represented in a 2DV model.

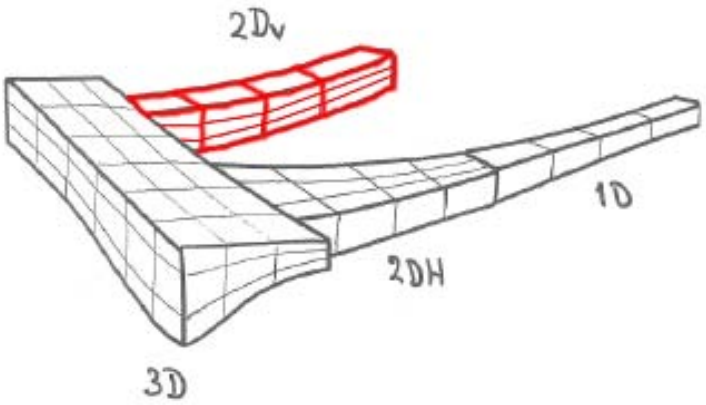

Figure 4.1: The 2DV grid composition in Delft3D

An overview of the basic equations used in Delft3D is given in appendix A.

4.3 Model set-up and model settings

As a basis for the schematized 2DV model, a numerical model developed by Rijkswaterstaat is used. The KustZuid model is based on the SIMONA (WAQUA) software package and simulates the water levels at the South-western coast of the Netherlands, forced by 94 astronomical tidal components. The model includes the two Scheldt estuaries, the Scheldt river and the coastline from Duinkerke (Belgium) in the south to the island of Goeree in the north. For the water level and flow velocity calculations the model uses maximum horizontal grid-cells of 150x200m and has one single depth-layer (2DH).

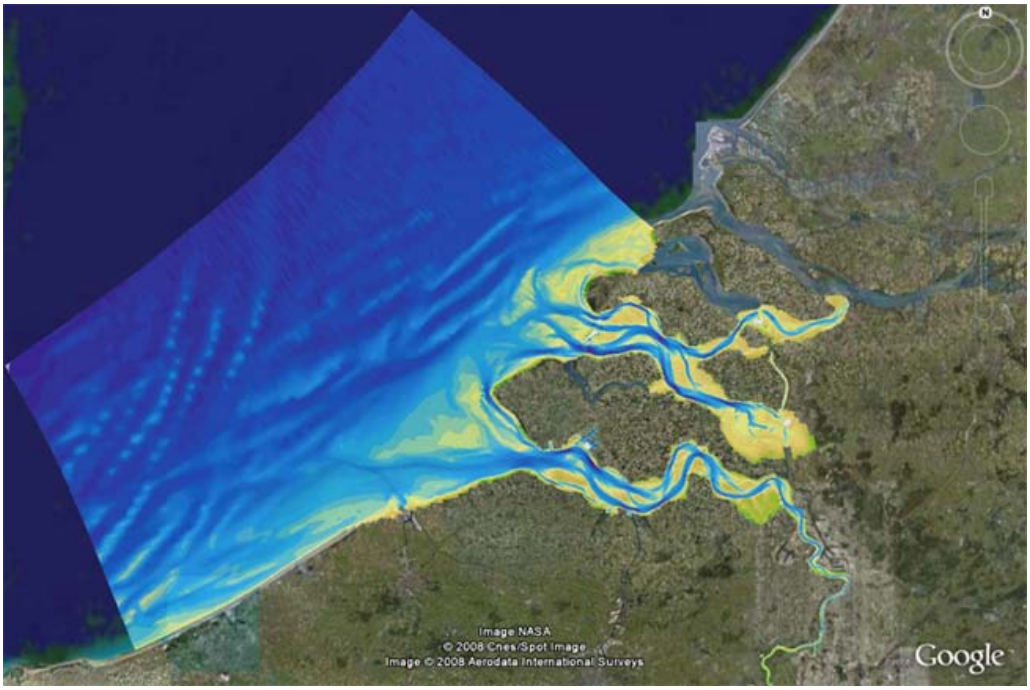

Figure 4.2: The 2DH KustZuid model

Because this model is based on a different software package, it has been converted to a Delft3D model and calibrated afterwards. The conversion and calibration of this model is described in appendix B. After this conversion and calibration, the KustZuid model is used to produce boundary conditions, and reference data for the calibration of the 2DV model.

4.3.1 Schematized 2DV model

To construct a 2DV model where the hydrodynamic behavior is representative for the real situation, the flow-characteristics has to fulfill certain criteria. It is important that the longitudinal velocities are dominant over the perpendicular velocities for the total length of the model. In figure 4.3 the velocities at maximum flood-flow are given. It is visible that due to the two converging channels at the west side of the Roompot (southern) inlet, velocities are not parallel to each other. Due to this convergence of streamlines, it is very difficult to represent the flow conditions around the Roompot channel in a 2DV model. At the Schaar van Roggenplaat the flow is nicely following the main channel. Therefore this channel is chosen to use in the 2DV model. Although the bathymetry of Roompot channel is more extreme (longer scour holes with slightly steeper slopes) than the Schaar van Roggenplaat bathymetry, it is expected that a model of the Schaar van Roggenplaat channel still gives a good understanding about the dominating processes that are influencing the sediment transport.

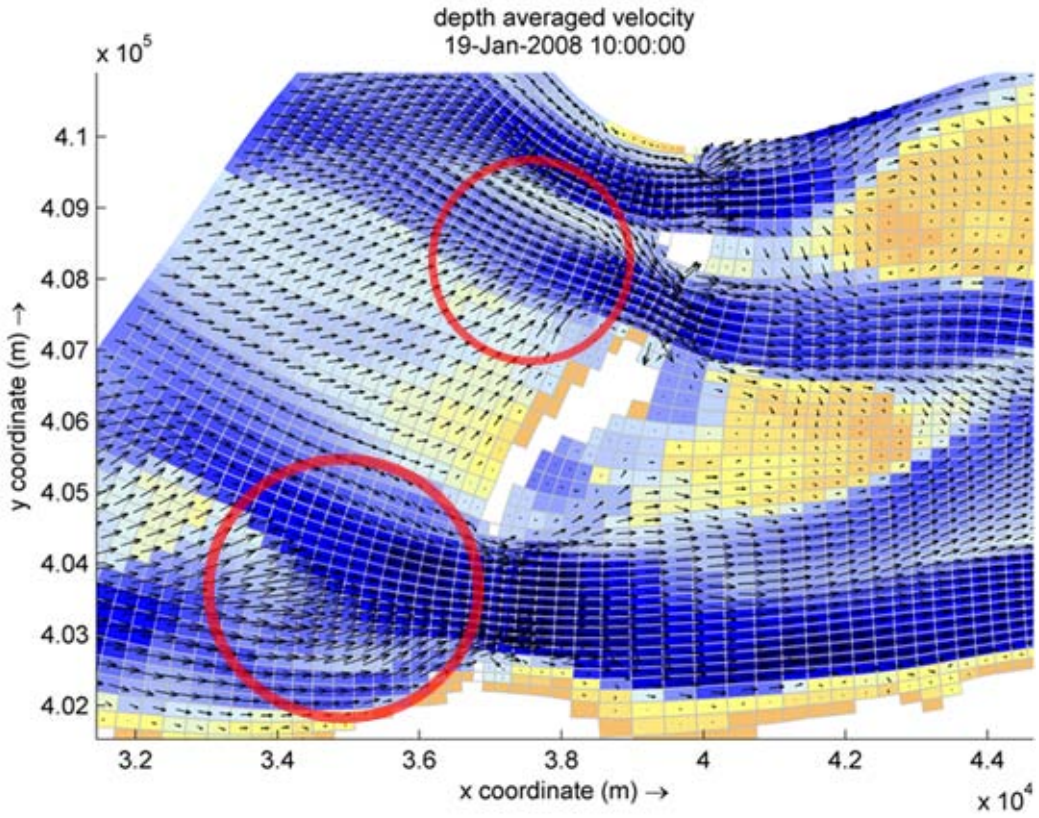

Figure 4.3: Flow velocity at maximum flood-flow in the Roompot(southern) channel, the Schaar van Roggenplaat(center) and Hammen(northern) channels

4.3.2 Bathymetry

The bottom geometry of the original KustZuid model is too coarse to be used in the detailed 2DV model. Therefore newer and more detailed measurements have been used. Rijkswaterstaat has measured the bottom around the storm surge barrier every year since the realization of the project. From the detailed 'multibeam' measurements of 2008 by Rijkswaterstaat, a cross-section has been constructed (figure 4.4) from which the steepness, depth and length of the real scour holes are extracted and schematized into the 2-dimensional model (figure 4.5).

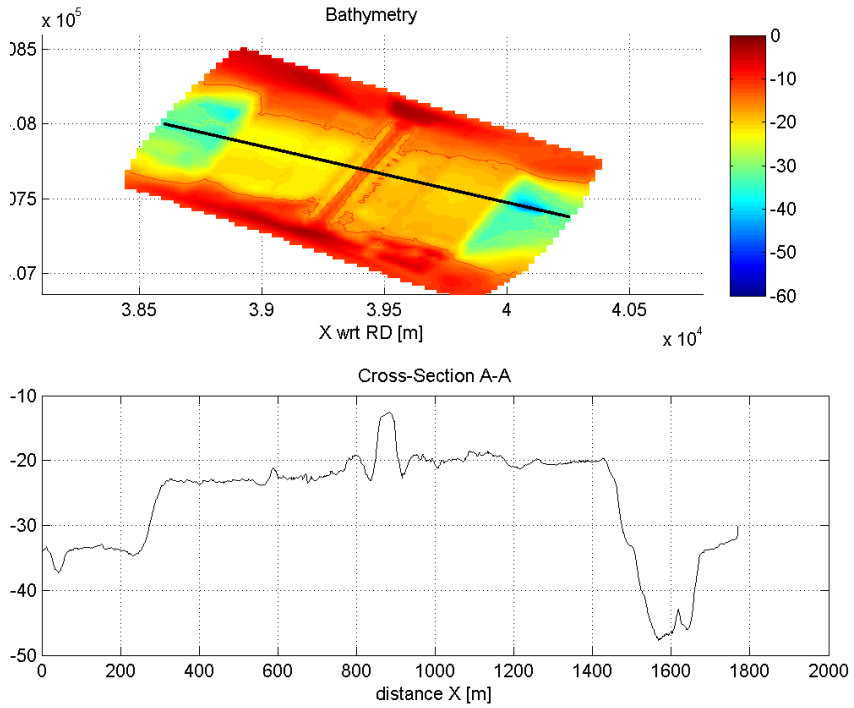

Figure 4.4: Original bathymetry of Roompot channel (2008)

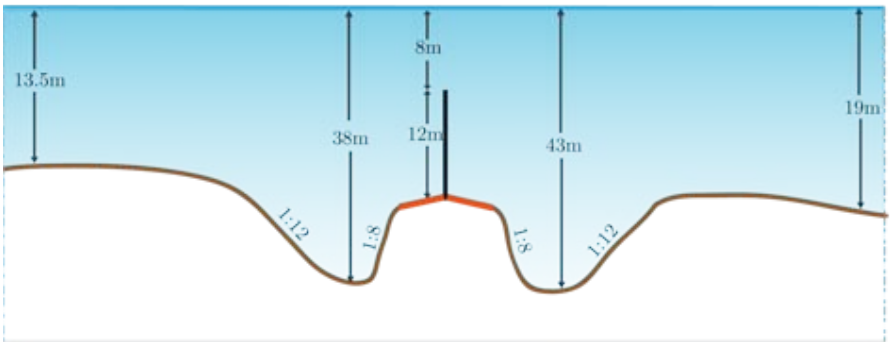

Figure 4.5: Schematized bathymetry used in the 2DV model

At the western end of the 2DV model the water depth is 13.5 meters, eastwards the slope of the scour hole slowly increases to a maximum of 1:12. After the deepest point has been reached at -38m below mean sea level, the depth is decreasing with a steepness of 1:8 to a fixed bed level of -20m. From here the fixed bottom protection prevents scouring around the barrier. In the middle of the 1100m wide bottom protection (550m east- and westwards) the sill of the storm surge barrier is situated. A main part of the sill is the concrete beam, which has different depths in every inlet of the barrier. In the center of the Schaar van Roggenplaat, where the 2DV model is based on, the top of this beam is constructed at 8m below M.S.L. On the east side of the barrier a similar scour hole can be found, only this one is slightly deeper (-43m) and longer.

4.3.3 Grid

Horizontal grid

The grid consists of 367 grid cells in longitudinal direction, and the model is one cell wide. As the main interest of the model are the scour holes around the barrier, the longitudinal width is refined from 30 meter at edges of the model, to 9 meter around the barrier and scour holes. To model the horizontal contraction of the flow, the cell width varies along the model. By narrowing the grid width towards the barrier, the flow will accelerate and reach maximum velocity around the narrowest point (barrier). The width of the model is determined by calibrating this 2DV model to the original KustZuid model. Along the model, 8 points are chosen where the velocity and water level of the two models are compared. The calibration process will be discussed in section 4.4, resulting that the width of the grid cells near the barrier is 55% of the cell-width at the open boundaries.

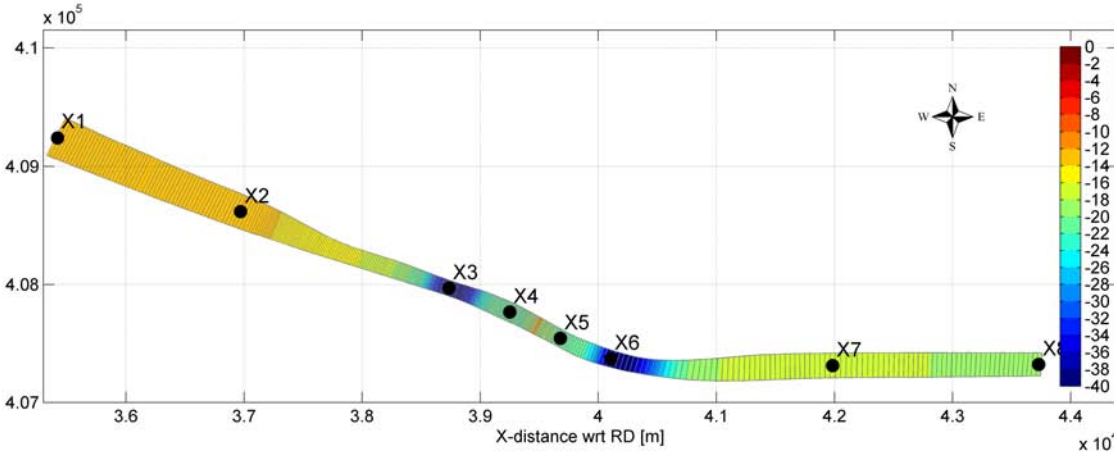

Figure 4.6: Horizontal grid with calibration points (section 4.4)

Vertical grid

For the vertical grid there are two possible grid compositions in Delft3D (figure 4.7):

- σ-layered grid composition, where the number of layers over the entire horizontal computational area is constant, irrespective of the local water depth.
- Z-layered grid composition, where the deepest water depth is divided by the vertical number of grid cells, the layer-thickness is constant along the model.

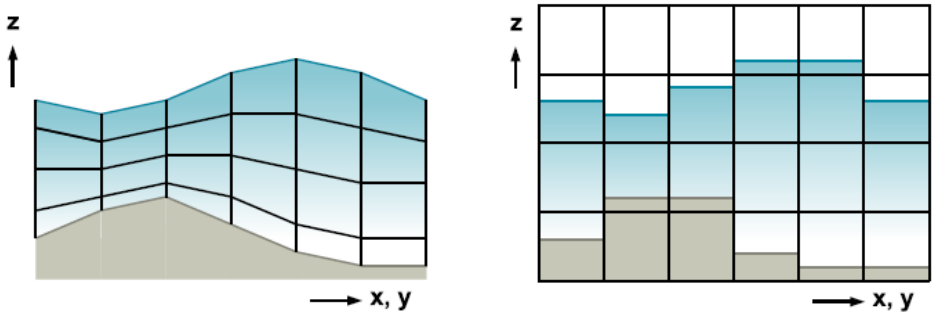

Figure 4.7: Vertical grid with σ-layers(left) and Z-layers(right) [Ullman, 2008]

A σ-coordinate model provide an accurate representation of the bathymetry and is therefore well suited for simulating bottom boundary layer processes. The coordinate system permits simple treatment of the boundary conditions at the bottom and free surface and makes efficient use of computer resources. Although the preceding advantages of the terrain-following coordinate system are evident, the method also has some drawbacks ([Bijvelds, 2001]). The relative thickness of the computational grid cells does not depend on the horizontal coordinates x and y which gives rise to unnecessarily high grid resolution in shallow areas and possibly insufficient grid resolution in deeper parts of the computational domain. For situations with steep bottom topography, the σ coordinate system can also give inaccuracies in the representation of the flow. Because the bottom cell of a σ-grid follows the bottom topography, there is the possibility that on steep slopes the flow sticks to the slope. While on the same slope in a Z-coordinate system, the flow 'overshoots' the downward slope. Besides the difference in the representation of the flow, there are different functional limitations to the σ- and Z-grids. The most important difference for this research project is that the combination of a Z-gridded model with the sediment transport module has not been fully developed in Delft3D. Therefore morphological results of such a calculation might not be sufficiently reliable to draw conclusions from. An advantage of the Z-grid model is that non-hydrostatic pressures can be implemented in the model. This might be necessary when the vertical acceleration component of the flow is no longer negligible to the acceleration of gravity. A more detailed description of differences between hydrostatic and non-hydrostatic modeling can be found in appendix A.1 and A.2. For the constructed 2DV model three different options will be modeled to make a hydrodynamic analysis:

- σ-grid model.
- Z-grid model with hydrostatic pressure assumption.
- Z-grid model coupled with non-hydrostatic module.

For all models 60 depth-layers are implemented, which means for the σ-model a layer thickness varying from 0.15m(around barrier) to 0.70m (in scour holes). For the Z-layer model the layer thickness has a uniform value of 0.80m along the model. Other runs with 40 and 100 vertical layers has also been performed to check the model sensitivity to the vertical grid resolution. In the model with 60 layers the velocities converge to the values of a model with 100 layers. A reduction to 40 layers gives too many inaccuracies, especially at the bottom and the steep slopes of the scour hole (figure 4.8 and 4.9).

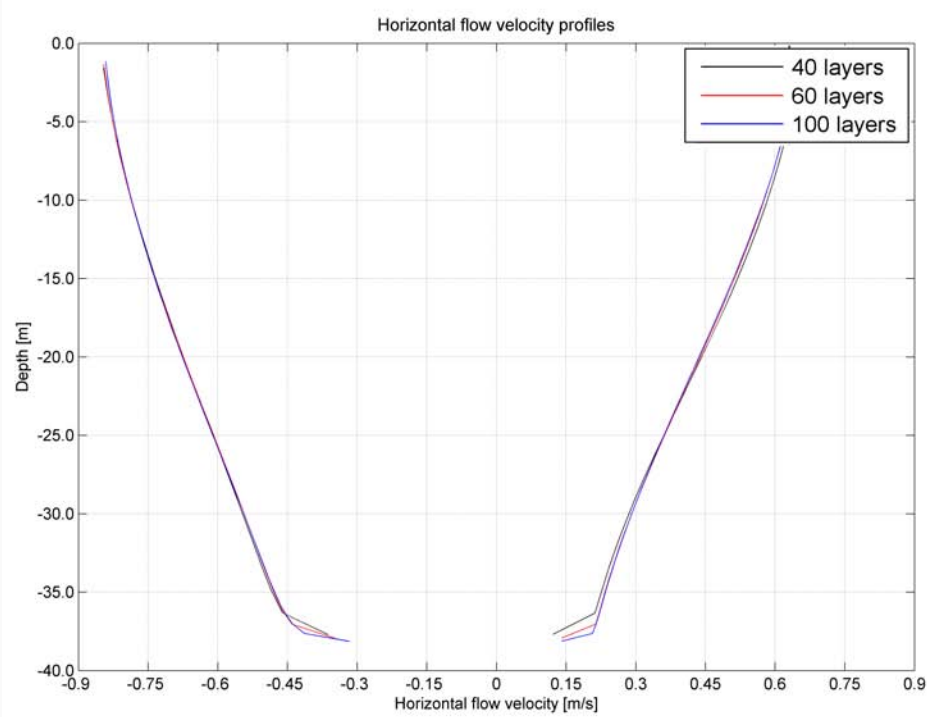

Figure 4.8: Flow velocity profiles for differentnumber of layers

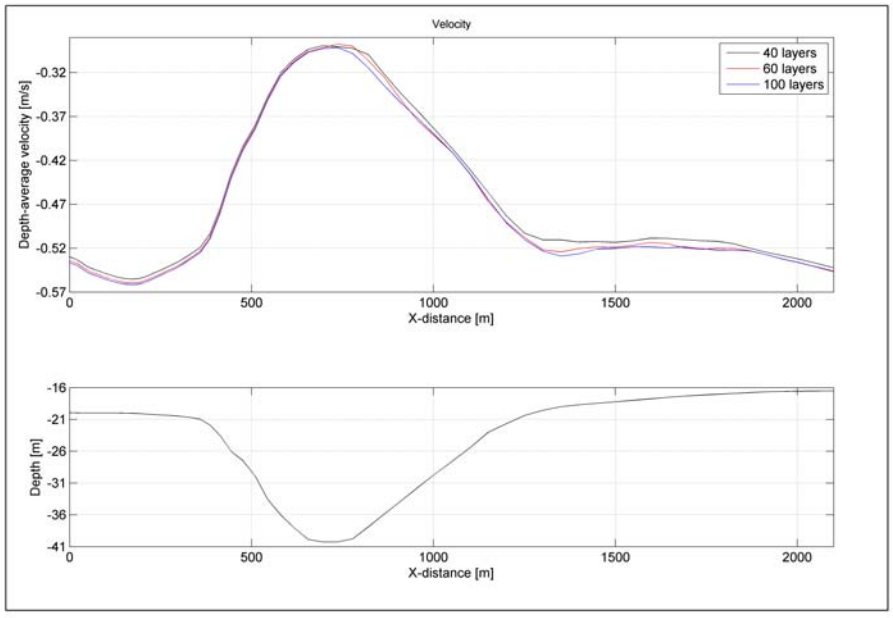

Figure 4.9: Depth-average velocity for different number of layers

4.3.4 Boundary conditions

Boundary conditions for the 2DV model are obtained from the larger KustZuid model. As a result all 94 tidal components are included (see appendix B). 5 Kilometer west of the storm surge barrier an output time series of the water level is generated over one spring-neap tidal cycle. Inside the Eastern Scheldt, 5 kilometer east of the barrier, an output time series of the depth-average flow velocity is generated over the same period. The time series of the water level (sea side) and flow velocity (basin side) are implemented as boundary conditions for the 10 kilometer long 2DV model. From the generated spring-neap cycle an average tidal wave has been chosen for the analysis of the hydrodynamic behavior during one daily tidal cycle.

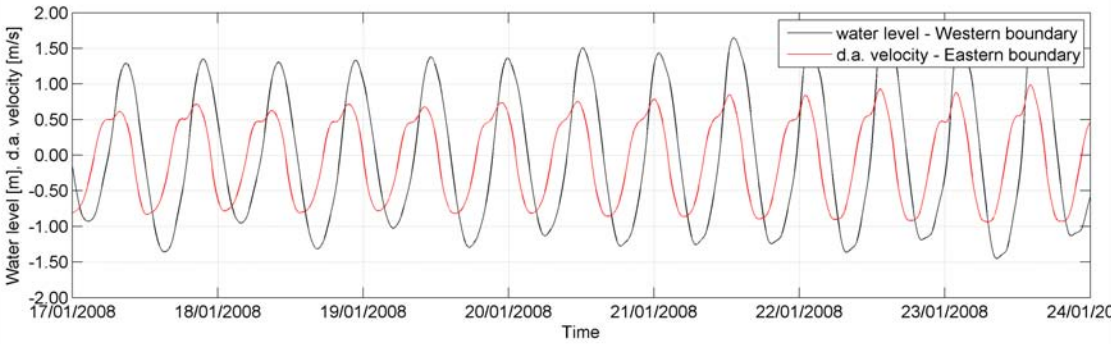

Figure 4.10: Time series of water level (western boundary) and depth average velocity (eastern boundary)

4.3.5 Time scale parameters

The hydrodynamic module of Delft3D uses an implicit scheme to solve the unsteady shallow water equations. Because an unconditionally stable scheme is used, the numerical stability is not restricted by the time step or the grid size. However, the accuracy of the flow computation decreases with an increasing Δt. Therefore a widely used parameter for the numerical stability of the flow, the Courant number, is evaluated to give an indication of the accuracy of the computation [WL|Delft-Hydraulics, 2007]:

$$Cr = \frac{\sqrt{gH}\Delta t}{\Delta x, \Delta y} \leq 10 \tag{4.1}$$

For the Z-coordinate model the following additional restriction apply:

$$\Delta t \leq \frac{min\left(\Delta x, \Delta y\right)}{max\left(|u|, |v|\right)} \tag{4.2}$$

With:

g =gravitational acceleration = 9.813 ms^{-2}
H =maximum water depth = 40 m
Δx,Δy =smallest grid size in x or y direction = 10 m
$|u|$ =maximum velocity $\approx$ 1.5 m s^{-2}

A maximum time step of 5 seconds fulfills both restrictions.

4.3.6 Barrier modeling

The storm surge barrier in the Eastern Scheldt constricts the flow in two directions. In horizontal direction the cross-section is narrowed by the piers of the barrier. Because the numerical model is only one cell wide, a single pier cannot be placed in the grid. Therefore the cell-width is varying along the model as mentioned in section 4.3.3. In vertical direction the flow is also constricted by the sill on the bottom of the inlet. For the Z-layered model this sill can be included in the bathymetry. The σ-layered model is not able to cope with the steep slopes (>1:3) of the barrier-sill when it is included in the bathymetry. Therefore a Delft3D hydraulic structure is implemented to represent the vertical constriction.

A 3D-gate is a very thin construction with a limited height, which closes off a number of layers in the vertical. The thickness of the construction is infinitely small, so it has no influence on the water volume in the area. The gate is located at a velocity point of a grid. Here the flow at all intermediate layers of the gate is set to zero. As a result of the gate the flow is accelerating upstream of the construction (contraction) and decelerating downstream of the gate (expansion). In the model the inlet is closed off from -8m (top of the sill) to -20m (bottom), which means that only the upper 27 (out of 60) layers of the model are left open.

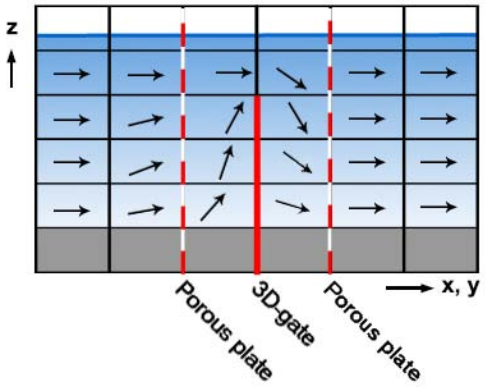

Figure 4.11: Principle of a 3D-gate and porous plate in Delft3D-FLOW

This 3D-gate structure underestimates the energy losses over the openings [WL|Delft-Hydraulics, 2007]. Therefore an additional 'porous plate' is placed on both sides of the gate to increase the resistance of the barrier. A porous plate is a partially transparent structure that extends into the flow over some or all layers in the vertical. Like the 3D-gate, the thickness of a porous plate is much smaller than the grid size in the direction normal to the porous plate. The porous plates are adding a quadratic loss term to the local momentum balance of the form λu^2. The energy loss coefficient in the quadratic friction term is defined by:

$$M_\zeta = -c_{loss-U} \frac{U_{m,n} \left| \vec{U}_{m,n} \right|}{\Delta x} \tag{4.3}$$

M_ζ = Quadratic friction term [m s^{-2}]
c_{loss-U} = Barrier resistance coefficient [-]
A_c = cross-sectional area below mean sea level [m^2]

In the KustZuid model the porous plates are used as a calibration parameter for the storm surge barrier (Appendix B). This energy loss coefficient resulting from the calibration, has also been used in the 2DV model.

4.3.7 Model parameters

Simulation start time	18-01-2008 00:00:00
Simulation stop time	19-01-2008 18:00:00
Number of horizontal grid cells	367
Number of vertical grid layers	60
Time step	6 sec
Gravitational acceleration	9.813 m s^{-2}
Water density	1023 kg m^{-3}
Bed roughness	60 $m^{1/2}$ s^{-1} (Chézy)
Vertical background viscosity	$1 \cdot 10^{-6}$ m^2/s
Turbulence model	k-ϵ-model
Barrier friction coefficient of the quadratic friction [-]	2.3

Table 4.1: 2DV model parameters

A small value for the background viscosity has been chosen, as the real viscosity is calculated by the k-ϵ turbulence model. For the gravitational acceleration, water density and the Chézy bed roughness realistic values have been used which are based on own insight.

4.4 Model calibration and validation

Simplification of the complex situation into the 2DV model is only useful if the hydrodynamics along the ray in the calibrated KustZuid model are approximated by the schematized 2DV model. The calibration of the velocities in the model is done by varying the cell-width along the grid, which represents the contraction of the flow around the barrier. Although the contraction can be included with this method, the ebb- and flood tidal jets as described in 3.2 are not represented in this 2-dimensional model. Because there are no reliable flow-velocity measurements over a longer period available (one tidal cycle for instance) in the vicinity of the inlet, calibration of the 2DV model has been done with the KustZuid model as reference.

Within the boundaries of the 2DV model eight observation points are placed. In these points the depth-average velocity is compared with the same observation points in the KustZuid model.

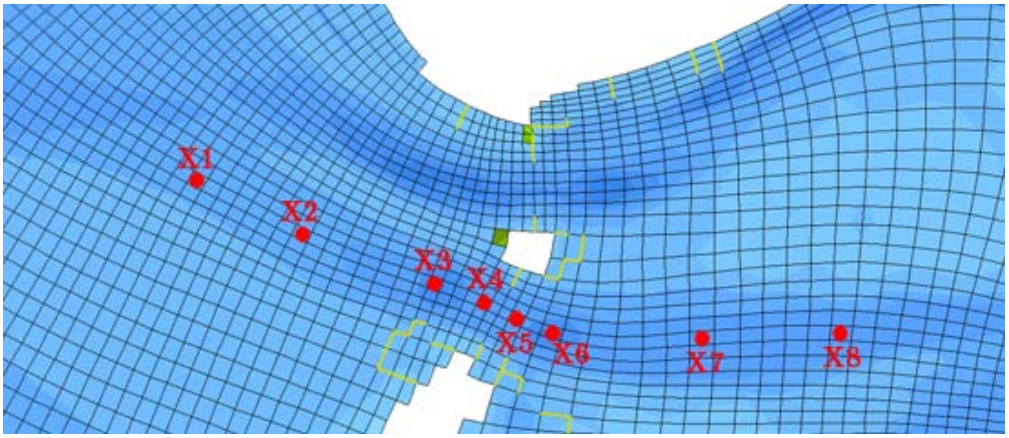

Figure 4.12: Observation points in the KustZuid model

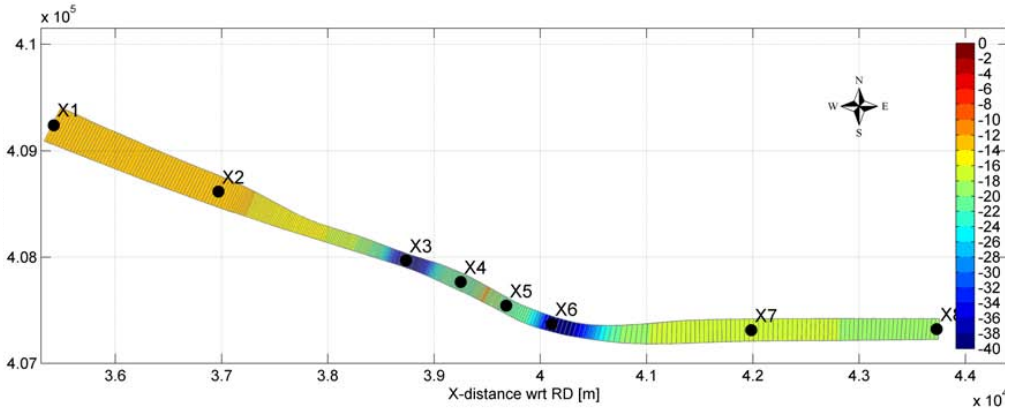

Figure 4.13: Observation points in the 2DV model

The cell-width in the 2DV model is adjusted until the flow velocities approximate the results of the KustZuid model. The approximation of the flow velocities are prioritized over the water level because the currents are the main driving force behind sediment transport. The results of the calibration are shown in figure C.4.1 in appendix C.

In the main interest area of this research project (sea side of barrier), the depth-average flow velocities are approximated fairly well and give a good representation of the real situation in the schematized 2DV model. Extra model runs did not result in a better approximation of the water levels in the interest area.

4.5 Model analysis

In this section, different runs of the model are compared and discussed. The analysis focuses mainly on the seaside of the storm surge barrier, because the outer scour hole is of main interest in this thesis.

The three discussed model runs are:

- σ-grid model
- Z-grid model with hydrostatic pressure assumption
- Z-grid model coupled with non-hydrostatic module

4.5.1 Hydrodynamic analysis

The overall hydrodynamics of the three models are quite similar. Flow velocities increase when the cross-sectional area decreases due to narrowing of the horizontal grid or an up sloping bottom and when the flow is entering the scour hole deceleration of the flow is observed. At eight observation points in the model, flow velocity profiles during ebb and flood are plotted in figure C.4.2 (Appendix C). The four flow profiles in the vicinity of the scour hole are shown in more detail in the figure below.

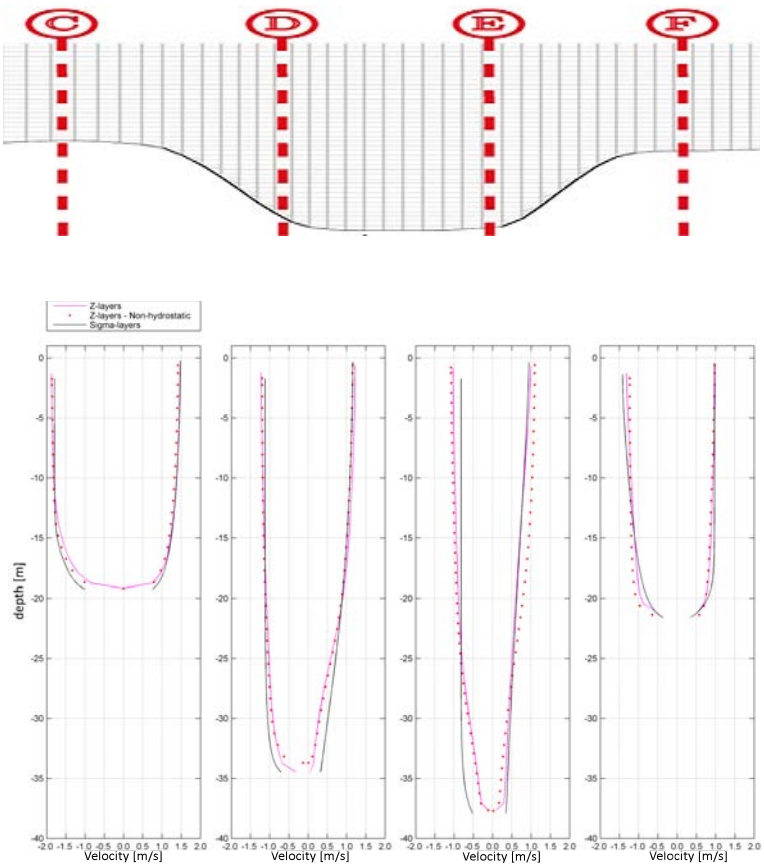

Figure 4.14: Flow velocity profiles around the outer scour hole

Comparing the flow velocity profiles for the different grid compositions, it is clear that the σ-grid model show significantly larger velocities than the Z-grid model, especially near the bottom of the scour hole. The approximation of strictly horizontal gradients in areas with steep bottoms causes errors in σ-models. This is caused by the fact that the horizontal derivatives in Cartesian

coordinates are split into two terms in σ-coordinates. Sometimes horizontal derivatives that are almost zero result from two large derivatives that should cancel. In that case, truncation errors in the approximation of both terms may result in a relatively large error. In particular the error in approximating the pressure gradient error has been addressed often in the literature [Bijvelds, 2001].

The difference between the Z-layers with and without the Non-hydrostatic module is very small, only at the bottom of the scour hole a small difference can be observed. Possibly the non-hydrostatic effects an these places play a less important role than the difference in grid-composition. However it is very difficult to verify which results are the most correct ones, as there are no measurements available to verify these numerical model results.

Flow recirculation

In a situation with very rapidly varying bed topography, reversal currents may be present at places where flow separation is occurring. Section 3.2 describes that recirculation of the flow can be expected where the bed slope exceeds a value of 1:5 [van Rijn, 1991], so in the model reverse currents behind the barrier sill (1:3) can be expected. In the z-coordinate model this flow recirculation develops behind the sill (figure 4.15). Due to the numerical structure of the barrier in the σ-coordinate model, this flow recirculation is not represented in this model. In the three models no reverse current is observed inside the scour holes, which is reasonable with the present bottom slope (1:8). However the slopes of the scour hole in the Roompot channel are slightly steeper (1:6), which give the possibility that flow recirculation will develop in that scour hole.

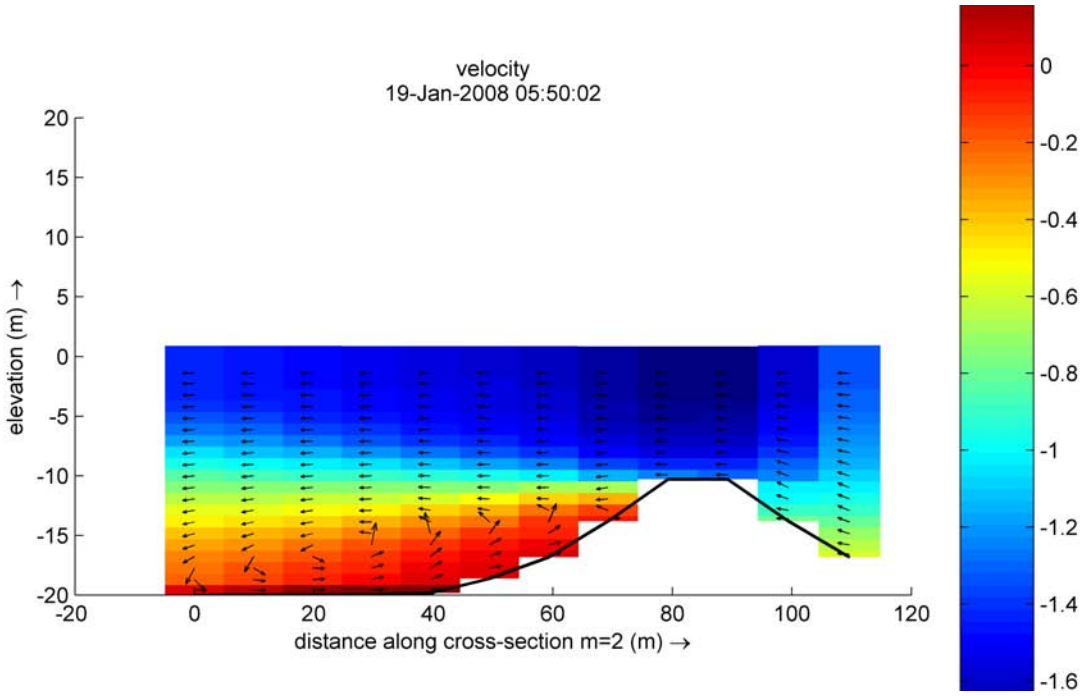

Figure 4.15: Flow recirculation behind the sill of the barrier during ebb-flow (Z-coordinate model)

Bed shear stresses

The bed shear stresses in the model give a good indication where sediment can be picked up from the bottom and where sedimentation can occur. When the longitudinal bed shear stresses around the outer scour hole during flood are plotted for the three model runs, some clear differences can be observed (figure 4.16).

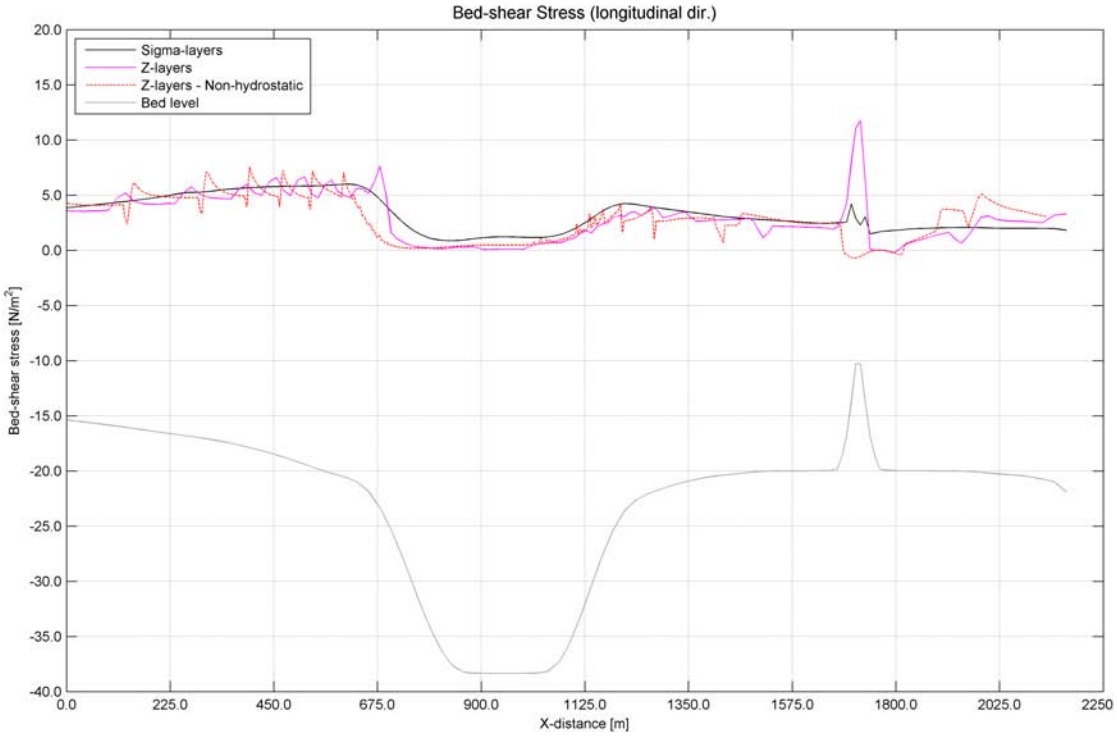

Figure 4.16: Bed shear stress during ebb-flow for different layer-types, in longitudinal direction along the model

The higher flow velocities in the σ-model at the bottom of the scour hole are directly translated to the bed shear stresses. While the bed shear stresses for the Z-model (hydrostatic and non-hydrostatic) are decreasing to almost zero, the stresses in the σ-model have a minimum value of about 1 Nm^{-2}. Another difference between the models are the irregularities in the Z-layered hydrostatic and non-hydrostatic models. According to [Fortunato and Baptista, 1994], the representation of the bottom leads to these inaccuracies in the approximation of the bed stress and the horizontal advection near the bed. This difference in the representation of the bottom boundary layer between the σ- and Z-coordinate is showed in figure 4.17, where the staircase effect in the bottom layer of the z-coordinate model is shown. Due to the vertical jumps in the bottom grid layer, errors in bed shear stresses at sloping bottoms occur for which no solutions are yet implemented in the Delft3D version which is used for this thesis. Runs with smaller grid sizes and time step did not result in smoother results of the Z-gridded model.

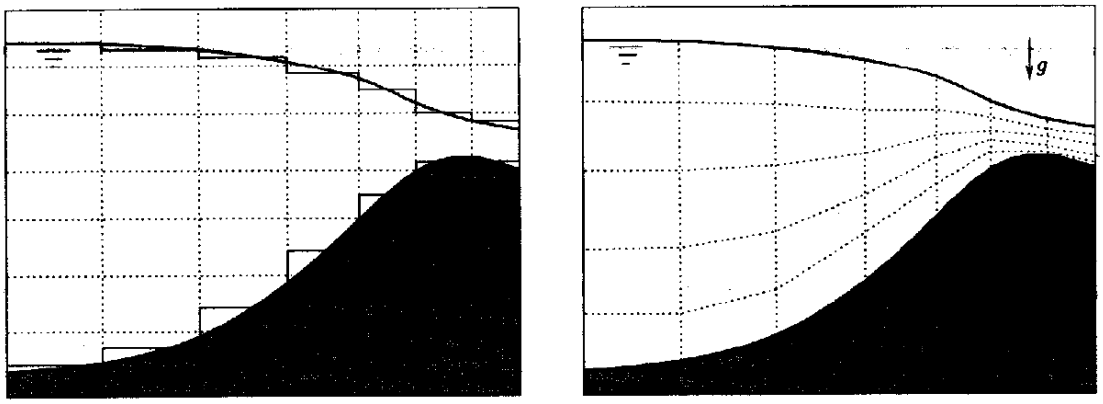

Figure 4.17: Representation of bottom boundary in the z-coordinate system (left) and the boundary fitted σ-coordinate system (right) [Bijvelds, 2001]

Another big difference between the runs, is the magnitude of the bed shear stress around the barrier. The hydrostatic Z-layered model results in significant larger bed shear stresses compared to the σ-layered model, this can be subscribed to the difference in modeling of the barrier. For the Z-model the barrier is included in the bathymetry, while in the σ-model a hydraulic structure has been applied (see section 5.2.5). The model where the non-hydrostatic module is included (red line), shows even small negative values for the bed-shear stress at the western side of the barrier. This is caused by the flow recirculation which develops downstream (left side of barrier in figure 4.16)during ebb-flow.

Conclusions

After various runs with the 2DV model, it can be used as a valuable addition to the existing theories as described in chapter 3. Flow behavior around the scour hole and storm surge barrier in the vertical direction, show patterns that can be expected in reality. Two main reasons for the differences between the model runs can be distinguished:

1. The difference in representation of the bottom boundary layer between the σ- and z-coordinate layer system. This numerical difference is described by Fortunato and Baptista [1994] and Bijvelds [2001] and causes especially irregularities in the representation of the bed shear stresses at sloping bottoms.

2. The models show a difference in the calculated local flow velocities, especially near the bottom and slopes of the scour hole. This difference is also described by Bijvelds [2001] and is caused by the conversion of horizontal derivatives in Cartesian coordinates to σ-coordinates.

According to personal communication with experts (ir. A. Luijendijk, Deltares), the σ-coordinate model represents the hydrodynamic behavior correctly for maximum slopes of about 1:9. Therefore is can be expected that the Z-coordinate model including the non-hydrostatic module represents the hydrodynamic behavior near these scour holes better than the σ-coordinate model. However the boundary conditions of this model at the bottom produces irregularities in the bed

shear stresses. This might be the reason that the combination of a Z-layered model with the sediment module in Delft3D is not yet fully developed.

4.5.2 Sediment transport

Although the hydrostatic σ-layered model might not represent the flow velocities correctly at the bottom of the scour hole, interesting results can be expected when sediment transport is implemented. When keeping the observed differences with the Z-coordinate models in mind, sediment concentration patterns can give a good idea about the sediment-trapping function of the scour hole. Therefore this section gives a short analysis of the σ-layer based model including sediment transport.

For this analysis an exact period of 4 tidal period is modeled (figure 4.18), within this period the ebb- or flood dominance and the mean sediment transports in this model can be determined.

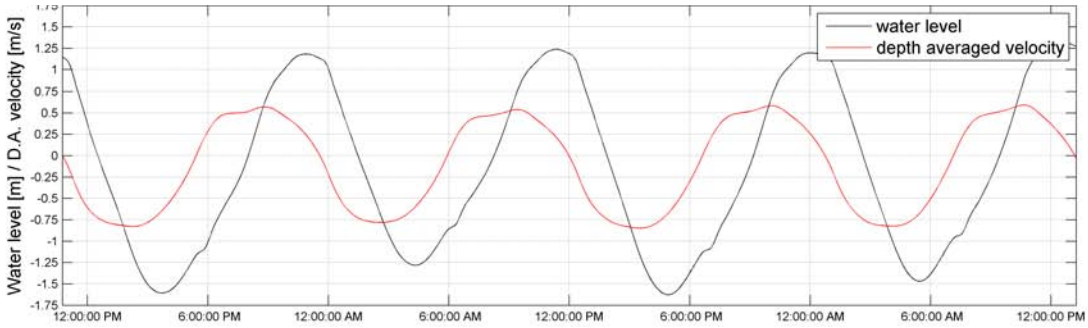

Figure 4.18: Water level and depth-average flow velocity

Sediment concentrations

At the seaward side of the barrier, the variance of sediment concentrations in the model show a significant decrease of the concentration when the flow enters the scour hole. During flood flow (figure 4.19) a large reduction can be observed at the down sloping bottom of the scour hole. Sediment is picked up again on the upward slope towards the bottom protection, however this increase is very small.

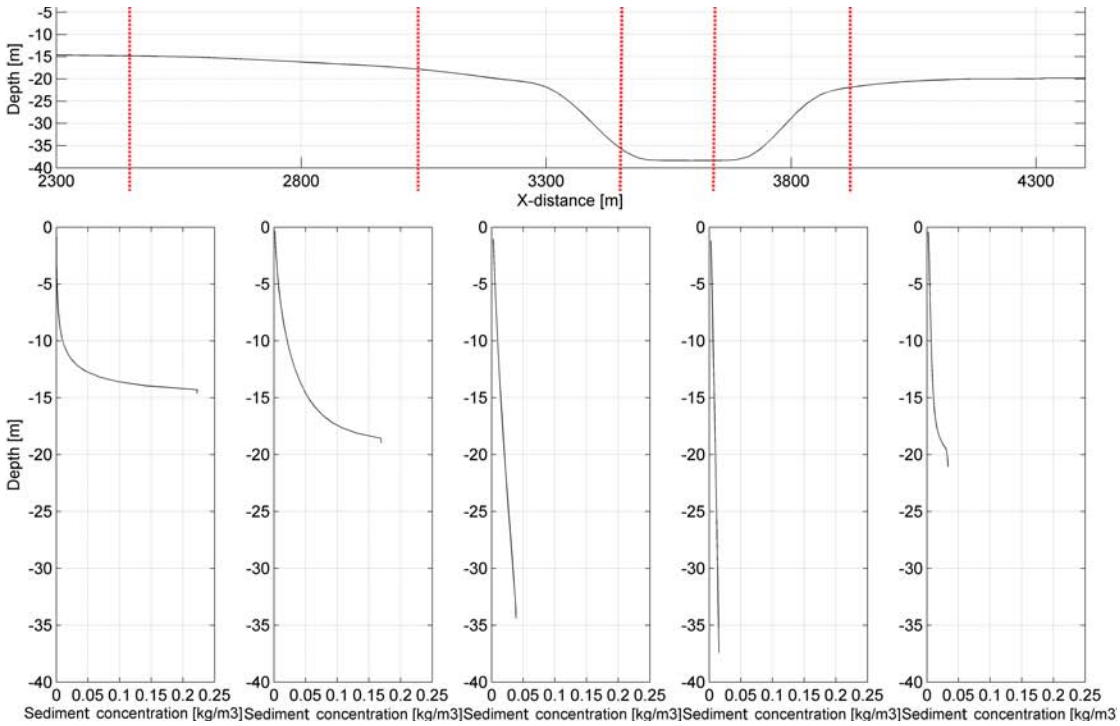

Figure 4.19: Sediment concentrations during maximum flood velocity

During ebb flow the situation is slightly different (figure 4.20). A smaller amount of sediment is transported from the barrier towards the scour hole, this concentration decreases again inside the scour hole. At the upward slope, a lot of sediment is picked up by the higher velocities which are caused by the flow through the barrier. This causes a large increase in the sediment transport from the scour hole to the ebb-tidal delta.

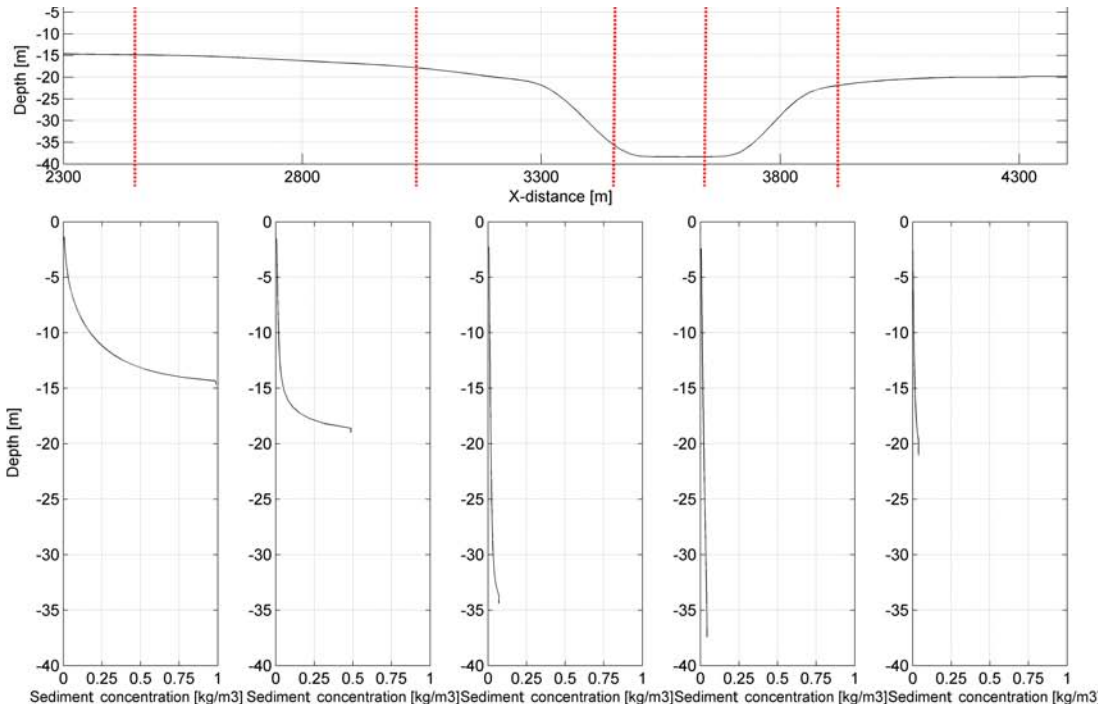

Figure 4.20: Sediment concentrations during maximum ebb velocity (note horizontal scale difference with figure 4.19)

In the model suspended sediment transport is significantly larger than bed-load transport.The variation of this suspended sediment transport in time for three locations near the scour hole is shown in figure 4.21, which show a large dominance in the transport toward the ebb-tidal delta.

During flood a decrease of the suspended transport is observed when the sediment enters the scour hole (black-red-blue line, above x-axis). At the bottom protection behind the scour hole the maximum transport during flood has reduced with 80%, compared to the transport in front of the scour hole.

During ebb less sediment is transported over the barrier (blue line, below x-axis), this transport increases slightly inside the scour hole and at the seaward slope of the scour hole a large amount of sediment is picked up and transported towards the ebb-tidal delta (red to black line, below x-axis).

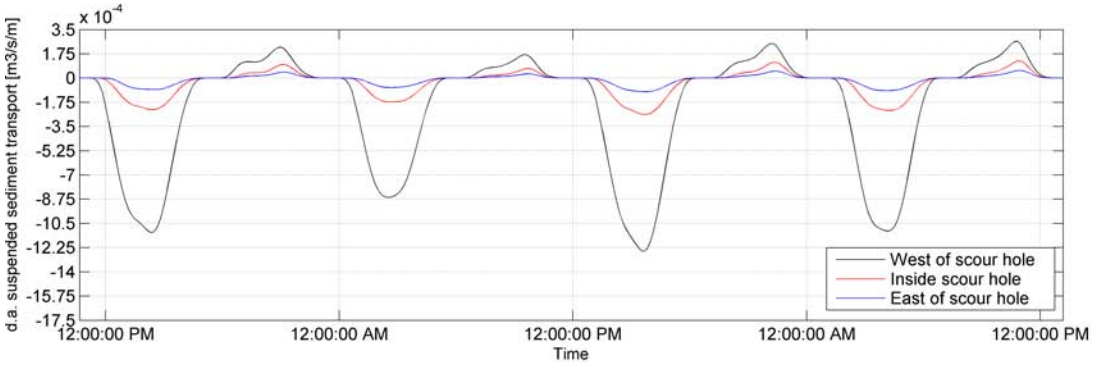

Figure 4.21: Depth-average suspended sediment transport (negative = seaward directed)

4.5.3 Adaptations to scour holes

As an experiment in this section the influence of two different interventions in the model will be discussed to determine their relative influence on the sediment transport. The two adaptations which will be compared to the original situation are:

- filling of the outer scour hole to the level of the bottom protection
- filling of both scour holes to the level of the bottom protection

Figure 4.22 shows the instantaneous transport at different locations near the outer scour hole for the three different scenarios. At these locations the filling of the inward scour hole (red line in 4.23) has minimal influence, therefore only the first scenario is plotted. For this situation during flood an increase of transport can be observed inside the (filled) scour hole, however during ebb the increase at this location is significant larger.

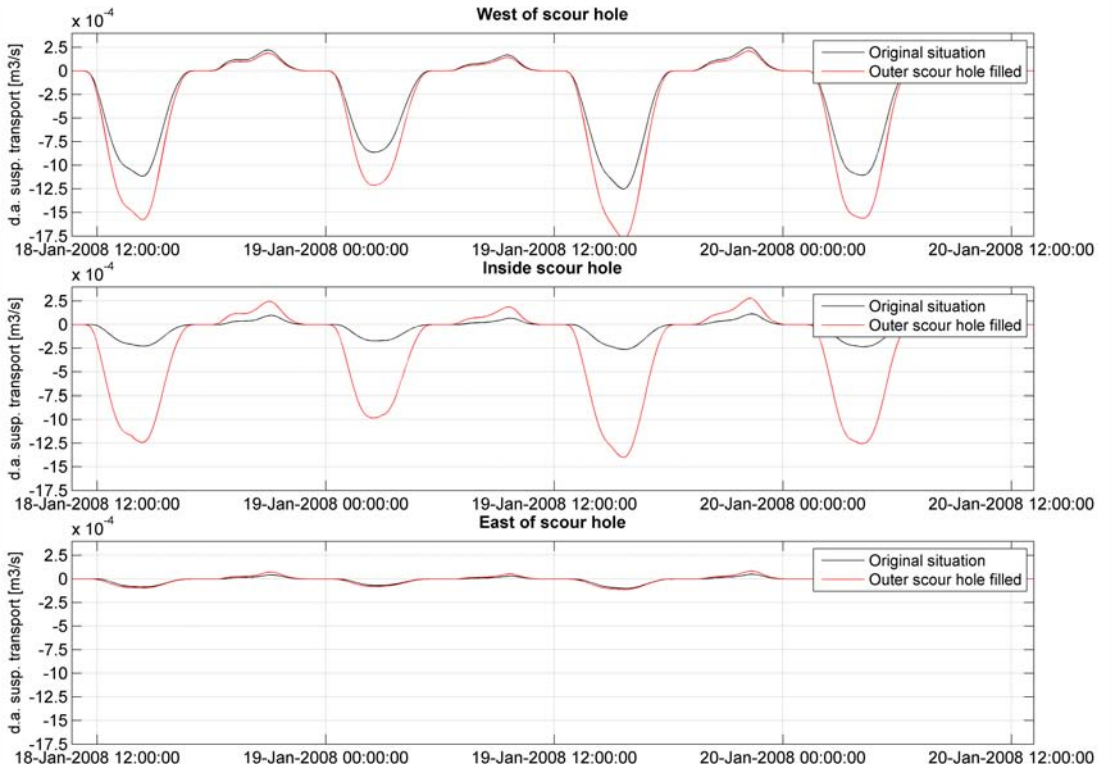

Figure 4.22: Depth-average suspended sediment transport at three points around the outer scour hole (negative = seaward directed)

The results of the mean sediment transport in the three different situations are shown in figure 4.23. For the first scenario (blue line) a significant increase of the mean sediment transport from the (filled) scour hole towards the ebb-tidal delta (negative values) is observed. While at the eastern side of the barrier the model shows a slight increase in the mean transport, however these values remain smaller than zero which means that all mean transports show an exporting trend.

The model shows for the scenario where both scour holes are filled (red line), no influence at the seaward side compared to the first scenario (blue line). At the eastern side of the barrier it shows increased negative values, which means that most of the sand which is used for the filling is transported in seaward direction.

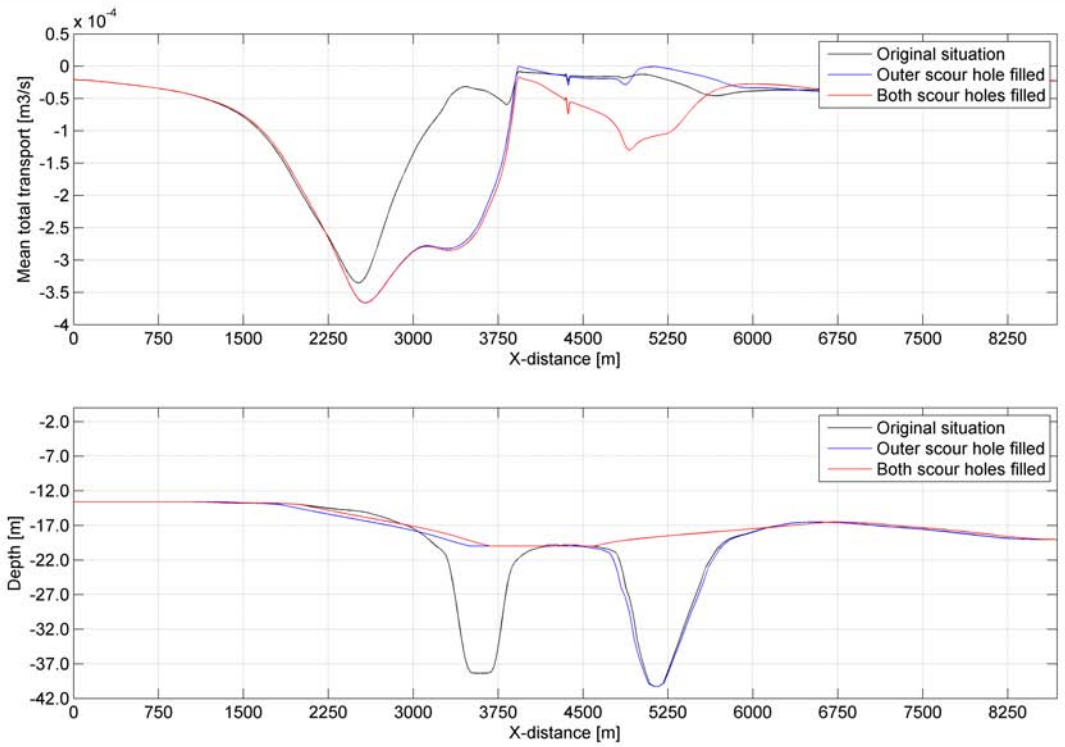

Figure 4.23: Mean total sediment transport (negative = seaward directed) and bed level for 3 scenarios

The fact that the model shows negative (seaward directed) mean sediment transports for all scenarios, can possibly be addressed to the limitation of the model that the side-boundaries are closed and no water can flow in from the shoals. The influence of these horizontal effects which cannot be included in the 2DV model will be discussed in the next chapter.

Chapter 5

2DH Roompot inlet analysis

5.1 Approach

Continuing on the schematized scour hole analysis in chapter 4, in this chapter a more detailed analysis of the Roompot inlet will be given, especially focused on the behavior of sediment near the scour holes. Although the schematized model in the former chapter gives a good impression of the numerical performance of the model and the hydrodynamic behavior of the flow around the scour holes, several effects cannot be taken into account in such a 2DV model. For instance the influence of the ebb- and flood tidal jets, as described in section 3.2, is probably not represented correctly in the schematized model.

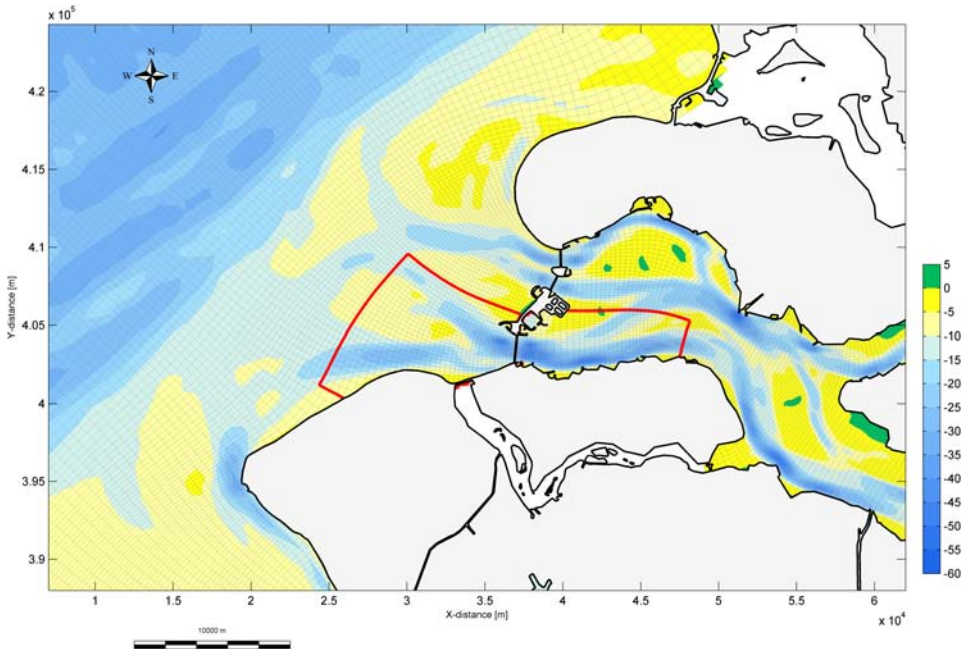

Figure 5.1: The nested Roompot model in the overall KustZuid model

This analysis of the Roompot channel will again be based on the numerical model Delft3D. The Waqua KustZuid model of the south-western Dutch coast is used to generate boundary conditions. The nested Roompot-model in (part of) the KustZuid model is shown in figure 5.1. For calculation-efficiency reasons the model will first be set-up and calibrated with a single depth layer (2DH), after which will be discussed whether a 3-dimensional application can give any significant improvements of the results. After calibration and validation of the hydrodynamics in the model, sediments are added. A uniform sediment diameter is used to investigate the influence of the scour holes on the sediment transport. By comparing the current situation with possible different scenarios, the relative impact of adaptations on the scour holes is quantified.

5.2 Model set-up and model settings

5.2.1 Bathymetry

Because the bathymetric data of the KustZuid model is too coarse to use in a detailed Roompot model, 2008 multi beam echo sounding measurements are used (see figure 5.2). With this system detailed bed level data is generated, with a resolution of about 0.1 meter.

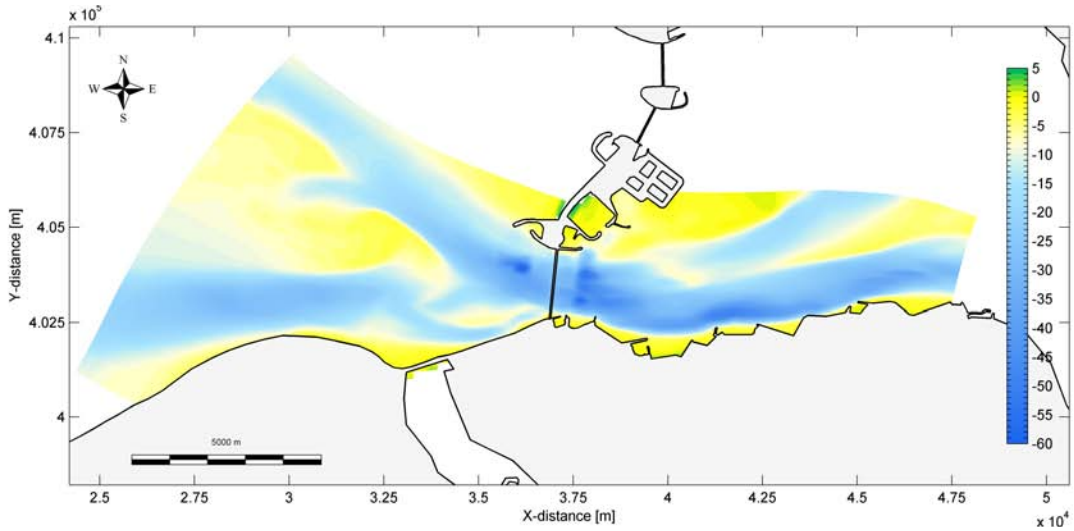

Figure 5.2: Bed level in the Roompot model

At the western side of the model, two channels are approaching the storm surge barrier. In front of the bottom protection the seaward scour hole measures a depth of 57m below mean sea level. From the scour hole a maximum slope of 1:6 reduces the depth to 26m at the border of the bottom protection. At the eastern side of the barrier the bottom protection is constructed at a depth of 30m. The scour hole at this side of the barrier is less deep (55m), but is larger and is smoothly connected to the channel at the southern side of the model. In this channel more places can be observed where deep scouring has taken place near coastal structures.

5.2.2 Grid

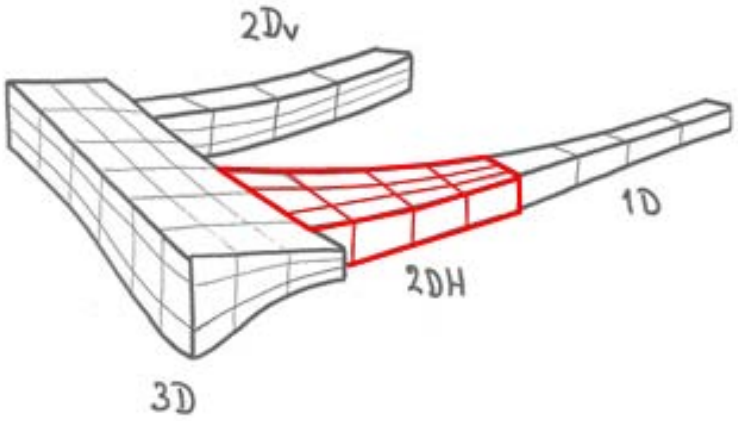

Figure 5.3: The 2DH grid composition in Delft3D

Horizontal grid

The horizontal grid for the model is constructed from the KustZuid model; an area of 10 km west and east of the barrier is cut out of the model. The resulting area has been refined with a factor of three in the x-direction and a factor of four in the y-direction, and smoothened out towards the borders of the model to avoid sudden increases of the grid-size. These operations result in a grid of 76 x 150 grid cells with a minimum size of 25x40m near the barrier and a maximum size of 400x500 m at the western- and eastern border.

Vertical grid

For this thesis the Roompot model is constructed with a single depth layer. This can be used to analyze the horizontal flow patterns, depth-average velocities, bed-shear stresses and sediment transport patterns. Due to the difficulties of σ-layers in combination with steep bottom topography, sediment analysis of the area are made with a single-layered 2DH model. For a more detailed analysis of vertical processes inside a scour hole, the model can be extended with multiple vertical layers in the future. However, for this step first more attention must be paid on the recommendations regarding the z-layered model in combination with sediment transport, which are given in section 6.2.

5.2.3 Boundary conditions

A combination of water-levels and flow-velocities at the seaward side of the barrier is used as boundary conditions. This results in realistic flow patterns on the intertidal flats at the northern side of the channel and the water levels at the open-sea boundary. On the landward side of the storm surge barrier two flow-velocity boundaries are imposed, one at the eastward side of the main channel and one boundary across the smaller channel which is entering the domain from north-eastern direction (figure 5.4).

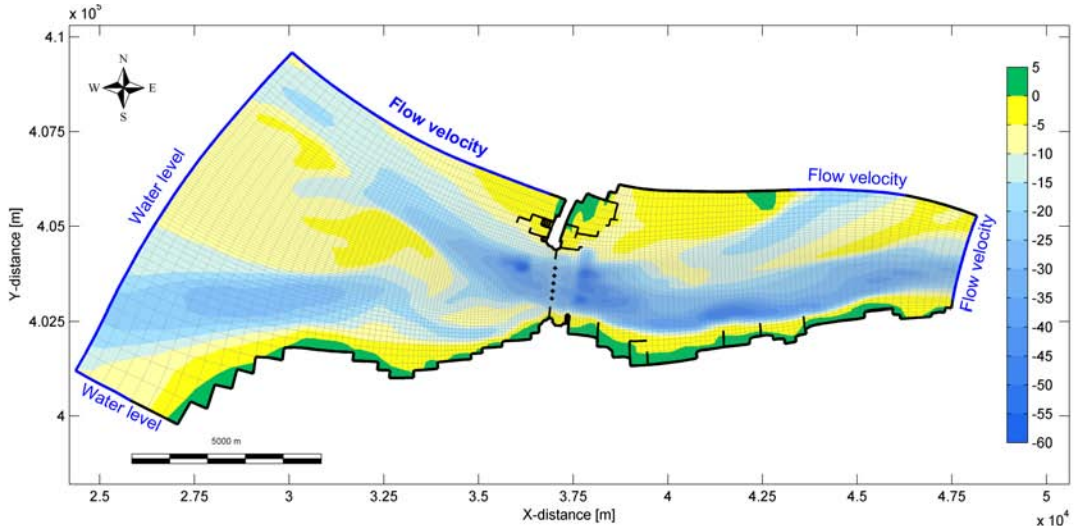

Figure 5.4: Open boundaries in the Roompot model

Nesting procedure

To generate a time serie of the water levels and flow velocities at the boundaries from the overall Kustzuid model, the nesting tool of Delft3D is used. The nesting procedure in Delft3D is executed in three steps, using two separate utilities and the Delft3D-FLOW program. The nested boundary conditions are generated by bi-linear interpolation of computational results at monitoring stations of the overall model. The procedure to generate nested boundary conditions consists of 3 steps [WL|Delft-Hydraulics, 2007]:

- Using the tool NESTHD1, a list of monitoring stations in the overall model, needed for the interpolation, is generated. In addition to this, the program generates the nesting administration, i.e. the link between the boundary support points in the nested model and the monitoring stations in the overall model.
- Running the overall model with the list of monitoring stations generated by NESTHD1.
- The actual boundary conditions for the nested model are generated by NESTHD2 using the history file of the overall model and the nest administration.

A time series of a complete spring-neap cycle for all boundaries are generated with above procedure.

5.2.4 Time scale parameters

Section 4.3.5 described the numerical stability and accuracy of a Delft3D model. For the Roompot model the same requirements apply.

$$Cr = \frac{\sqrt{gH}\Delta t}{\Delta x, \Delta y} \leq 10 \tag{5.1}$$

A maximum time step of 6 seconds fulfills this criterion.

5.2.5 Barrier modeling

In the Roompot channel, 32 piers have been placed on the bottom protection. These piers have a width of 5.5 meters and a mutual distance of 45 meters. To overcome an excessive calculation time of the model, not all single piers are modeled separately. Therefore an equivalent percentage of 13.5% of the total open width (1490m) is closed off by 5 dry cells which are equally distributed along the cross-section of the channel. By modeling the barrier this way, it is not necessary to narrow the grid cells near the barrier to the width of a single pier (5.5m), which saves calculation time. For the vertical constriction of the barrier, the sill is included in the bathymetry of the model. The sill depth varies along the inlet, with the deepest point (10m) at the center of the inlet (figure 5.5).

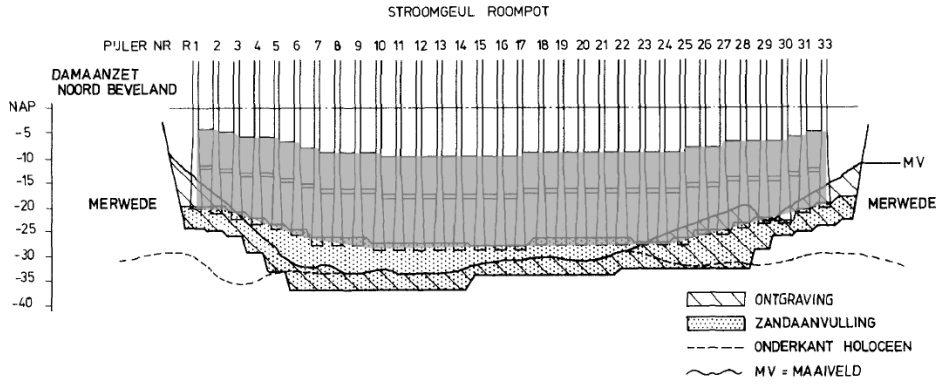

Figure 5.5: Level of the Roompot-sill in the storm surge barrier design [Rijkswaterstaat, 1991b]

Bottom protection

Around the piers of the storm surge barrier, a large bottom protection prevents erosion near the piers (see section 2.3.1). In the numerical model this bottom protection is represented by an area where the Chézy value is decreased to 45, which represents the higher roughness of the block mattresses. Besides the higher bottom roughness, the availability of sediment at the bottom protection is reduced to zero.

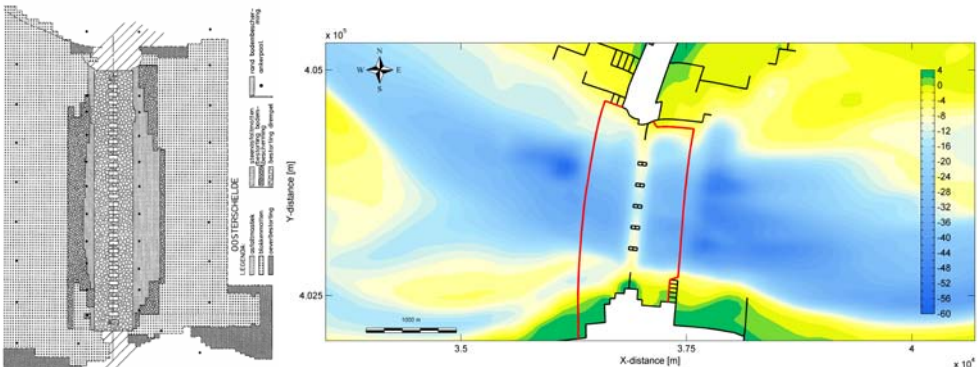

Figure 5.6: Bottom protection at the Roompot inlet in the storm surge barrier design [Rijkswaterstaat, 1991a] (left) and in the model (right)

5.3 Model calibration and validation

Calibration of the model is done by a comparison of water levels and flow velocities at six calibration points in the model. These calibration points are positioned in the major flow channels and in the two major scour holes (figure 5.7). In the calibration points ("cal1" to "cal6"), time series of water levels and flow velocities of the Roompot model are compared with the overall KustZuid model (figure C.5.1, appendix C).

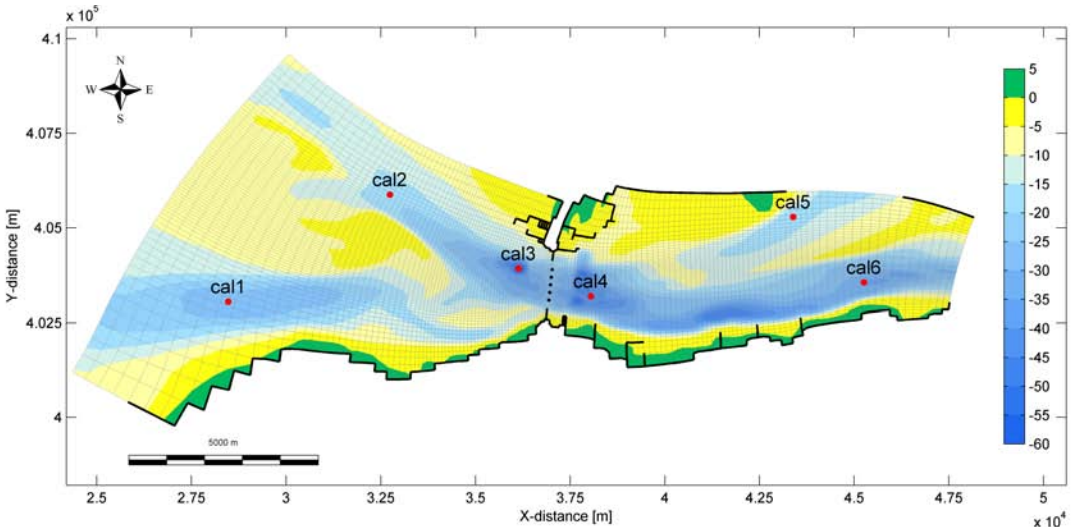

Figure 5.7: Calibration points in the Roompot model

Due to the differences in coarseness of the grids, local differences in hydrodynamic behavior can be expected. Especially locally around structures and rapidly changing bathymetry, a fine grid can capture phenomena that cannot be observed in a coarser model. One obvious difference between the models is the small irregularity of the flow velocity around flood, at the seaward side of the barrier (cal3). Analysis of the flow pattern in the model show that this is caused by a horizontal eddy, which develops after slack water northwest of the barrier (figure 5.8). Variation of the boundary definitions in the model indicate that this eddy is not caused by mismatching boundaries, and probably develops due to a combination of the slack water, bottom geometry and the presence of the barrier. Due to this kind of phenomena, the comparison in the calibration between the two models (figure C.5.1) should not be seen as a 1-on-1 calibration of water levels and flow velocities. However this comparison gives a good indication of the order of magnitude and phase differences of the depth-averaged velocities and water levels. After the comparison in the calibration points, the overall flow patterns in the Roompot model are checked on irregularities and unusual patterns.

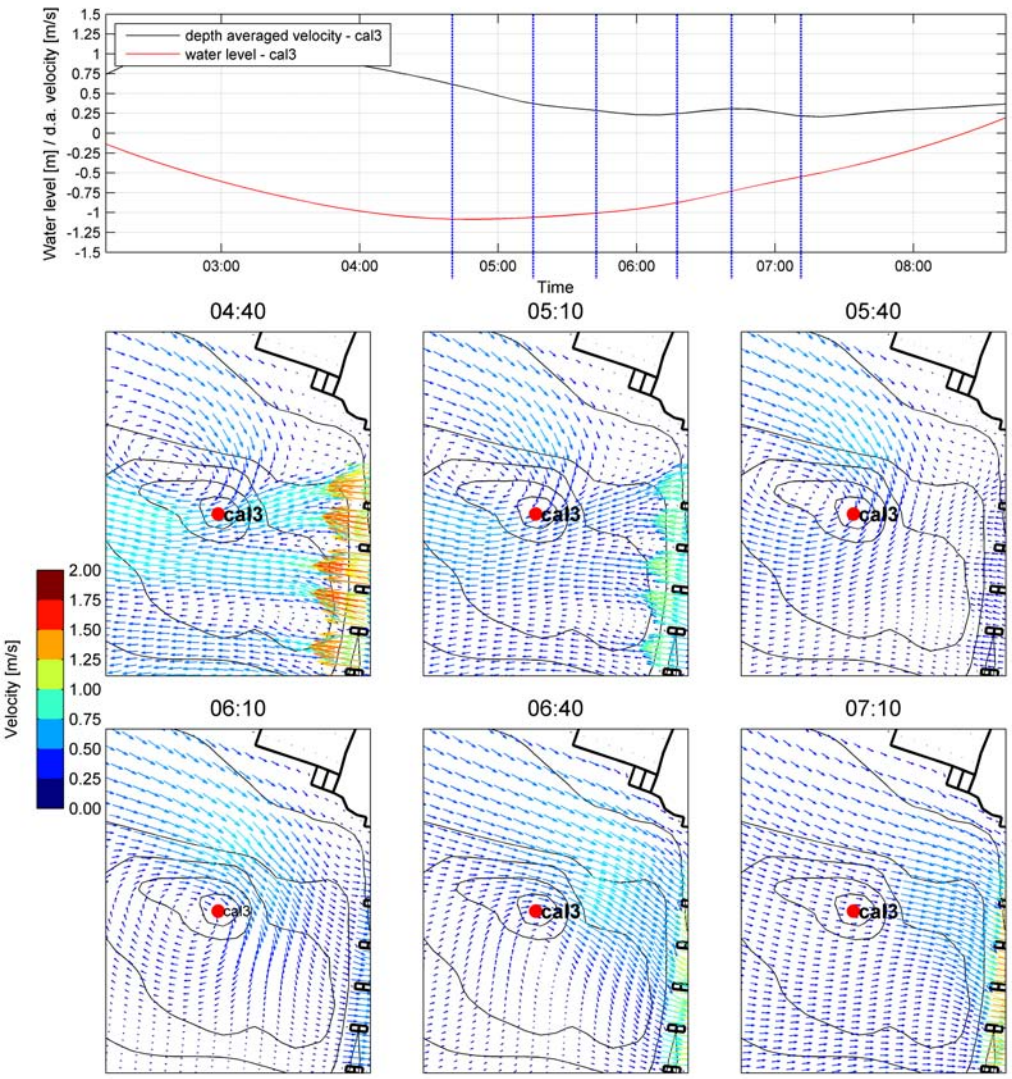

Figure 5.8: Horizontal eddy development near calibration point

5.3.1 Model validation

As there are no useful field-measurements or previous studies that give a detailed representation of the flow around the storm surge barrier, it is difficult to verify the accuracy of this Roompot 2DH model.

The overall KustZuid model is calibrated with measurements at the North Sea and inside the Eastern Scheldt (appendix B.2). Therefore, the boundary conditions which are extracted from this KustZuid model, at large distance (kilometers) from the barrier, are supposed to give an accurate representation of the real hydrodynamic conditions. With these boundary conditions and accurate bottom geometry measurements, particularly the representation of the storm surge barrier is a sensitive 'parameter' which can influence the flow behavior significantly. To optimize

the reliability of the model, the characteristics of the real barrier are modeled as accurate as possible in both the KustZuid and the Roompot model. The characteristics of the barrier in the real situation and the two models are shown in the next table.

	Real situation	KustZuid model	Roompot model
Total width [m]	1369	1484	1467
Piers [#]	32	1	5
Single pier width [m]	5.5	134	33
Effective flow width [m]	1293	1350	1302
Average flow depth [m]	8.56	8.36	8.49
Cross-sectional area below NAP [m^2]	11068	11286	11054

Table 5.1: Characteristics of the storm surge barrier

With the accurate boundary conditions, bottom geometry and these barrier characteristics, the modeling area is reproduced adequately in the Delft3D model. However, it is uncertain if the numerical model capacities are accurate enough to give locally sufficiently reliable results. The main uncertainty in this 2DH model is the representation of the flow near very steep bottom geometry where non-hydrostatic effects might play an important role. The representation of small scale turbulent flow caused by the bottom protection might also not be accurate enough. By taking the influence of these uncertain factors into account during the analysis of the results, conclusions can still be drawn on specific parts of the research.

Because this thesis only describes the influence of the scour holes and not the exact sediment transport in the vicinity of the barrier-sill, the exact representation of the bottom protection is not a limitation for good results. Even without taking the exact influence of the bottom protection into account, the sediment transport patterns around the scour holes can be analyzed. This is done by determining transports from the scour hole at the border of the bottom protection, in the direction of the barrier. Hereby the behavior of sediments between the border of the bottom protection and the sill is not of significant importance for the results. The same applies for the non-hydrostatic effects near the barrier-sill. In chapter 4 it was shown that the non-hydrostatic effects of the sill do not reach the scour holes. The influence of non-hydrostatic effects in the scour holes itself however, might not be neglected. Possible overestimation of bed shear stresses at the bottom of the scour holes results in higher erosion and lower sedimentation rates at these places. Therefore this limitation of the 2DH model should be kept in mind when analyzing the results. For the scenario-analysis of the scour holes, these uncertainties are not directly relevant as the steep slopes are not present (scour hole is filled up).

The most important assumptions and limitations of the model are listed below:

- No waves are included in the model; this might give an underestimation of the transport towards the Eastern Scheldt.
- A single (uniform) grain diameter is used.
- No bathymetry updating; this means that yearly transports are based on the actual bathymetry.
- Depth-average modeling; local non-hydrostatic effects near the barrier or scour hole might

not be represented correctly.

- Turbulence caused by the bottom protection cause uncertainties in the sediment transport on the bottom protection.

Overall it is expected that the 2DH model will especially give a good representation of the horizontal flows and transports, and when keeping the above mentioned limitations in mind, well-founded conclusions can be drawn on the important processes in this area.

5.3.2 Model parameters

Simulation start time	03-01-2008 00:05:00
Simulation stop time	01-02-2008 16:30:00
Horizontal grid cells in m-direction	76
Horizontal grid cells in n-direction	150
Time step	6 sec
Gravitational acceleration	9.813 m s^{-2}
Water density	1023 kg m^{-3}
Bed roughness (Chézy)	65 $m^{1/2}s^{-1}$
Bed roughness bottom protection (Chézy)	45 $m^{1/2}s^{-1}$
Background horizontal eddy viscosity	0.1 m^2s^{-1}
Background horizontal eddy diffusivity	0.5 m^2s^{-1}
Sand density	2650 kg m^{-3}
Dry bed density	1600 kg m^{-3}
Median diameter (D_{50})	200 μm
Barrier friction coefficient of the quadratic friction [-]	2.3
Horizontal large eddy simulation(HLES)	activated

Table 5.2: 2DH Roompot model parameters

Default values for the gravitational acceleration, water density and sediment characteristics have been used in the model. Especially varying the sediment characteristics can influence the model outcomes, therefore this will be recommended for further research (see section 6.2). For the bed roughness a large Chézy value is used at the sandy bottom and at the bottom protection this value has been decreased to represent the higher bed roughness at this location. The values are based on own insight, because no field measurements are available. Small background values for horizontal eddy viscosity and diffusivity are used as the exact values for these parameters are calculated by the HLES module in Delft3D. For the quadratic friction coefficient of the barrier structure, the same value is applied as the friction coefficient that has been used as a calibration parameter in the KustZuid model.

5.4 Sediment transport analysis

For the analysis on the behavior of sediment in the Roompot area, the sediment module of Delft3D is used. For the model a 'virtual' sediment layer thickness on the bottom is prescribed. From this layer, sediment can be picked up when the critical flow velocity is reached. Although erosion and sedimentation of this layer can take place, the bathymetry of the model is not updated. This means that the flow is not influenced by bottom changes.

The sediment layer has a uniform thickness of 5m in the model. Only at the location of the bottom protection of the storm surge barrier, there is no sediment available and a layer thickness of 0m is prescribed. At the open inflow boundaries of the model, an equilibrium sediment concentration is defined. Above settings will result in sediment transports that are likely to be overestimating the real sediment transports in the area. In reality the availability of sediment at the boundaries is fluctuating in time and depending on the supply of sediment from the North Sea and Eastern Scheldt. In the model there is always as much sediment available as can be transported by the flow. This means that the resulting sediment transports are based on the maximum transport capacities of the flow.

Results of the model show a relative large variation of the sediment transport over a single month (figure 5.9). To make a reliable quantification of the sediment transports in the model, two tidal cycles (approximately one month) are calculated during every model run. Multiplying cumulative transports by 12 gives a good approximation of yearly transports in the model. However, it should be noted that these resulting yearly transports are based on instantaneous transport in the model. Because the bathymetry in the model is not updated during the calculation, variation of the transport capacity in time due to erosion or sedimentation is not included.

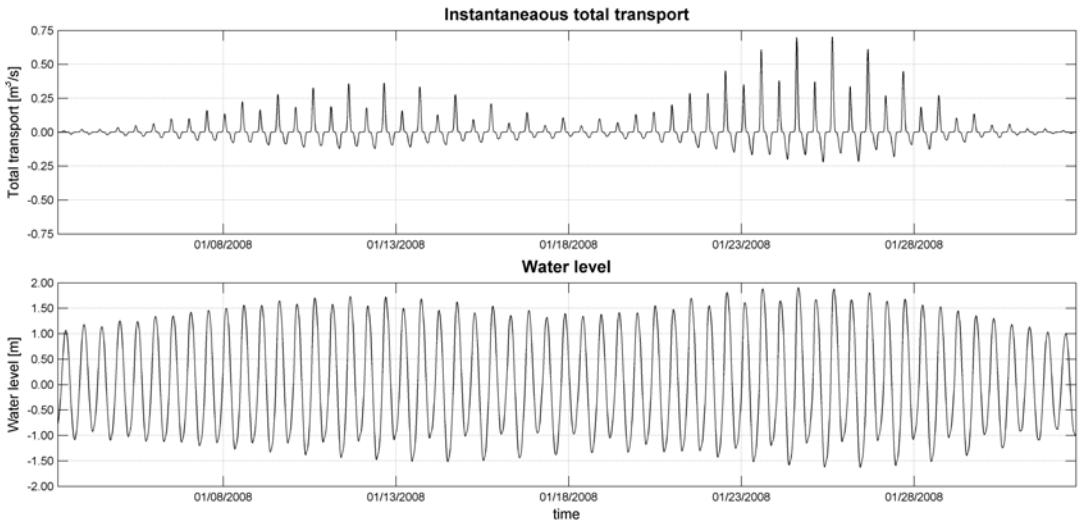

Figure 5.9: Monthly variation of sediment transport (negative values indicate seaward directed transports) through an arbitrary cross-section, 2.5km west of the storm surge barrier

5.4.1 Transport patterns

The yearly net transports are based on the single-month cumulative transport through cross-sections in the model. Interpretation of the transport rates in the model results in the net sediment transport patterns which are shown in figure 5.10. Large transports are entering the model through the south-western channel and from the shoal in the west. Sediment rates with the same order of magnitude are also transported trough the northern channel, in north-western direction. At the basin-side of the storm surge barrier the transports are significantly smaller compared to the seaward side of the barrier. Exact results of the net yearly transports in the model are shown in figure C.5.2a.

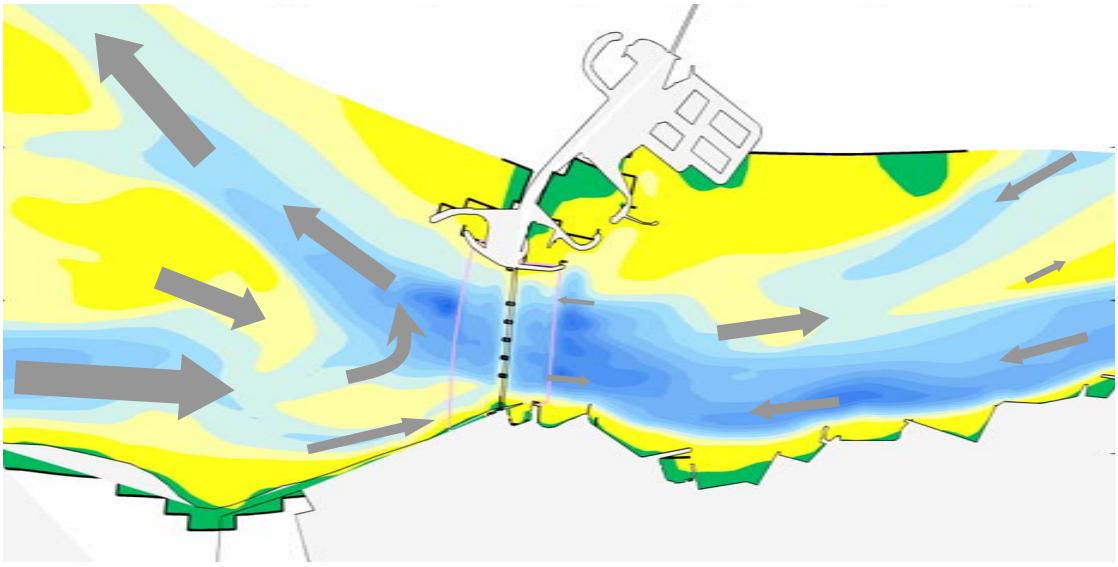

Figure 5.10: Interpretation of overall net transports in Roompot model

Huisman and Luijendijk [2008] studied the morphology around the storm surge barrier, based on a different(coarser) morphological model. From the model results they interpreted a net transport from the south-west (channels north of Walcheren) to the Roompot, from where it is expected to be transported to the north-west. This is the same pattern as can be seen in the model results described in this chapter, and the relative order of magnitude between the different channels in the two models correspondent relatively well. The absolute values in this Roompot model are a factor 4-5 smaller than in the results of Huisman and Luijendijk [2008]. This can partly be ascribed to the waves which are included in their model and not in this Delft3D model. Results of both models are shown in figure 5.11 and 5.12. No other detailed studies on this part of the Eastern Scheldt entrance were found in literature.

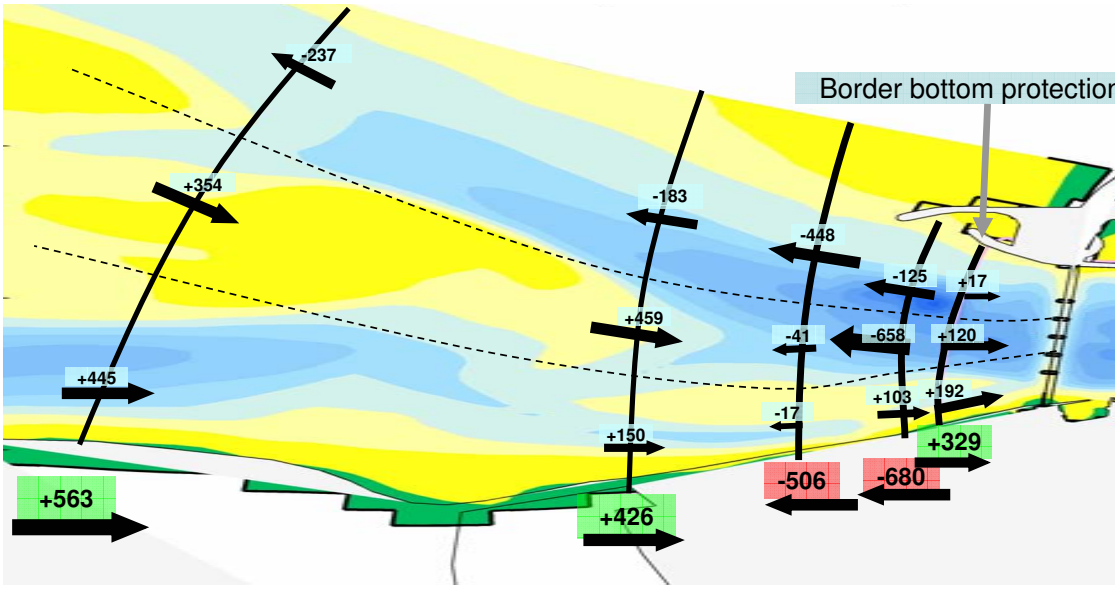

Figure 5.11: Net yearly transports ($\cdot 10^3 m^3 year^{-1}$) at western side of barrier

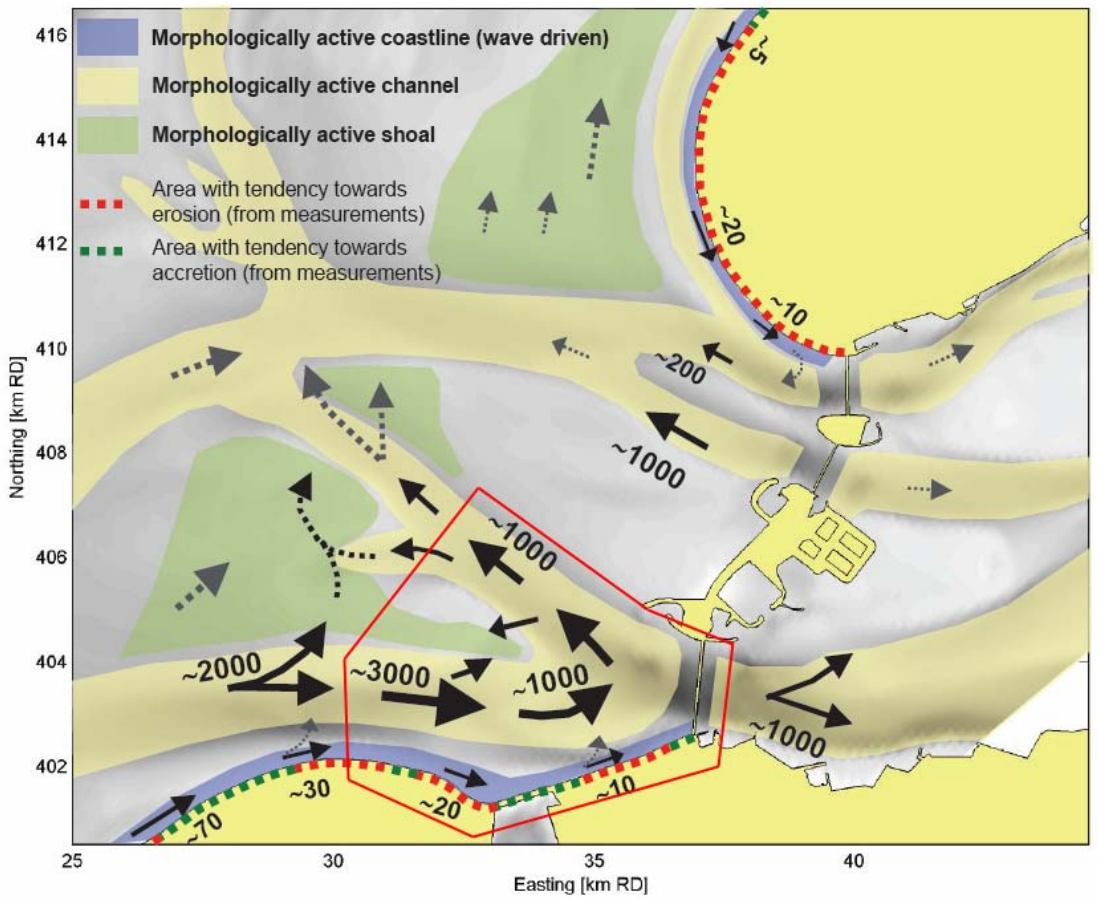

Figure 5.12: Yearly transports ($\cdot 10^3 m^3 year^{-1}$) according to Huisman and Luijendijk [2008]

For a more detailed view of the net transport patterns around the seaward scour hole in the Roompot inlet, a large number of cross-sections is defined between the large shoal at the western side and the storm surge barrier. In the top panel of figure 5.13 the position of the boundary cross-sections is given (red lines), in between them 19 cross-sections are defined, which are all divided in a northern, center and southern part. In the lower panel of this figure the magnitude of the yearly net sediment transport is given for these cross-sections, where negative values indicate seaward transports and positive values transports towards the storm surge barrier.

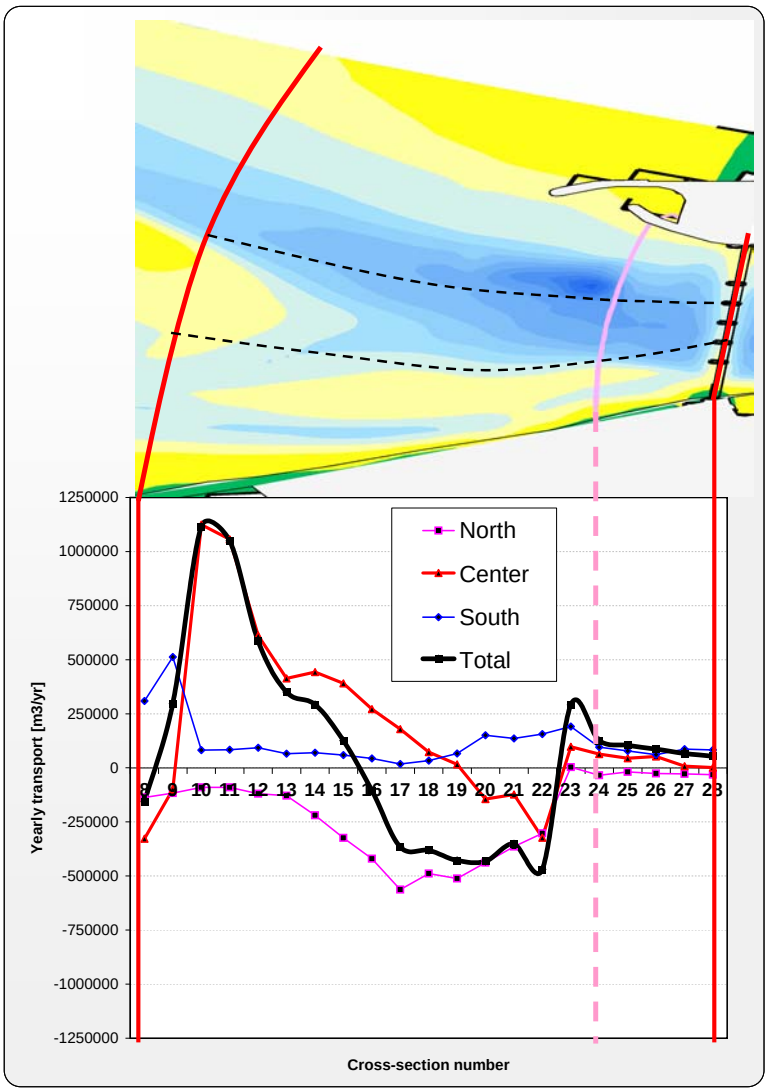

Figure 5.13: Net yearly sediment transport through cross-sections (negative values indicate seaward directed transports)

Figure 5.13 results in the following observations:

- Large net import at the western side of the model, mainly caused by transport over the shoal in the center (red line).
- A switch from import to export of the cumulative transport over the whole cross-section is

observed between cross-section 15 and 16.

- Near the scour hole, the center and northern part mainly contribute to seaward directed net transport of the total cross-section.
- The southern side of the model show barrier-directed transport over the whole length (blue line).
- The northern side of the model show ebb-tidal delta directed transport over the whole length (purple line).
- Over the bottom protection, a tendency towards Eastern Scheldt directed transport is observed at the southern and central side of the inlet. The net transports at the northern side and center over the bottom protection are very small compared to the other transports.

The derivative of the graph gives an indication for an erosion or sedimentation tendency:

- Large negative derivative between cross-section 11 and 16, which indicates a sedimentation trend in this part of the model.
- Large positive derivative between cross-section 22 and 23, which indicates an erosive trend in the scour hole.

Taking a closer look inside the scour hole at the seaward side of the storm surge barrier, the significant ebb-dominance of the flow velocities as described in section 3.2 is also represented in the model. This is also translated to the bed-shear stresses at the bottom of the scour hole. Time series of water level and bed-shear stresses (figure 5.14) show significant larger bed-shear-stresses during ebb- than during flood-flow, this explains the erosive trend as described in the last section and the dominance of seaward directed transports at this location.

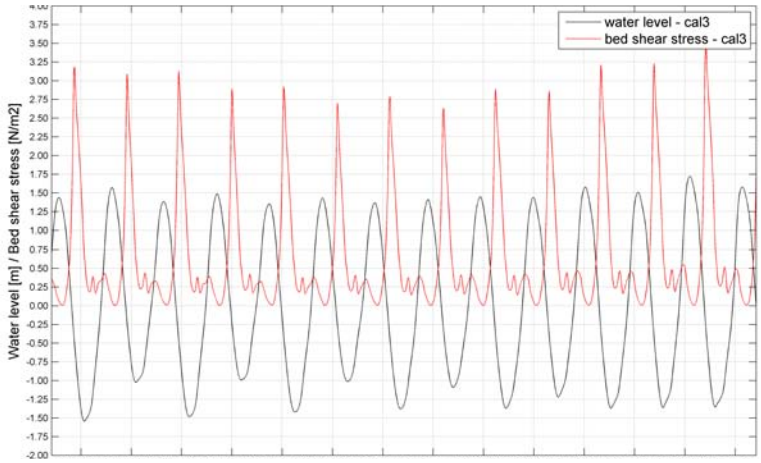

Figure 5.14: Ebb-dominance of bed shear stress in point 'cal3' (see figure 5.7) at deepest point in the seaward scour hole

5.5 Scenario analysis

In this section three different scenarios are discussed which might have a positive effect on the sediment transport towards the Eastern Scheldt. First an analysis on 2 scenarios with adaptations to the seaward scour hole will be made, after which one adaptation to the landward scour hole will be discussed.

5.5.1 Adaptations to the seaward scour hole

With the model results of the sediment transport in the actual situation in mind, two different scenarios are modeled and compared with the results in section 5.4. As filling of the seaward scour hole is considered as a possible solution to increase the sediment transport into the Eastern Scheldt, two variations on this solution are compared with the actual situation (figure 5.15):

- Filling the seaward scour hole to the depth of the bottom protection (-26m MSL)
- Filling the seaward scour hole to the depth of the bottom protection (-26m MSL) and extend the bottom protection over the scour hole

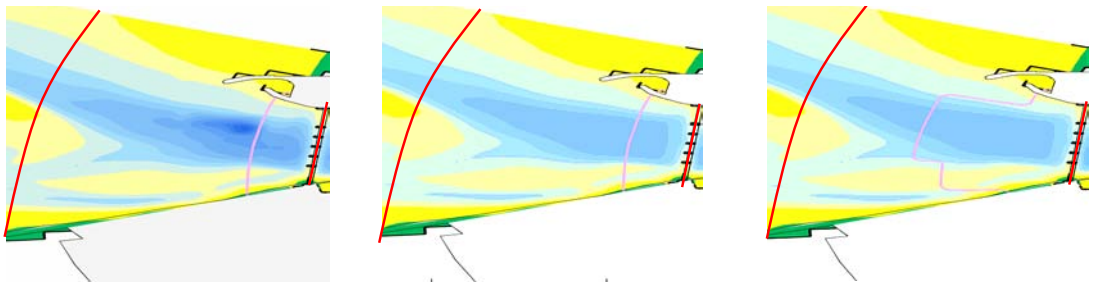

Figure 5.15: Actual situation(left), Filling the landward scour hole(center) and filling+protecting the landward scour hole (right)

The above mentioned two adaptations are extreme human interventions regarding the amount of sand ($13 \cdot 10^6\ m^3$) and extension size of bottom protection ($2.5 \cdot 10^6\ m^2$) that is applied. However, with these scenarios the 'most positive' result can be determined. This is because in the first scenario it is not expected that dumping a smaller amount of sand will result in larger sediment import than completely filling of the scour hole. And in the second scenario the bottom protection is so large that the scouring is reduced significantly due to the much smaller local flow velocities at the border of the bottom protection. With the results of these scenarios, a conclusion can be drawn whether further detailed research on these adaptations is valuable.

Filling the scour hole (figure 5.17)

Whereas in the actual situation (figure 5.16) the net transport at the second cross-section is directed towards the storm surge barrier, this trend changes to a large transport in the direction of the ebb delta when the scour hole is filled with sand (from +426 to -1194 $\cdot 10^3 m^3 year^{-1}$). At

the third cross-section (located at the border of the bottom protection), an increase of sediment transport towards the barrier is observed (from 329 to 875 $\cdot 10^3 m^3 year^{-1}$). At the eastern bottom protection of the storm surge barrier, the influence of the adaptation is visible too. In the actual situation a transport towards the barrier is present. But due to the adaptation this changes to a net transport towards the Eastern Scheldt (from -89 to +213 $\cdot 10^3 m^3 year^{-1}$).

Filling and protecting the scour hole (figure 5.18)

For the situation with the extended bottom protection the changes with respect to the actual situation are smaller. Again a net exporting trend at the second cross-section is observed, however this is smaller compared to the unprotected scenario (from +426 to -454 $\cdot 10^3 m^3 year^{-1}$), due to the smaller amount of sand that is available for transport. At the border of the (original) bottom protection, a decrease instead of an increase of the net import is observed, which changes again behind the barrier where the net export changes to a net import.

In the next table the influence of the two scenarios directly east and west of the scour hole is given in absolute numbers and the relative change with respect to the actual situation.

	Actual situation	Scenario 1		Scenario 2	
Cross-section 1	+563	+569	+1%	+560	-1%
Cross-section 2	+426	-1194	-380%	-454	-207%
Cross-section 3	+329	+857	+160%	+275	-16%
Cross-section 4	-89	+213	+339%	+17	+119%
Cross-section 5	+161	+155	-4%	+163	+1%
Cross-section 6	-12	-12	0%	-12	0%

Table 5.3: Comparison of absolute and relative net yearly transports for the two scenarios [$\cdot 10^3 m^3 year^{-1}$]

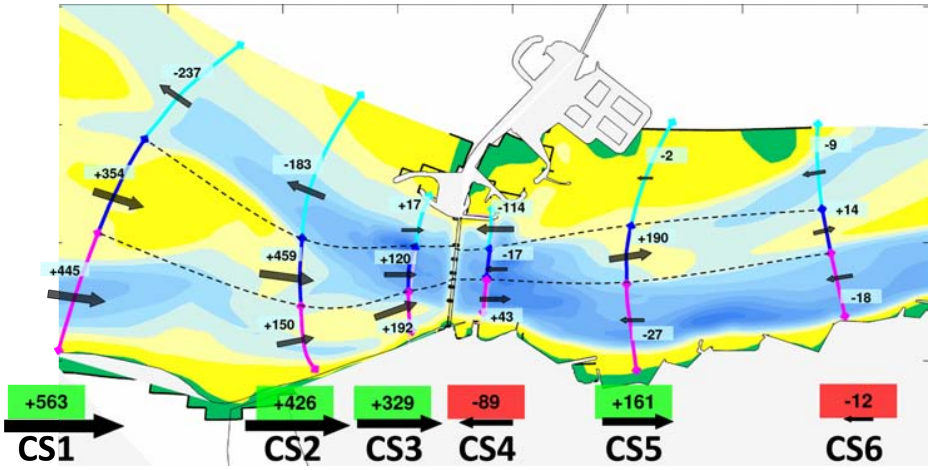

Figure 5.16: Net yearly transports in *actual situation* $[10^3 m^3 year^{-1}]$

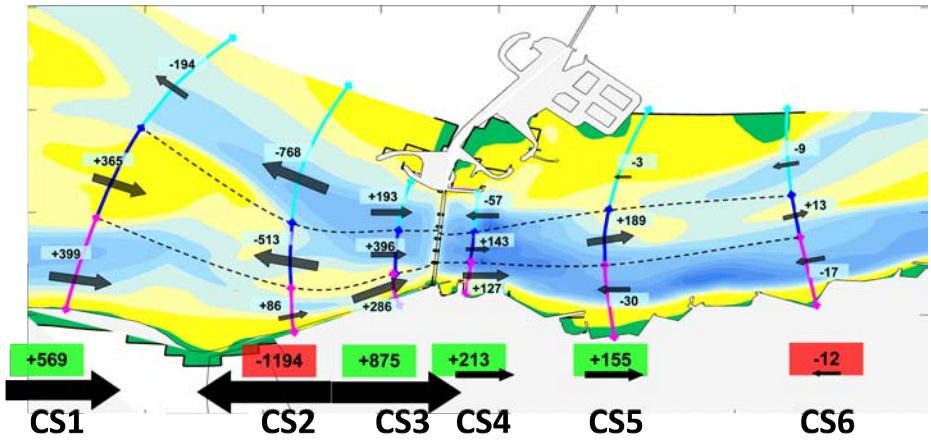

Figure 5.17: Net yearly transports for *filled scour hole* $[10^3 m^3 year^{-1}]$

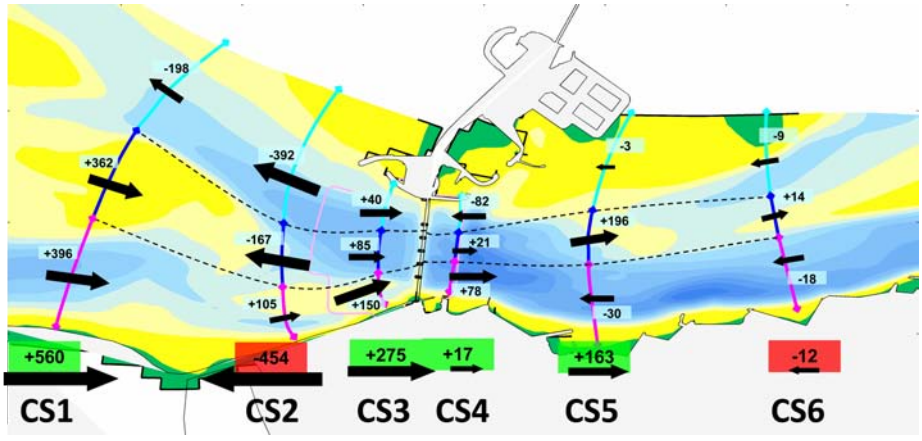

Figure 5.18: Net yearly transports for *filled and protected scour hole* $[10^3 m^3 year^{-1}]$

For a more detailed analysis on the scenarios, the same detailed cross-sectional diversion as used in section 5.4.1 is used. The above mentioned adaptations are discussed in more detail in the next sections (see also figure B.5.3).

Filling the seaward scour hole

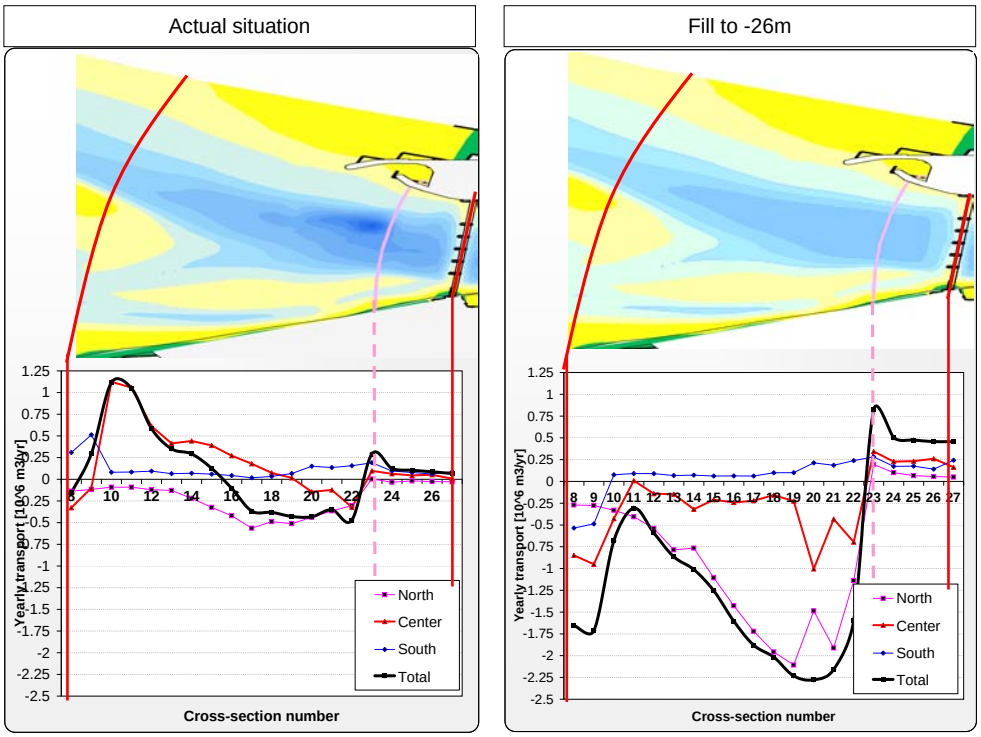

(a) Actual situation (b) Filling the scour hole

Figure 5.19: Longitudinal net sediment transports through cross-sections [$10^6 m^3\ year^{-1}$], negative values indicate seaward directed transports

In the scenario where the scour hole is only filled-up with sand and not protected, a lot of sand will be eroded behind the bottom protection. In fact this situation is the same as in 1986, when the storm surge barrier was just finished and no large scouring had taken place. The main question in this scenario is where the dumped sediment is transported to: will it be transported towards the storm surge barrier (and Eastern Scheldt) or towards the ebb tidal delta and further to the North sea?

Figure 5.19b shows that the negative (ebb delta directed) net transports increase with a factor 4.8 (from -0.47 to 2.27 $10^6 m^3\ year^{-1}$) at the west side of the scour hole. The positive transports from the shoal near cross-section 8 to 14, are counteracted by the large net transports which take place from the filled scour hole towards the ebb delta. Zooming in at the locations where these transports take place results in main export through the northern side of the model, while the net importing trend at the center section (red line) has turned into an exporting trend. No significant changes at the southern side of the model are observed; in the actual situation and

the scenario with the filled scour hole small transport towards the barrier takes place.

From the border of the bottom protection and eastward, small increase over the whole cross-section can be seen. Although no conclusions can be drawn on exact transport over the bottom protection (section 5.3.1), the transports just behind the transition from sand to bottom protection are trustworthy. At this point (cross-section 23) an increase in sediment transport with a factor 2.8 (from 0.29 to 0.82 $10^6 m^3\ year^{-1}$) over the total cross-section is observed.

Filling and protecting the seaward scour hole

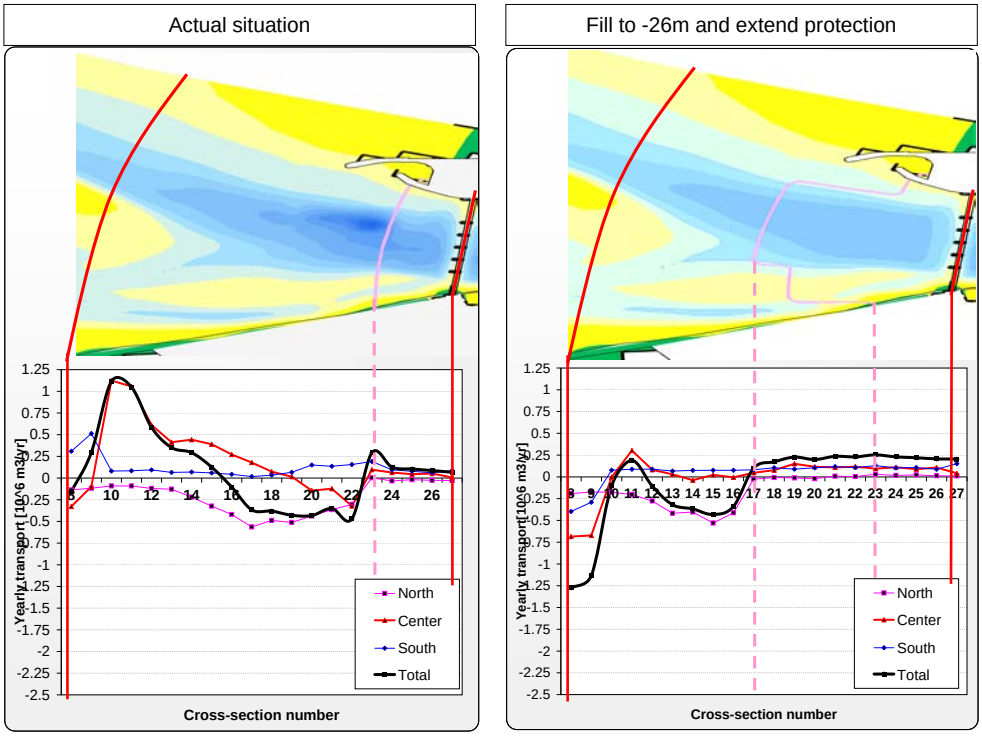

(a) Actual situation

(b) Filling and protecting the scour hole

Figure 5.20: Longitudinal net sediment transports through cross-sections $[10^6 m^3\ year^{-1}]$, negative values indicate seaward directed transports

The scenario where the seaward scour hole is not only filled up, but also partially protected against erosion, shows a less extreme exporting trend. Especially less erosion takes place behind the extended bottom protection, compared to the unprotected scour hole. However, still an exporting trend between cross-section 12 and 17 is seen in figure 5.20b. At the most western cross-section in this model, the increase of sediment export is clearly visible. This has been increased with a factor 8 (from 0.15 to 1.27 $10^6 m^3\ year^{-1}$). Compared to the actual situation, the sediment transport in the direction of the storm surge barrier is increased with a factor 2 (from 0.12 to 0.23 $10^6 m^3\ year^{-1}$). Again only the center and northern part of the model are dominated by a net transport directed to the ebb delta. The most southern channel shows no significant changes and transports sediment in the direction of the storm surge barrier.

5.5.2 Adaptations to the landward scour hole

After analysis of the adaptations to the seaward scour hole, one scenario where the landward(eastern) scour hole is filled with sand will be discussed. The idea behind this scenario is that sediment is nourished directly inside the Eastern Scheldt by means of a permanent pipeline from the seaside of the barrier to the scour hole at the eastern side of the storm surge barrier. Dredging vessels can pump sediment from the seaside of the barrier directly into the Eastern Scheldt, where it will initially fill up the tidal channels and over the longer term will also be beneficial for the flats.

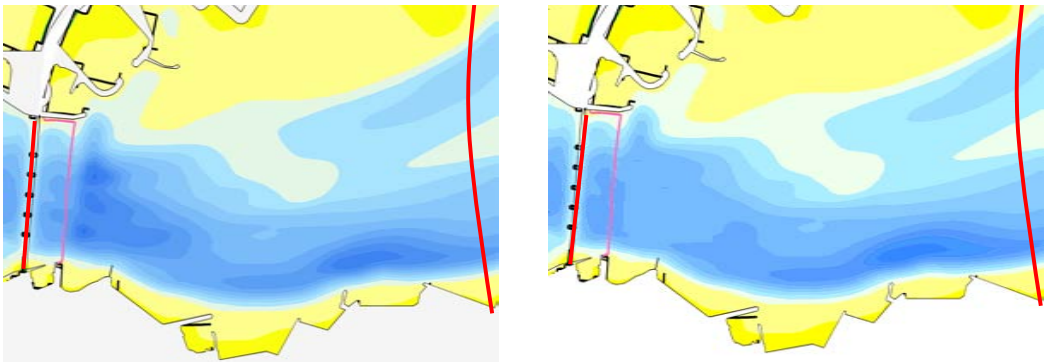

Figure 5.21: Actual situation(left) and filling the seaward scour hole (right)

This scour hole inside the Eastern Scheldt is slightly less deep but much longer compared to the seaward hole. Therefore only the area directly behind the bottom protection is filled with sand. For this scenario again an amount of $13 \cdot 10^6\ m^3$ sand is used to fill the scour hole (figure 5.21).

The results of the net yearly transports in the actual situation and in this scenario are shown in figure 5.22 and 5.23. The most significant differences caused by the filling of the scour hole, are visible at the borders of the bottom protections. At the cross-section just west of the filled scour hole, the adaptation causes an increase of the sediment export compared to the actual situation (from 89 to 530 $10^3 m^3\ year^{-1}$). The net import at the southern side of this cross-section changes to a net export in this scenario. The influence of the sand nourishment can also be seen at the seaward side of the storm surge barrier, at the border of the bottom protection the sediment import is decreased (from 329 to 439 $10^3 m^3\ year^{-1}$) due to the larger transport from the basin towards the ebb-tidal delta. East of the filled scour hole no significant influence of the adaptation is observed (from 161 to 164 $10^3 m^3\ year^{-1}$). Because the cross-section east of the scour hole is situated at a large distance from the intervention, a more detailed analysis on the east side of the storm surge barrier will be made with the same method as used in section 5.4.1.

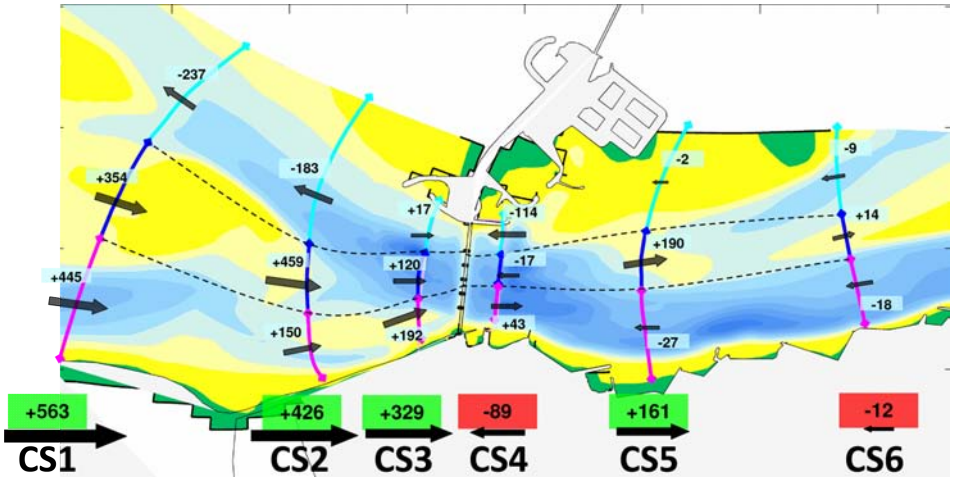

Figure 5.22: Net yearly transports for *actual situation* $[10^3 m^3 year^{-1}]$

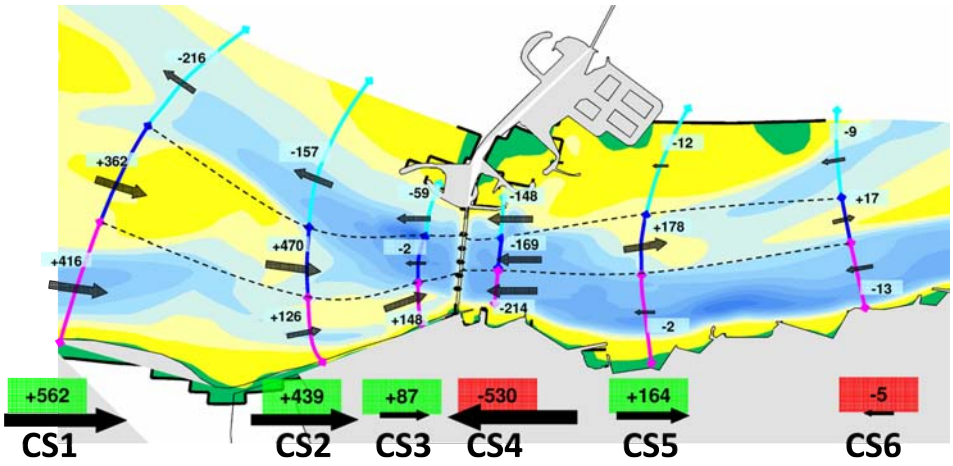

Figure 5.23: Net yearly transports for *filled landward scour hole* $[10^3 m^3 year^{-1}]$

	Actual situation	Scenario 3	
Cross-section 1	+563	+563	0%
Cross-section 2	+426	+439	+3%
Cross-section 3	+329	+87	-74%
Cross-section 4	-89	-530	+495%
Cross-section 5	+161	+164	+2%
Cross-section 6	-12	-5	-58%

Table 5.4: Comparison of absolute and relative net yearly transports for the scenario $[\cdot 10^3 m^3 year^{-1}]$

The area east of the barrier is divided by 25 cross-sections, each used to calculate the net sediment transport at the northern, center, southern side of the cross-section. This results in a more detailed view of the influence of the adaptation, which is shown in figure 5.24

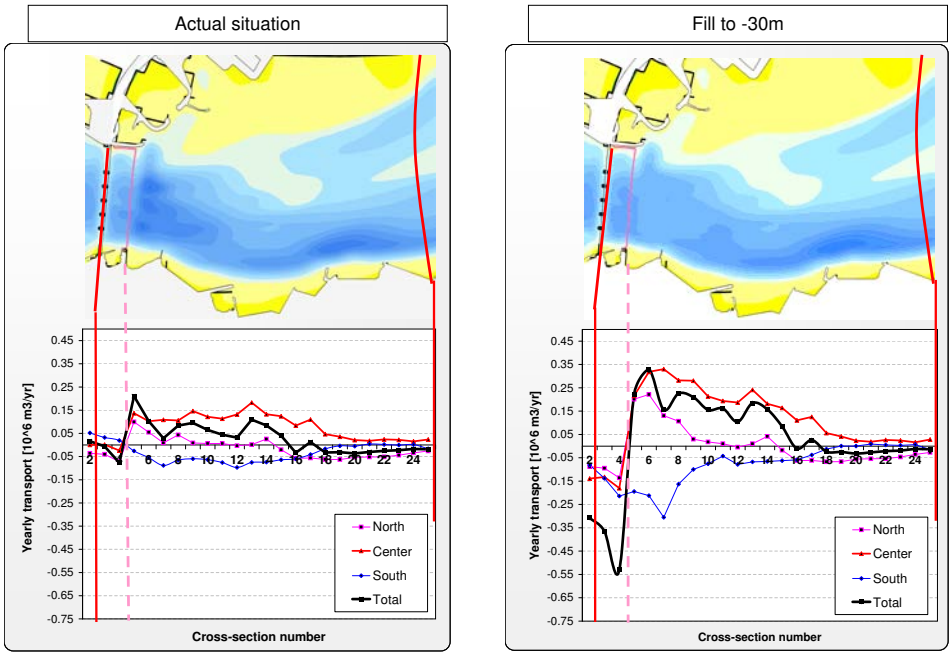

(a) Actual situation (b) Filling the landward scour hole

Figure 5.24: Longitudinal net sediment transports through cross-sections [$10^6 m^3\ year^{-1}$], negative values indicate seaward directed transports

The above figures show an increase of sediment transport from the filled scour hole in the direction of the Eastern Scheldt by a factor 1.5 (from 0.21 to 0.33 $10^6 m^3\ year^{-1}$). The sediment transport from the filled scour hole directed towards the storm surge barrier, increases with a factor 8 (from 0.07 to 0.55 $10^6 m^3\ year^{-1}$). While this flood-dominant area in the current situation shows larger net yearly import than export rates, this has changed due to the filling of the scour hole. After the adaptation, the model shows larger net yearly transports towards the barrier rather than towards the Eastern Scheldt.

Along the individual (northern, center, southern) cross-sections no change in direction of the net transport is observed; the figures mainly show an enlargement of the existing net transports. The southern side of the model shows a significant increase in barrier-directed transport especially in the first part of the basin (between cross-section 5 and 10). Near the deepening of the channel (cross-section 10-20) the model shows positive gradients in the net transports which indicates that probably due to the increasing depth, sedimentation takes place in the channel. Net sediment transports are reduced to zero at this large second scour hole (depth 48m) just in front of the coast.

Chapter 6

Conclusions and recommendations

This study investigates the influence of the scour holes near the Eastern Scheldt storm surge barrier on the sediment transport from the ebb-tidal delta towards the Eastern Scheldt. This primary objective is attained by answering the research questions posed in chapter 1:

1. Obtain more insight in the hydrodynamic and morphodynamic processes that are taking place inside the scour holes.
2. Determine the capabilities of the process-based model Delft3D to reproduce hydrodynamic and morphodynamic behavior around the scour holes correctly.
3. Increase the insight on the influence of scour holes on the sediment transport around the Eastern Scheldt storm surge barrier.
4. Determine the influence of human adaptations to the scour holes near the Eastern Scheldt storm surge barrier on the sediment transport.

After the conclusions, recommendations resulting from this study are presented in section 6.2. As final part of this report, a short personal opinion on this study with respect to the whole 'Eastern Scheldt sand demand' problem is added in section 6.3.

6.1 Conclusions

Research objective 1: Obtain more insight in the hydrodynamic and morphodynamic processes that are taking place inside the scour holes.

By studying literature, existing theories and numerical model simulations more insight is gained on the processes that are taking place in the scour holes near the Eastern Scheldt storm surge barrier:

- No vertical flow recirculation is developing during ebb- or flood-flow inside the scour holes. Theories show that flow separation and reversal is expected for slopes of 1:5 and steeper. Analysis of actual bottom geometry measurements show maximum slopes of 1:8 at the Hammen and Schaar van Roggenplaat inlets. Furthermore, the non-hydrostatic numerical model of the Schaar van Roggenplaat scour hole show no indication that a flow separation takes place. At the Roompot inlet slightly steeper slopes are observed; from the bottom protection towards the deepest point of the scour hole, the slope approaches a value of 1:6. Still no large flow recirculation is expected here either.
- Model results from the 2DH Roompot model show significant larger ebb-velocities than flood-velocities at the bottom of the seaward scour hole. This supports the idea that sediment settles down during flood and is transported towards the ebb-tidal delta during ebb.
- Ebb- and flood jets through the barrier play an important role in the asymmetry of flow velocities near the barrier, and consequently for the direction and magnitude of the net sediment transports around the scour holes. Higher near-bed velocities in the scour holes (during ebb in the seaward scour hole and during flood in the landward scour hole) are mainly induced by this flow asymmetry. No vertical flow recirculation has been observed which can result in higher near-bed velocities.

Research objective 2: Determine the capabilities of the process-based model Delft3D to reproduce hydrodynamic and morphodynamic behavior around the scour holes correctly.

- The schematized 2DV model of the Schaar van Roggenplaat inlet show significant differences in the hydrodynamic behavior for the three applied vertical layer-distributions. The hydrostatic σ-layered model shows significant larger flow velocities at the bottom of the scour hole compared to the hydrostatic and non-hydrostatic Z-layered model.
- Bed-shear stresses are not represented correctly for the hydrostatic and non-hydrostatic Z-layered model, near the scour holes unrealistic irregularities are observed caused by the staircase effect in the bottom boundary layer of Z-layered model.

Research objective 3: Increase the insight in the influence of scour holes on the sediment transport around the Eastern Scheldt storm surge barrier.

By looking at theories and numerical models the sand-trapping function of the scour holes is studied. The idea is that lower velocities during flood than during ebb inside the seaward scour hole cause a blockage for the sediment transport from the ebb-tidal delta to the Eastern Scheldt.

- Sedimentation theory of Van Rijn show a large sediment trapping efficiency and also the 2DV model show a very large decrease in sediment transport capacity along the seaward scour hole in the Schaar van Roggenplaat inlet. This supports the hypothesis that sediment is trapped during flood-flow due to the low transport capacity inside the scour hole.
- The numerical 2DV model of the Schaar van Roggenplaat inlet shows a large ebb-directed sediment transport due to the tidal asymmetry. In this model the exact representation

of the asymmetry due to ebb- and flood-jets through the barrier is not included. This results in an underestimation of the ebb-transport inside the seaward scour hole and an underestimation of the flood-transport inside the landward scour hole.

- In the numerical 2DH model of the Roompot channel, net sediment transport patterns at the seaward side of the bottom protection show an importing trend at the southern side of the channel and an exporting trend at the northern side of the channel. The turning point of these two main transports is located close to the scour hole. This supports the hypothesis that sediment is trapped in the scour hole during flood and transported towards the ebb-tidal delta during ebb.
- At the landward side of the storm surge barrier in the 2DH Roompot model, net sediment transports are significantly smaller. Through the southern channel, net transports are mainly directed towards the barrier, while the center and northern part of the landward scour hole show transports towards the Eastern Scheldt basin.

Research objective 4: Determine the influence of human adaptations to the scour holes near the Eastern Scheldt storm surge barrier on the sediment transport.

To determine possible solutions to decrease the negative influence of the scour holes on the sediment import, three scenarios are examined on their efficiency to increase sediment transport into the Eastern Scheldt.

- The scenario where the seaward scour hole is filled up with sand shows especially an increase in sediment transport towards the ebb-tidal delta rather than an increased sediment transport from the filled scour hole towards the storm surge barrier (net transport ratio westward : eastward = 4.8 : 2.8).
- By filling and protecting the seaward scour hole, the erosive process behind the bottom protection is reduced significantly. Despite the extended protection, erosion at the transition from sand to bottom protection is unavoidable. The erosion of sediment at this place is again mainly transported in the direction of the ebb-tidal delta rather than towards the storm surge barrier (net transport ratio westward : eastward = 8.0 : 2.0).
- Partly filling of the landward scour hole show an increase of net transport in both directions, but especially the barrier-directed transport shows a large increase rather than the net transport in the direction of the basin (net transport ratio westward : eastward = 8.0 : 1.5).

6.2 Recommendations

For further research on the influence of scour holes on the sediment transport through the Eastern Scheldt storm surge barrier, several recommendations are made regarding improvements of this study.

- Field-measurements of flow velocities in the vicinity of the storm surge barrier are necessary to increase the trustworthiness of the numerical model results. With measurements over a full tidal period, the flow behavior in the numerical model can be validated.

- Although this study shows that the hypothesis that sediment is trapped during flood and transported towards the ebb-tidal delta during ebb is conceivable, this can be confirmed by field-measurements. It is advised to measure sediment concentrations and flow velocities near the bottom of a scour hole over a tidal period to determine their variation over time.
- Extend the 2DH numerical model of the Roompot channel to a three-dimensional model with non-hydrostatic vertical Z-layers and a sediment transport module. A three-dimensional model is able to reproduce more accurate hydrodynamic and morphodynamic behavior inside the scour hole and near the sill of the storm surge barrier.
- Include waves in the model of the Roompot inlet. This might result in higher sediment transport rates in the direction of the Eastern Scheldt.
- Include different sediment fractions in the model to determine their influence on the sediment transport rates. Apply very fine sediment fractions (silt) in the model to validate the hypothesis that mainly silt rather than sand is imported to the Eastern Scheldt at this moment ([ten Brinke et al., 1994]).
- Include bathymetric changes in the model to analyze sedimentation and erosion patterns in the area, also a more accurate time-development of the erosion after a sand-nourishment can be made.
- Further research on the exact influence of the bottom protection and barrier-sill on the sediment transport through the barrier. No indication has been found that the barrier-sill poses a blockage for the sediment transport. However uncertainties in the model have to be studied to confirm this.
- Further research on the net sediment transports in a larger area around the storm surge barrier. The current 2DH study especially focused on the horizontal transport patterns near the Roompot inlet. However, there might be larger net transport patterns which interconnect with the other two inlet channels. Also scenarios where sand is nourished further away from the storm surge barrier, has not been discussed as these interventions are too close to the model-boundaries. Further research should be done on these scenarios.

6.3 Closure

This thesis resulted in more insight and conclusions regarding the influence of the scour holes near the storm surge barrier. It was shown that the sand-trapping function of the seaward scour hole is very likely and that ebb- and flood tidal jets play a very important role in the sediment transport near the storm surge barrier. In the part where different possible solutions are examined on their effectiveness for an increased sediment import, the model shows that for all scenarios, mainly the seaward directed transport is increased by adding extra sand to the system.

When looking at the whole system of the Eastern Scheldt and its ebb-tidal delta, an amount of 400 to 600 million m^3 sand is required to restore the dynamic equilibrium of the basin. The 2DH numerical model which has been discussed in this report shows net transport rates in the order

of 200.000 $m^3 \cdot year^{-1}$ at the basin-side of the barrier. Adaptations to the scour holes result in a maximum increase of these transports in the direction of the basin by a factor 2.8, at the same time increase of the transports in the the ebb-tidal delta direction which are two or three times larger. Therefore the adaptations with the intention to increase the inward transport, seem to be very inefficient. Moreover, the transports in the direction of the basin are such small, compared to the 400 to 600 million m^3, that these have a very small impact on the whole system.

It is expected that within 40 to 90 years most of the intertidal areas in the Eastern Scheldt will have disappeared [van Zanten and Adriaanse, 2008]. Therefore, it can be said that partially restoring the equilibrium by nourishing sand at the entrance of the basin evolves on a much larger timescale than the decrease of the amount of intertidal areas in the basin. Filling of the scour holes alone will not have a short-term significant impact to contribute to preserve the unique ecological values of the Eastern Scheldt; it might only be useful in combination with other measures, such as nourishing and/or protecting the intertidal areas themselves.

The above opinion is based on this first investigation on the subject and there are too many uncertainties in the numerical models to disregard the studied scenarios in future discussions on the sand demand of the Eastern Scheldt. It is advised to continue this research with more advanced models and verify these with field-measurements.

Bibliography

M.D.J.P. Bijvelds. *Numerical modelling of estuarine flow over steep topography.* PhD thesis, Delft University of Technology, March 2001.

H.N.C. Breusers and A.J. Raudkivi. *Scouring, Hydraulic structures design manual.* A.A. Balkema, Rotterdam, 1991.

C. Cleveringa. Morphodynamics of the delta coast: quantitative analysis and phenomenology of the morphological evolution 1964-2004. Final report A1881R1r2, Alkyon, January 2008.

C. de Bok. Long-term morphology of the Eastern Scheldt. Werkdocument RIKZ/2002.108x, Ministerie van Verkeer en Waterstaat, 2002.

EcoShape. EcoShape - Building with Nature information brochure. Technical report, EcoShape Building with Nature, 2008a.

EcoShape. ZW 3.2 Morphodynamic coupling between estuary and outer delft. Work plan, EcoShape Building with Nature, May 2008b.

A.B. Fortunato and A.M. Baptista. Fine sediments in the Oosterschelde tidal basin before and after partial closure. *ET AL., Peters A. (ed), Computational methods in water resources*, 1: 1045–1052, 1994.

F Gerritsen, H. de Jong, and A Langerak. Cross sectional stability of estuary channels in the Netherlands. *ASCE 22nd Int. Conf. Coastal Engineering*, 3:2922–2935, 1990.

A.J.M. Geurts van Kessel. Verlopend tij - Oosterschelde, een veranderend natuurmonument. Rapport RIKZ/2004.028, Ministerie van Verkeer en Waterstaat, December 2004.

A.W. Hesselink, D.C. van Maldegem, K. van den Male, and B. Schouwenaar. Verandering van de morfologie van de Oosterschelde door de aanleg van de stormvloedkering. Werkdocument RIKZ/OS/2003.810x, Ministerie van Verkeer en Waterstaat, 2003.

G.J.C.M. Hoffmans. *Two-dimensional mathematical modelling of local-scour holes.* PhD thesis, Delft University of Technology, June 1992.

G.J.C.M. Hoffmans. A study concerning the influence of the relative turbulence intensity on local-scour holes. Report W-DWW-93-251, Ministerie van Verkeer en Waterstaat, February 1993.

B.J.A. Huisman and A.P. Luijendijk. Sand demand of the Eastern Scheldt, part3: morphology around the barrier. Draft report, Deltares, December 2008.

T.H.G. Jongeling. Zandhonger Oosterschelde - maatregelen ter vergroting van doorstroomcapaciteit en zanddoorvoer stormvloedkering Oosterschelde. Rapport bureaustudie Q4264, WL|delft hydraulics, November 2007.

R.E. Jorissen and F.M. Stroeve. Ontgrondingsprocessen bij de stormvloedkering Oosterschelde. *Land+Water*, 1(7), 1997.

R.E. Jorissen and J.K. Vrijling. Local scour downstream hydraulic constructions. *International Association for Hydraulic Research XXIII congress, Ottawa, Canada*, August 1989.

T. Louters, J.H. van den Berg, and J.P.M. Mulder. Geomorphological Changes of the Oosterschelde Tidal System During and After the Implementation of the Delta Project. *Journal of Coastal Research*, 14(3), 1998.

D.C. Maldegem and J.A. van Pagee. Zandhonger Oosterschelde - een verkenning naar mogelijke maatregelen. Werkdocument RIKZ/2005.802w, Ministerie van Verkeer en Waterstaat, 2005.

J.P.M. Mulder and T. Louters. Changes in basin geomorphology after implementation of the Oosterschelde estuary project. *Hydrobiologia*, 282/283(1):29–39, May 1994.

Rijkswaterstaat. Ontwerpnota stormvloedkering Oosterschelde boek 1. Technical report, Ministerie van verkeer en waterstaat, 1991a.

Rijkswaterstaat. Ontwerpnota stormvloedkering Oosterschelde boek 2. Technical report, Ministerie van verkeer en waterstaat, 1991b.

G.J. Schiereck. *Introduction to bed, bank and shore protection.* VSSD, 2004. Lecture notes CT4310.

M.J.F. Stive, H.J. de Vriend, J. Dronkers, A van Dongeren, and Z.B. Wang. *Coastal inlets and tidal basins.* VSSD, aug 2006. Lecture notes CT5303.

W.B.M. ten Brinke, J. Dronkers, and J.P.M. Mulder. Fine sediments in the Oosterschelde tidal basin before and after partial closure. *Hydrobiologia*, 282/283:41–56, 1994.

S. Ullman. Three-dimensional computation of non-hydrostatic free-surface flows. Master's thesis, Delft University of Technology, 2008.

J van de Kreeke and J Haring. Equilibrium flow areas in the Rhine Meuse delta. *16th International conference for coastal Engineering, Volume 3, p97-111*, 1979.

L.C. van Rijn. Sedimentation of dredged channels and trenches . *Handbook of coastal and ocean engineering, volume 2, chapter 9*, 282/283:611–650, 1991.

L.C. van Rijn. Principles of sedimentation and erosion engineering in rivers, estuaries and coastal seas. Technical report, WL|Delft Hydraulics, 2005.

R. van Zanten and L.A. Adriaanse. Verminderd getij - Verkenning naar mogelijke maatregelen om het verlies van platen, slikken en schorren in de Oosterschelde te beperken. Hoofdrapport, Rijkswaterstaat, May 2008.

Jacques Vroon. Hydrodynamic characteristic of the Oosterschelde in recent decades. *Hydrobiologia*, 282/283(1):17–27, May 1994.

Z.B. Wang, C Jeuken, and H.J. de Vriend. Tidal asymmetry and residual sediment transport in estuaries. Technical Report Z2749, WL|delft hydraulics, November 1999.

WL|Delft-Hydraulics. *Delft3D-FLOW User Manual*, 3.14 edition, oct 2007.

List of Figures

List of Tables

Appendices

Appendix A

Delft3D

In this section, a description about the governing equations in Delft3D will be given. For a more extensive description of Delft3D-FLOW, it is referred to [WL|Delft-Hydraulics, 2007].

A.1 hydrostatic pressure

For the part of this study where the 2DH model is used, Delft3D FLOW computation contains the shallow water equations, under the condition of some assumptions, like a hydrostatic pressure profile over the depth. The depth averaged equations (2DH) are developed from a combination between the momentum and continuity equation. The depth-averaged continuity equation is given by:

$$\frac{\partial \zeta}{\partial t} + \frac{\partial}{\partial x}(HU) + \frac{\partial}{\partial y}(HV) = 0 \tag{A.1}$$

The 2D Momentum equation reads:

$$\frac{\partial U}{\partial t} + U\frac{\partial U}{\partial x} + V\frac{\partial U}{\partial y} = -g\frac{\partial \zeta}{\partial x} + fV + \upsilon_H\left[\frac{\partial^2 U}{\partial x^2} + \frac{\partial^2 U}{\partial y^2}\right] - \frac{gU\sqrt{U^2+V^2}}{HC^2} + \frac{\rho_{air}C_d W_x\sqrt{W_x^2+W_y^2}}{\rho_0 H} \tag{A.2}$$

$$\frac{\partial V}{\partial t} + U\frac{\partial V}{\partial x} + V\frac{\partial V}{\partial y} = -g\frac{\partial \zeta}{\partial y} - fU + \upsilon_H\left[\frac{\partial^2 V}{\partial x^2} + \frac{\partial^2 V}{\partial y^2}\right] - \frac{gV\sqrt{U^2+V^2}}{HC^2} + \frac{\rho_{air}C_d W_y\sqrt{W_x^2+W_y^2}}{\rho_0 H} \tag{A.3}$$

where

ζ = water level with respect to some reference level [m]
d = depth with respect to some reference level (downwards is positive) [m]
H = total water depth (H=ζ + d) [m]
U,V = depth averaged velocity in x and y-direction [ms^{-1}]
W_x,W_y = wind speed in x and y-direction [ms^{-1}]
f = Coriolis parameter [s^{-1}]
g = gravitational acceleration [ms^{-2}]
C = Chezy coefficient [$m^{1/2}s^{-1}$]

C_d = Wind drag coefficient [-]
ρ_0 = Density of water [kgm^{-3}]
$\rho_a ir$ = Density of air [kgm^{-3}]
υ_H = Horizontal eddy viscosity [$m^2 s^{-1}$]

A.2 Non-hydrostatic pressure

Because in some parts of the model in this thesis a abruptly changing bottom topography and a hydraulic structure (barrier) are present, there might be relatively large vertical acceleration component expected. In order to capture non-hydrostatic phenomena in the flow, the Z-grid model of Delft3D has been extended with a non-hydrostatic module. For small density differences, the Reynolds-averaged Navier-Stokes equation may be written as [WL|Delft-Hydraulics, 2007]:

$$\frac{\partial u_j}{\partial t} + u_i \frac{\partial u_j}{\partial x_i} + \frac{1}{\rho_0} \frac{\partial \tau_{ij}}{\partial x_j} + \epsilon_{ijk} 2\Omega_j u_k = \frac{\rho}{\rho_0} g \delta_{i3} \tag{A.4}$$

This non-hydrostatic pressure gradient can be split into two parts, a hydrostatic ρgh part and a hydrodynamic *(q)* part.:

$$p = p_{atm} + g \int_z^\zeta \rho \, dz' + q \tag{A.5}$$

Combining the momentum equations with this non-hydrostatic pressure, we get:

$$\frac{\partial u}{\partial t} + \frac{1}{\rho_0} \frac{\partial}{\partial x} \int_z^\zeta \rho g \, dz' + \frac{1}{\rho_0} \frac{\partial q}{\partial x} = \text{RHS}_x \tag{A.6}$$

$$\frac{\partial v}{\partial t} + \frac{1}{\rho_0} \frac{\partial}{\partial y} \int_z^\zeta \rho g \, dz' + \frac{1}{\rho_0} \frac{\partial q}{\partial y} = \text{RHS}_y \tag{A.7}$$

$$\frac{\partial w}{\partial t} + \frac{1}{\rho_0} \frac{\partial q}{\partial z} = \text{RHS}_z \tag{A.8}$$

Where the right hand side contains the acceleration due to advection, turbulent stresses and Coriolis.

Appendix B

KustZuid model

SIMONA (SImulatie MOdellen NAtte waterstaat) is a knownledge system at Rijkswaterstaat. Which is a collection of mathematical simulationmodels to describe hydrodynamic processes. Within this knowledge system, WAQUA is a water movement and water quality simulation system, to simulate hydrodynamic processes in lakes, rivers, seas and estuaries. The system calculates depth-average currents and concentrations of constituents and supposes that these do not vary in depth of the simulated river or sea. In this research the KustZuid schematization of the south-western Dutch coast has been used to define boundary conditions for smaller numerical models. KustZuid describes the Western- and Eastern Scheldt estuaries, including the Scheldt river and the coastline from Duinkerke (Belgium) in the south to the island of Goeree in the north.

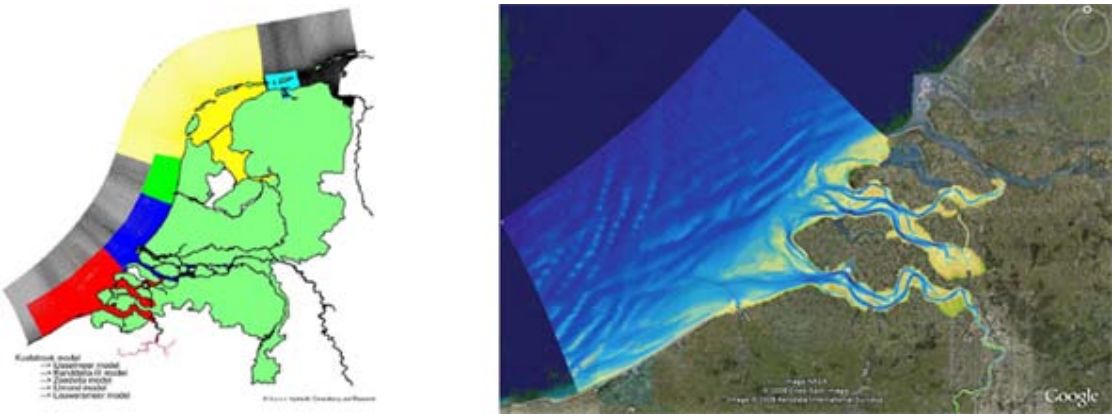

Figure B.1: SIMONA numerical models of the Dutch Coast; KustZuid in red (left). KustZuid model (right)

In this version of the KustZuid model, a bed topography of 2004 is included. For the boundary conditions, 94 astronomical components are given as input to represent the tide.

B.1 Model adjustments

The storm surge barrier in WAQUA is modelled in a different way than in the converted Delft3D model. The inlets of the Eastern Scheldt storm surge barrier in the model are 5(Hammen), 6(Schaar) and 11(Roompot) cells wide. To represent the horizontal constriction in the WAQUA model the width of every cell is limited to a certain percentage of the original cell width. The vertical constriction is represented by a given sill-depth. In the converted DELFT3D model, the vertical constriction is defined by a vertical plate extending from a reference level downwards in the flow. To represent the energy losses by the barrier, a porous plate is added on both sides of the barrier. The energy loss coefficient of the porous plate is used as a calibration parameter (see also section 5.2.5). The other difference between the original and converted model is the bottom roughness. In the original WAQUA model the bottom roughness is space-varying, especially on the Scheldt river and parts of the Western Scheldt distinct Manning-values are used. Due to difficult conversion and minimal influence on the area of interest, the bottom roughness is considered uniform in the Delft3D model. The main model parameters of the converted model are listed in table B.1.

Coriolis acceleration	52 ^{o}N
Number of grid cells	37181
Grid resolution	250x750 to 125x125
Time step	1 min.
Reference date	01-01-2004
Tidal components	94
Gravity	9.813 m s^{-2}
Water density	1023 kg $m-3$
Bottom roughness	0.025 (Manning)
Horizontal eddy viscosity	1 m^2s-1
Energy loss coefficient	2.3

Table B.1: KustZuid model parameters

B.2 Calibration

After conversion of the model, it is calibrated by comparing water levels in- and outside the Eastern Scheldt basin. As reference water levels, predictions by HMCZ (Hydro Meteo Centrum Zeeland) are used. These predictions are in fact a direct output of the KustZuid model in WAQUA, so only water level variations due to tidal forcing are included. In the model 4 observation points are defined to compare the "measurements" with the converted Delft3D model (see figure B.2):

- Oosterschelde11: 15km offshore from the storm surge barrier
- Roompot buiten: Sea-side of the Roompot-sluize
- Roompot binnen: Estuary-side of the Roompot-sluize
- Stavenisse: 22km inwards the Eastern Scheldt Estuary

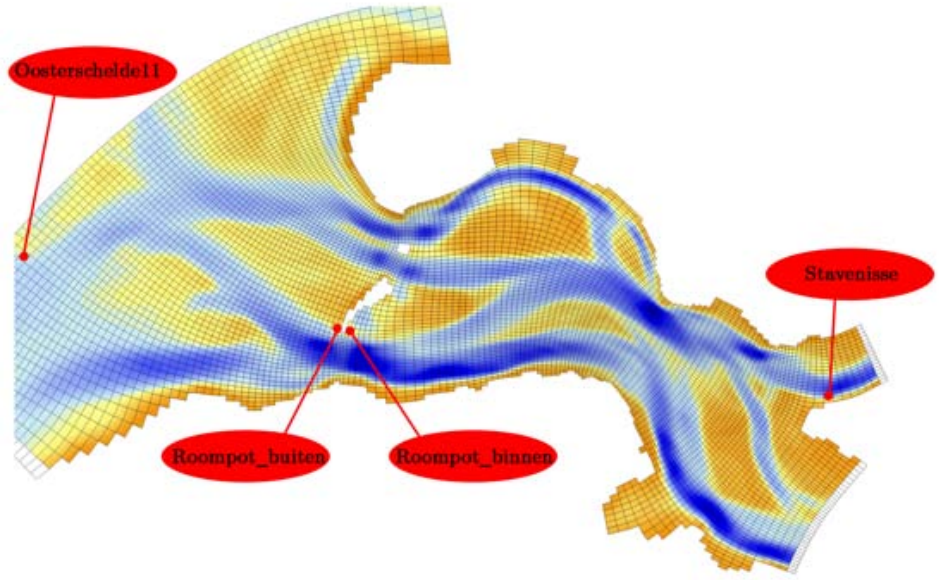

Figure B.2: Observation points for model-calibration

By varying the energy loss coefficient of the storm surge barrier, the model is calibrated to the original KustZuid model. With the water levels in the four observation points, it is also important that the phase differences between the observation points along the model are correct. An error in the phase can give significant flow velocity errors. By comparing the phases between the two observation points at the Roompot sluize (sea-side and basin-side), velocities near the storm surge barrier can accurately be reproduced in the new model. The results of this calibration are shown in figure B.3

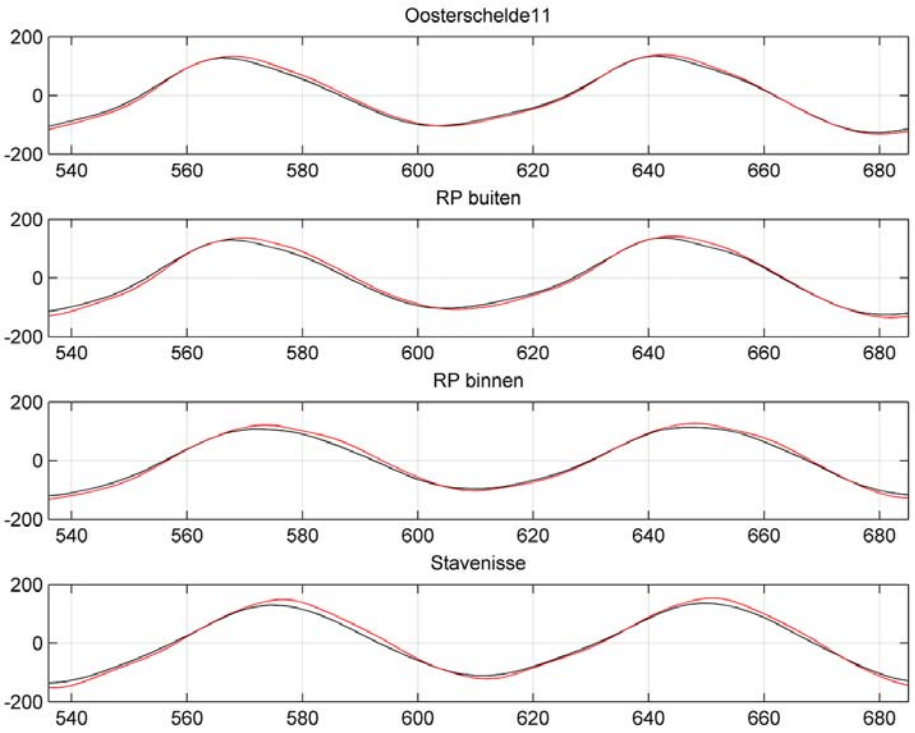

Figure B.3: Calibration of the KustZuid model; Water level in four observation points

Appendix C

Figures

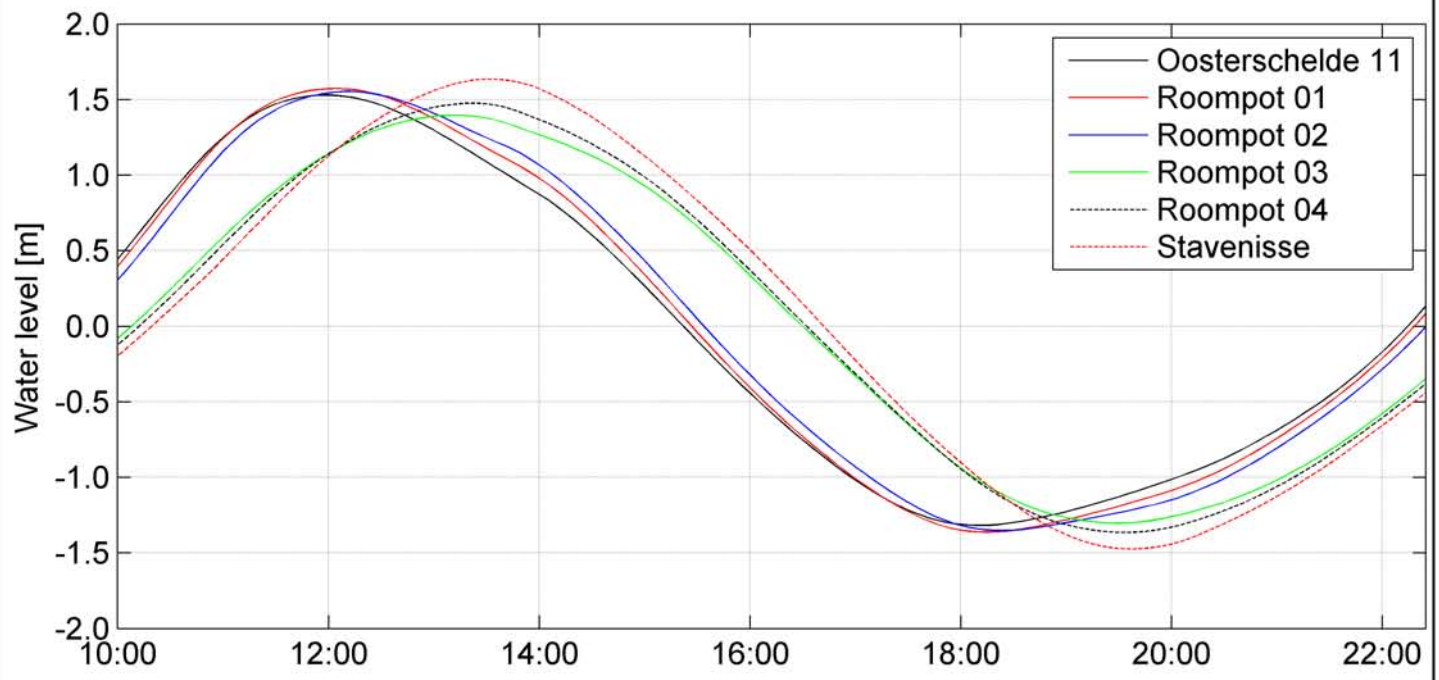

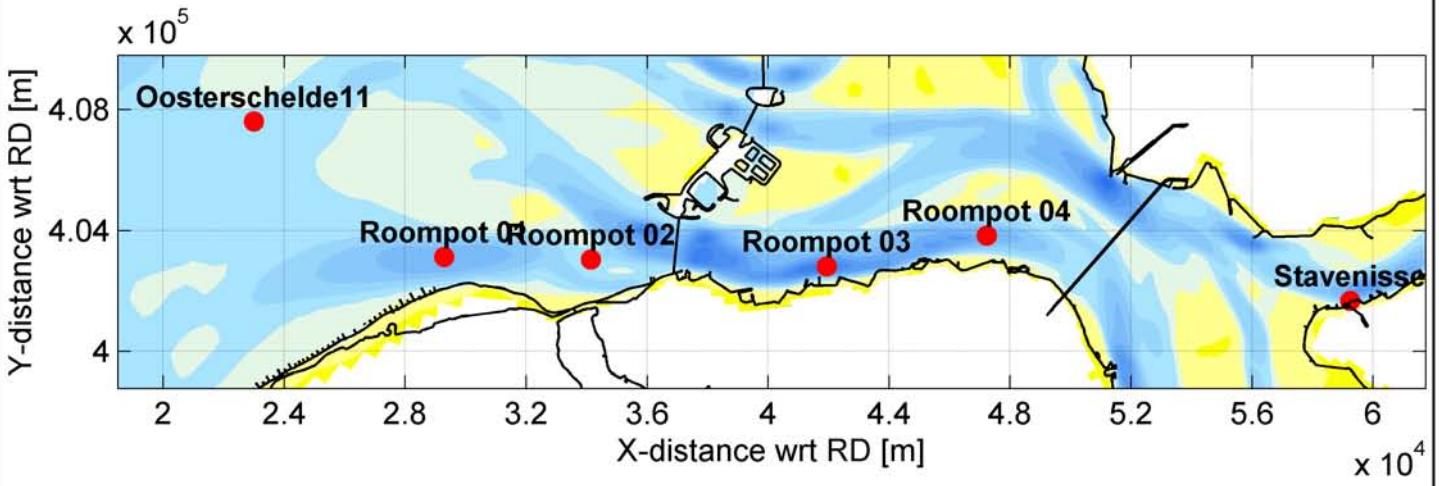

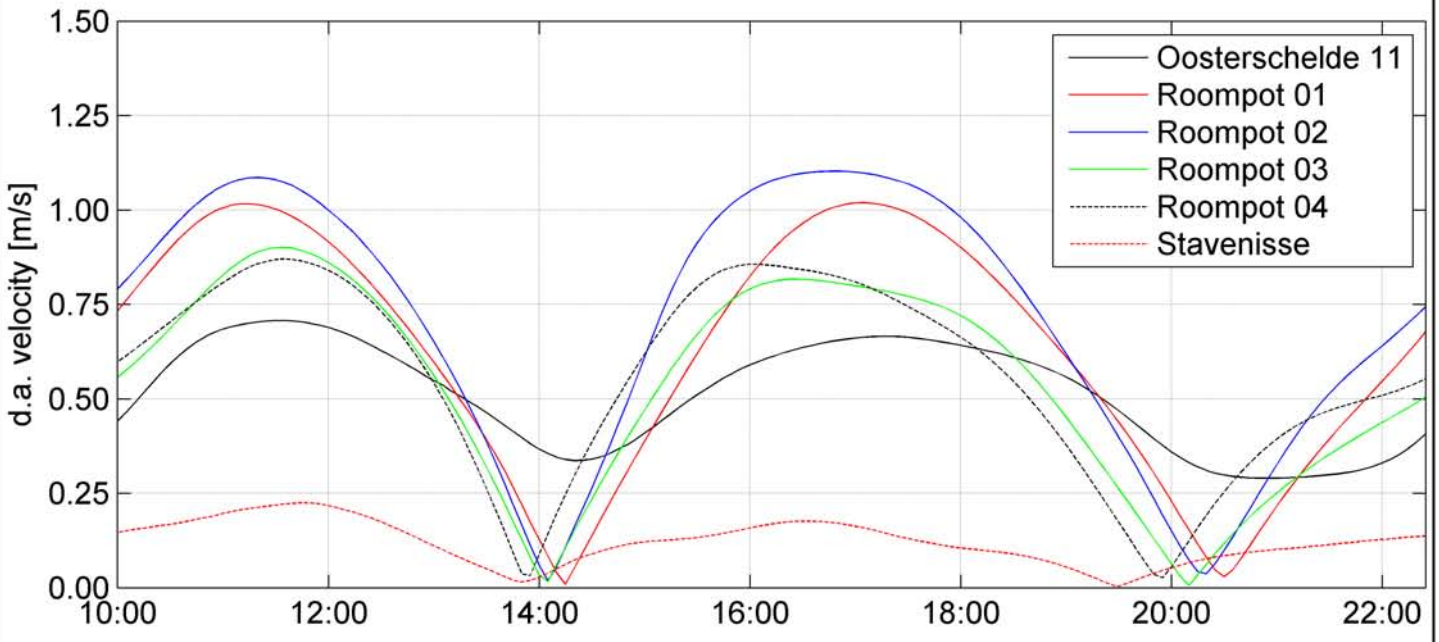

Deformation of tidal wave through storm surge barrier
Water level [m] (top)
Depth-average velocity [m/s] (bottom)

TUDelft EcoShape Van Oord Deltares

C.3.1

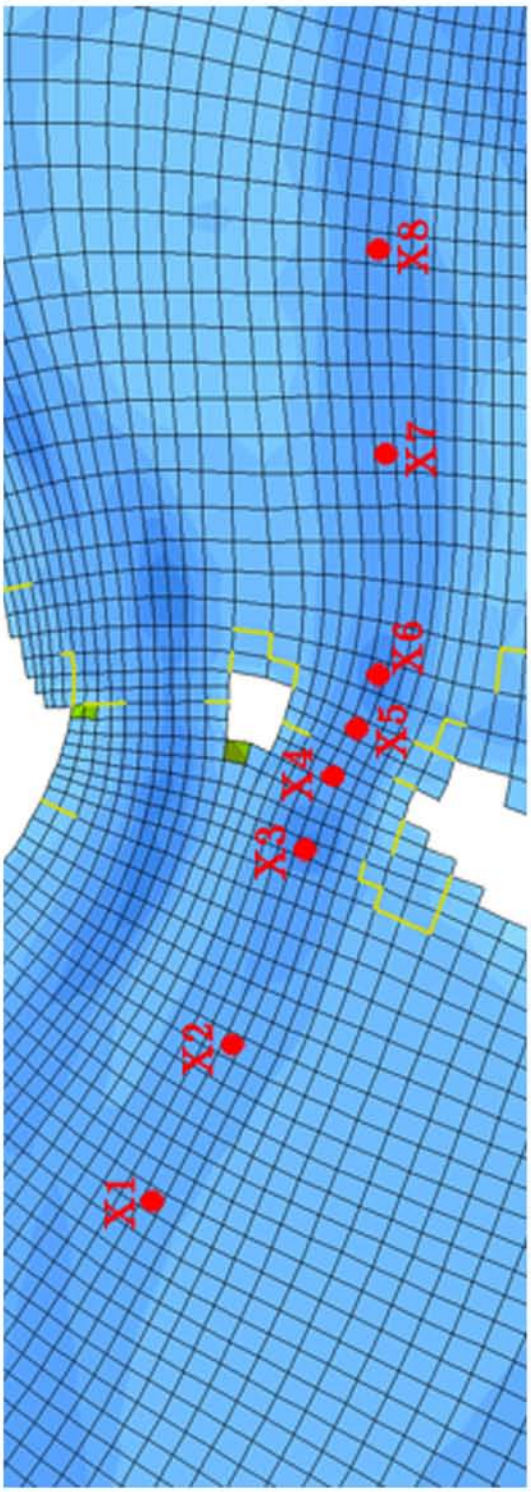

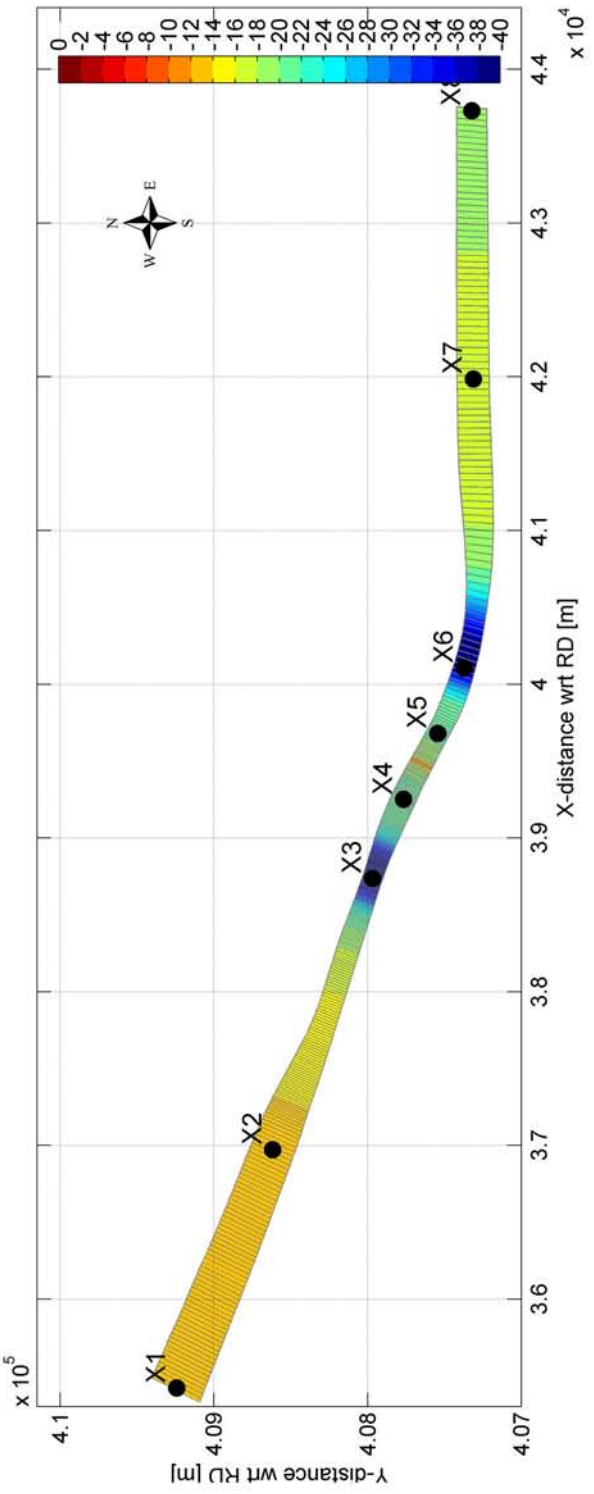

Calibration points X1 to X8
in KustZuid model (top) and in 2DV model (bottom)

TUDelft EcoShape Van Oord Deltares

C. 4.1a

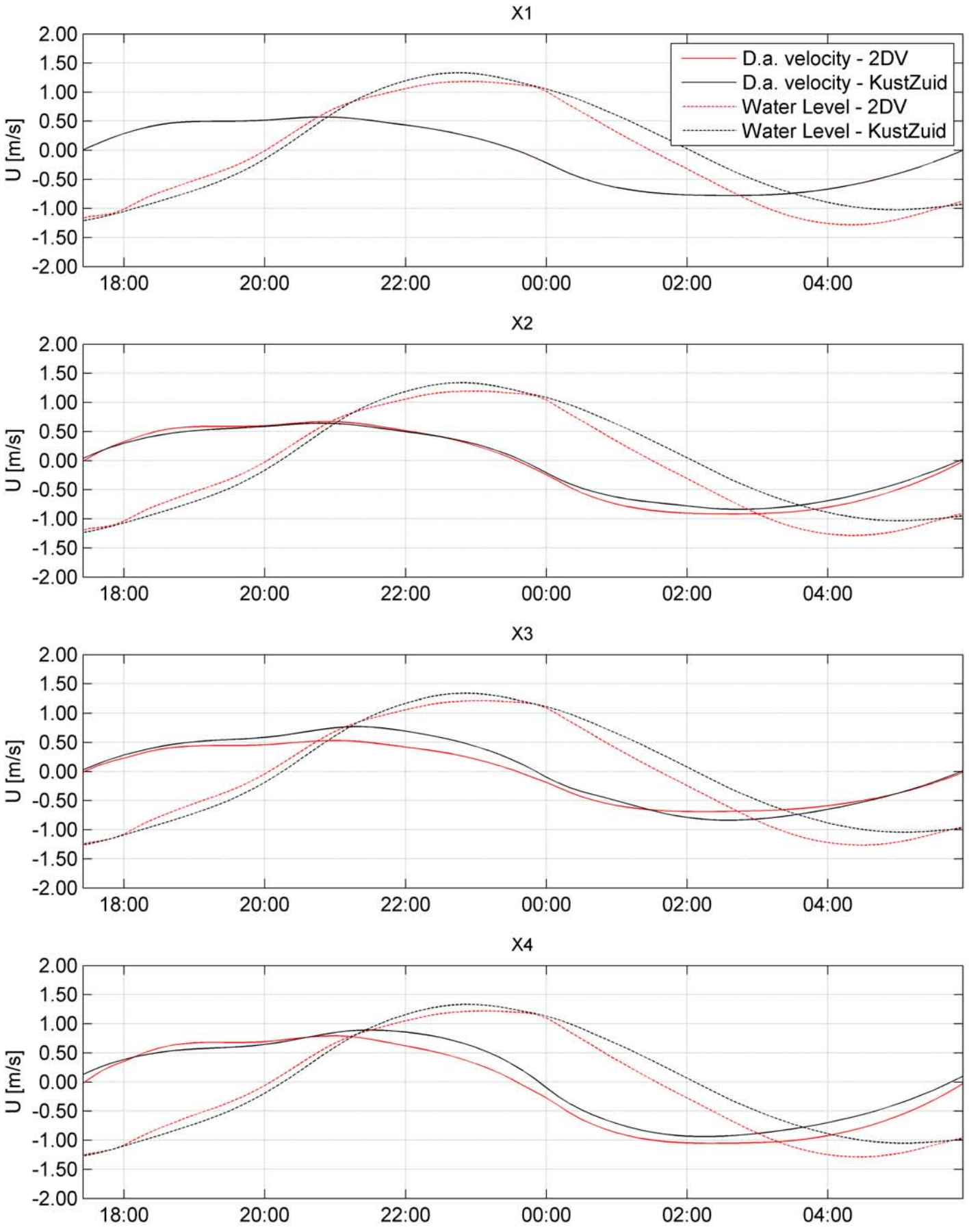

Calibration of 2DV model to KustZuid model
X1 (western boundary) - X4 (west of barrier)

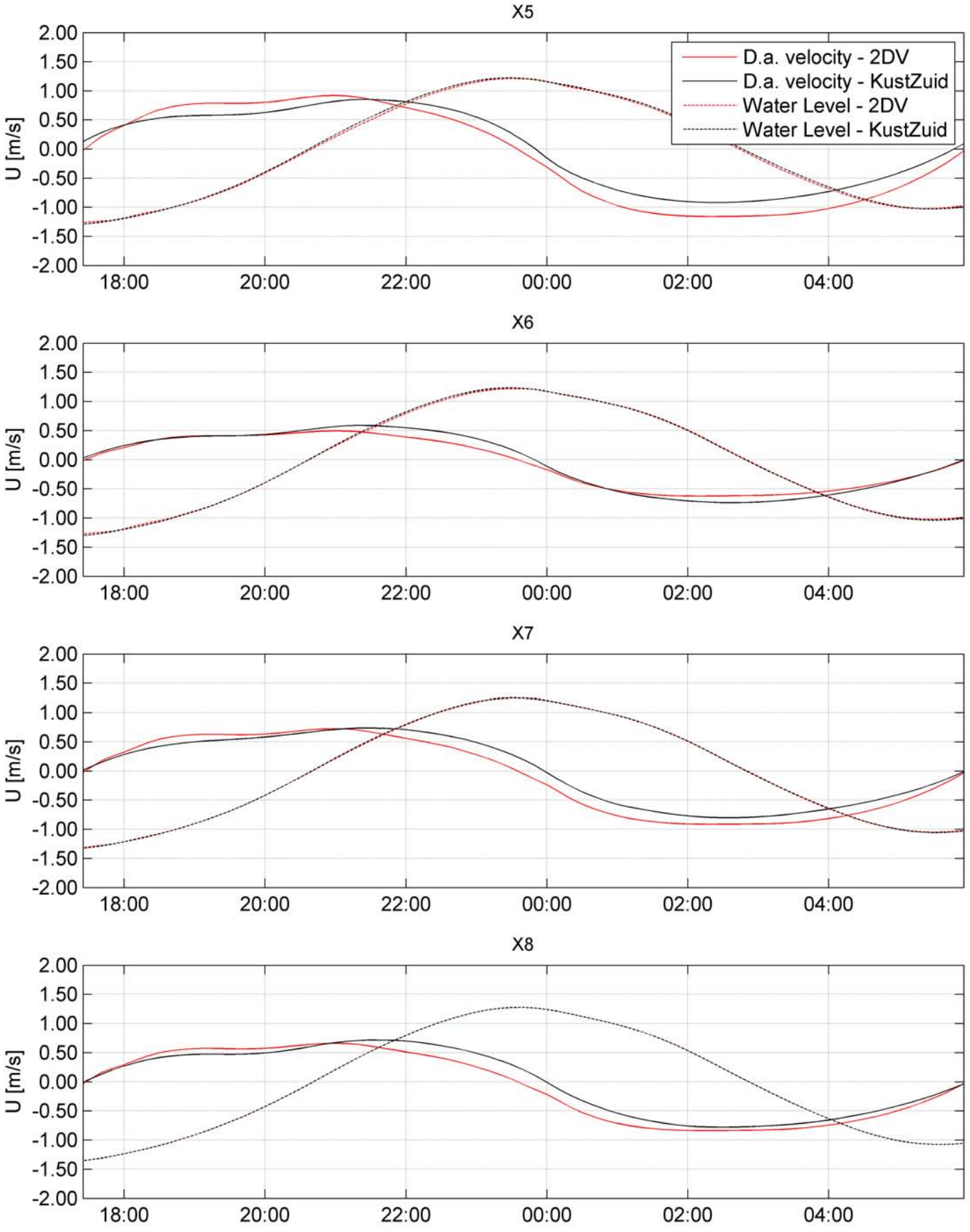

Calibration of 2DV model to KustZuid model
X5 (east of barrier) - X8 (eastern boundary)

Velocity profiles X1 X8 during ebb and flood flow

TUDelft EcoShape Van Oord Deltares

C.4.2

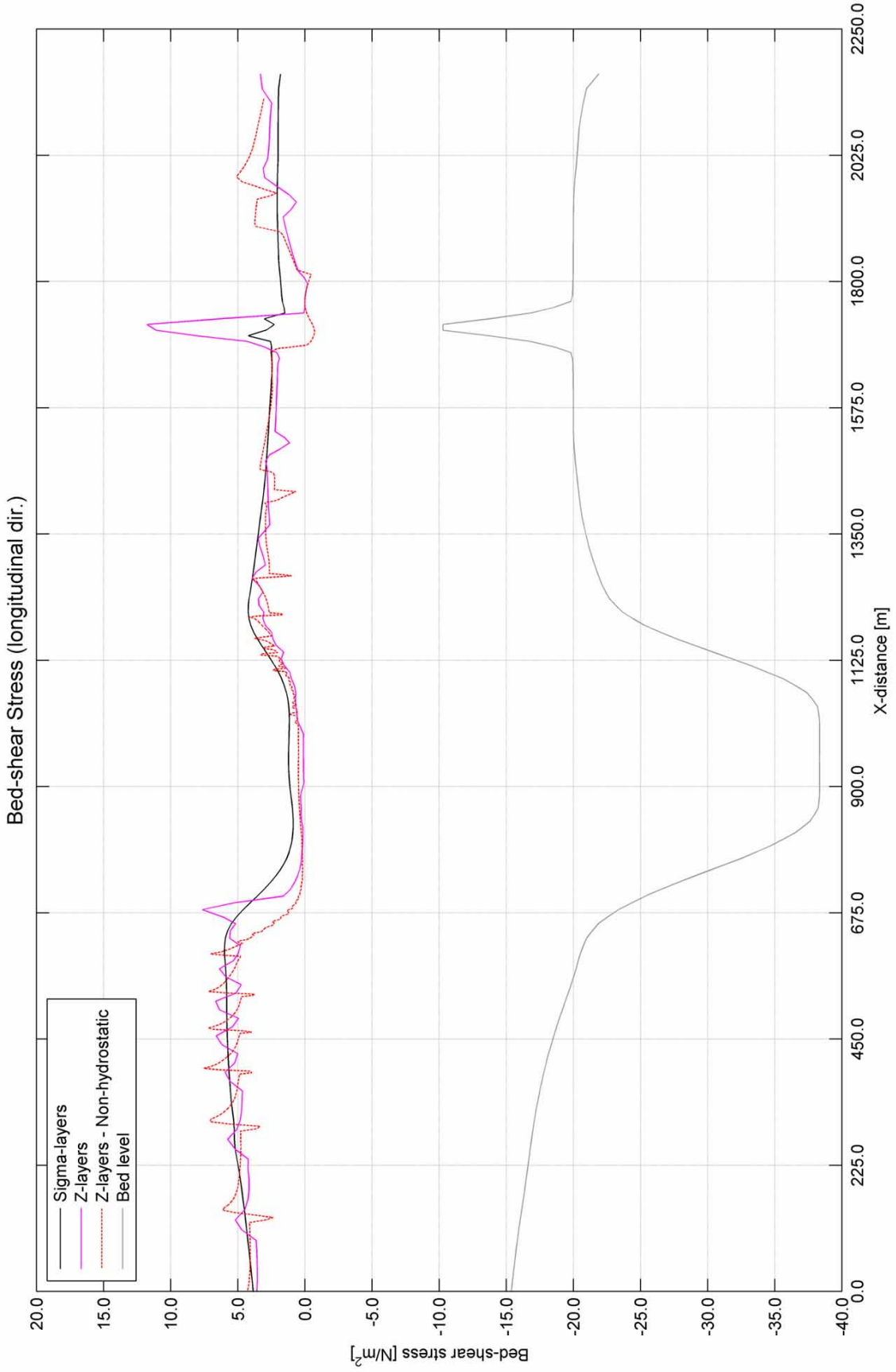

Bed shear stress in 2DV model
For sigma-layers and Z-layers (Hydr. & Non-hydrostatic)

TUDelft EcoShape Van Oord Deltares

C.4.3

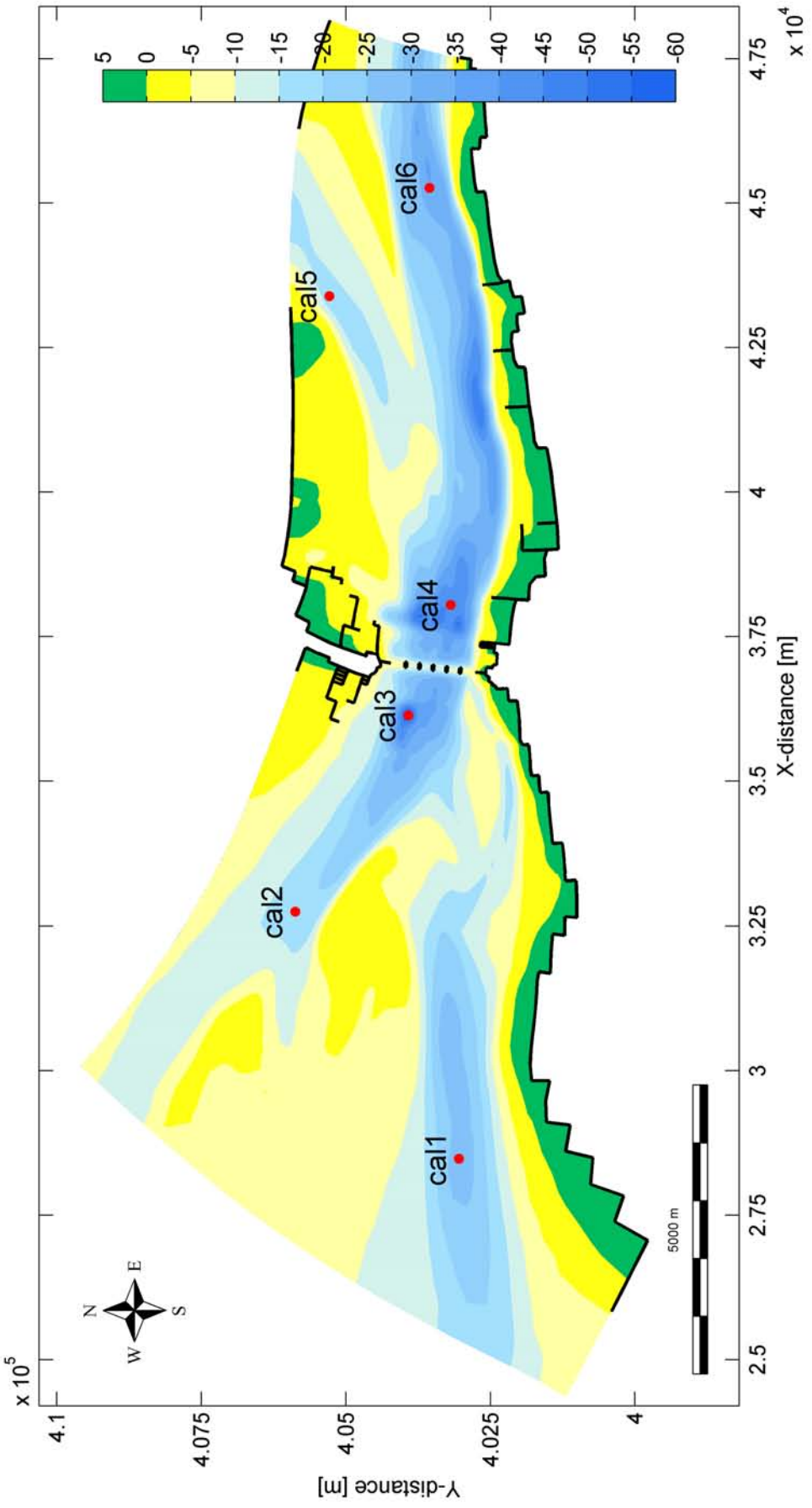

Calibration of Roompot model to KustZuid model
Position of calibration points cal1 - cal6

C.5.1a

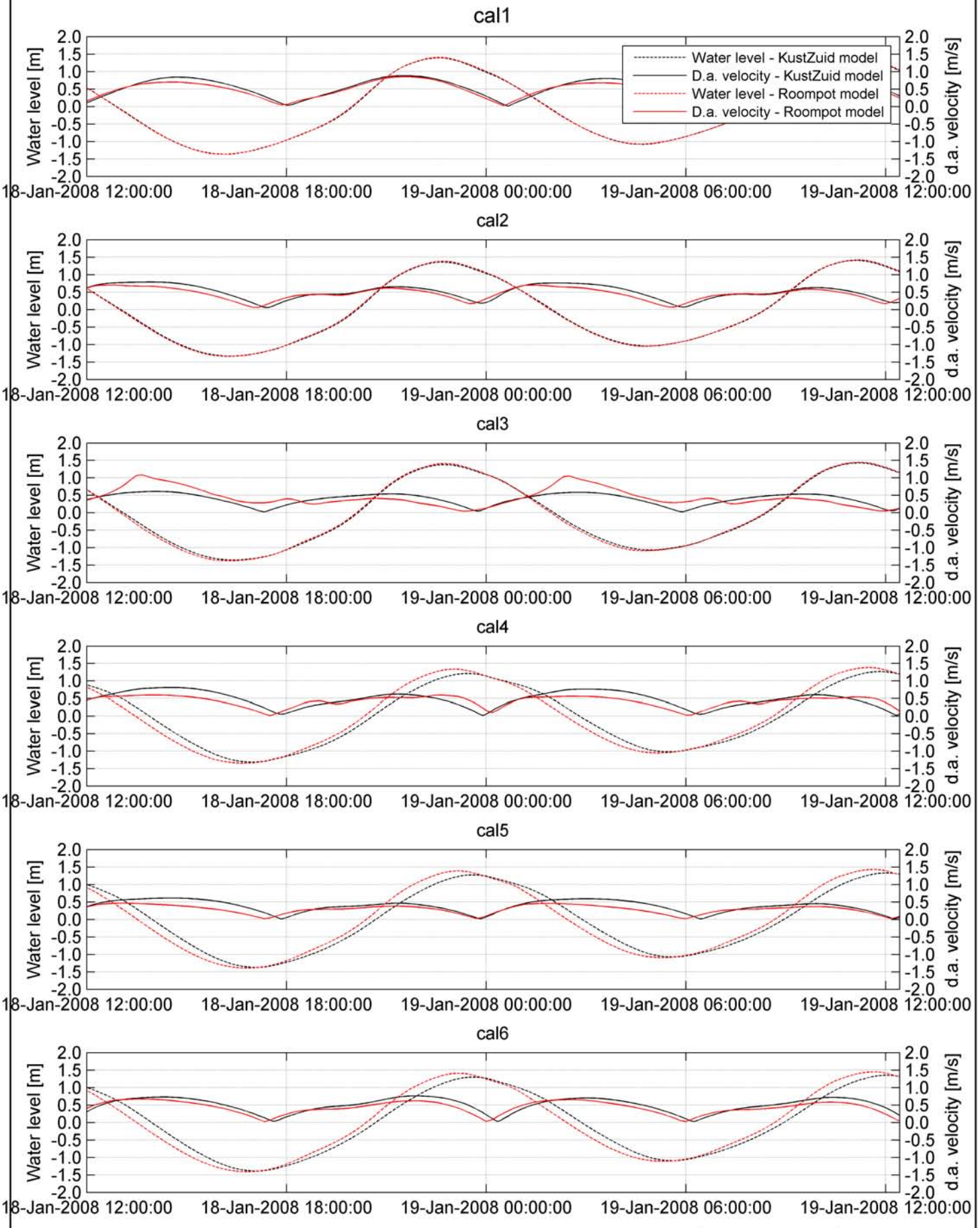

Calibration of Roompot model to KustZuid model
Calibration points cal1 - cal6 (see figure C.5.1a)

TUDelft EcoShape Van Oord Deltares

C.5.1b

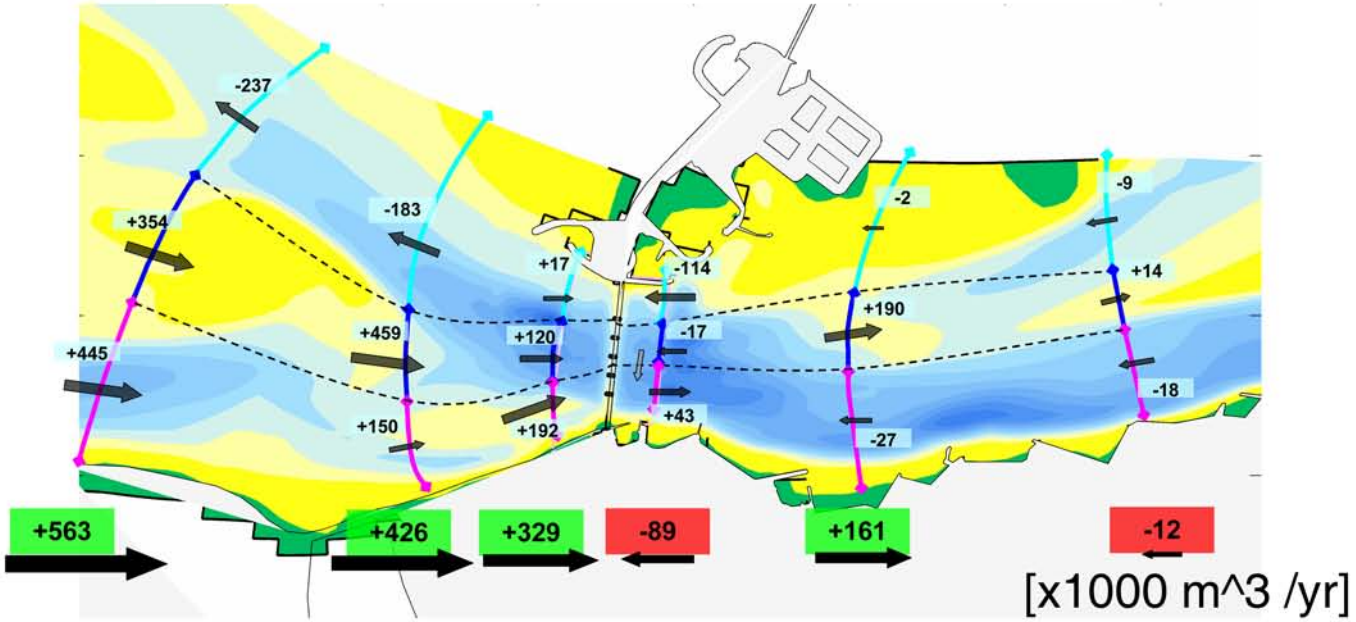

Actual situation

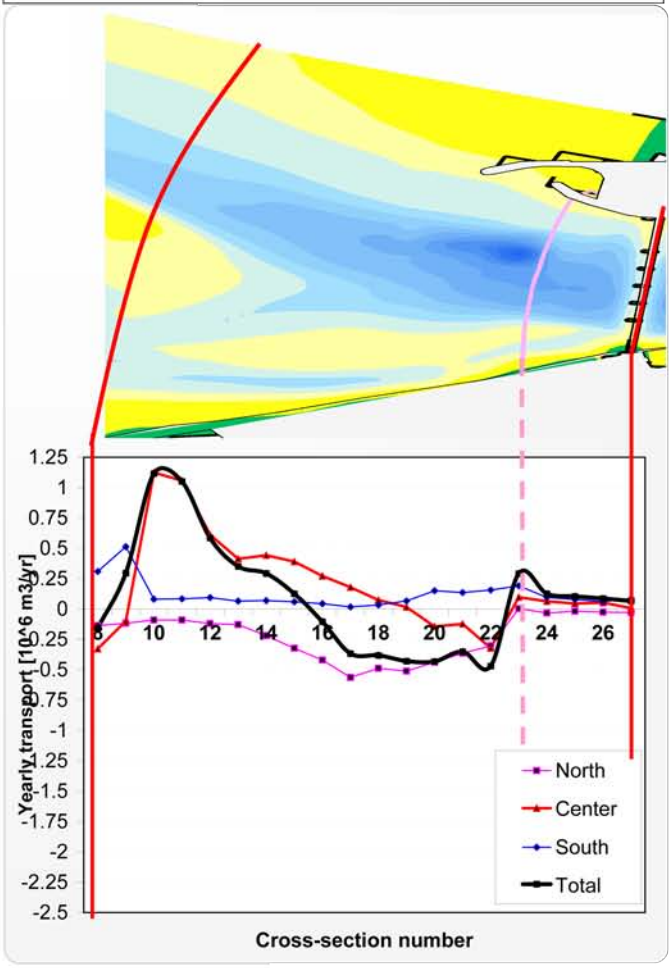

Actual situation

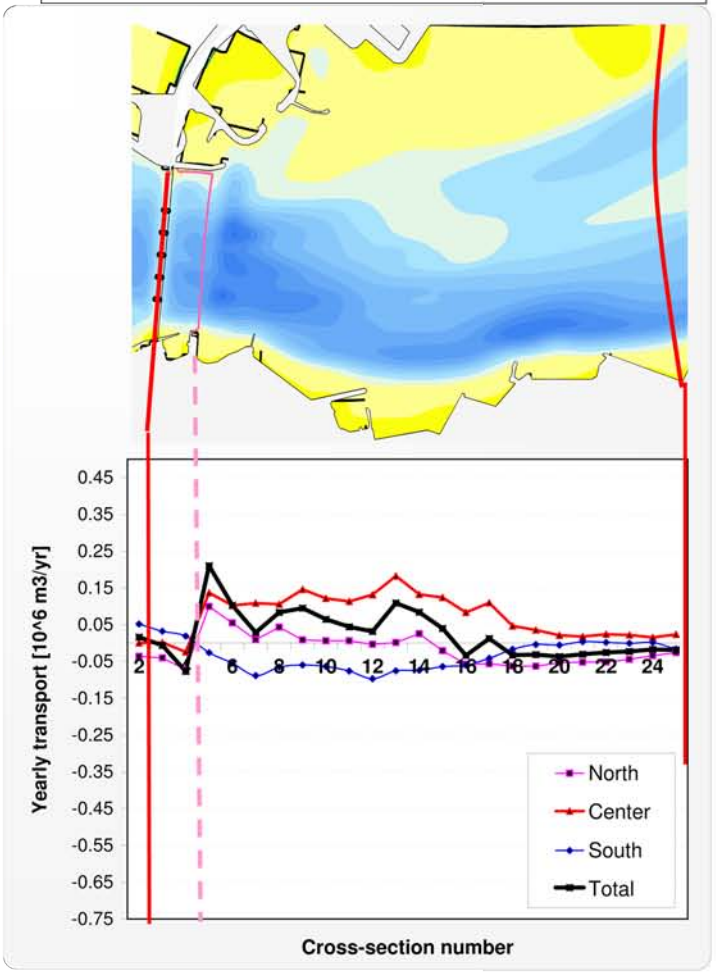

Longidudinal net yearly transports
Actual situation

TUDelft EcoShape Van Oord Deltares

C.5.2a

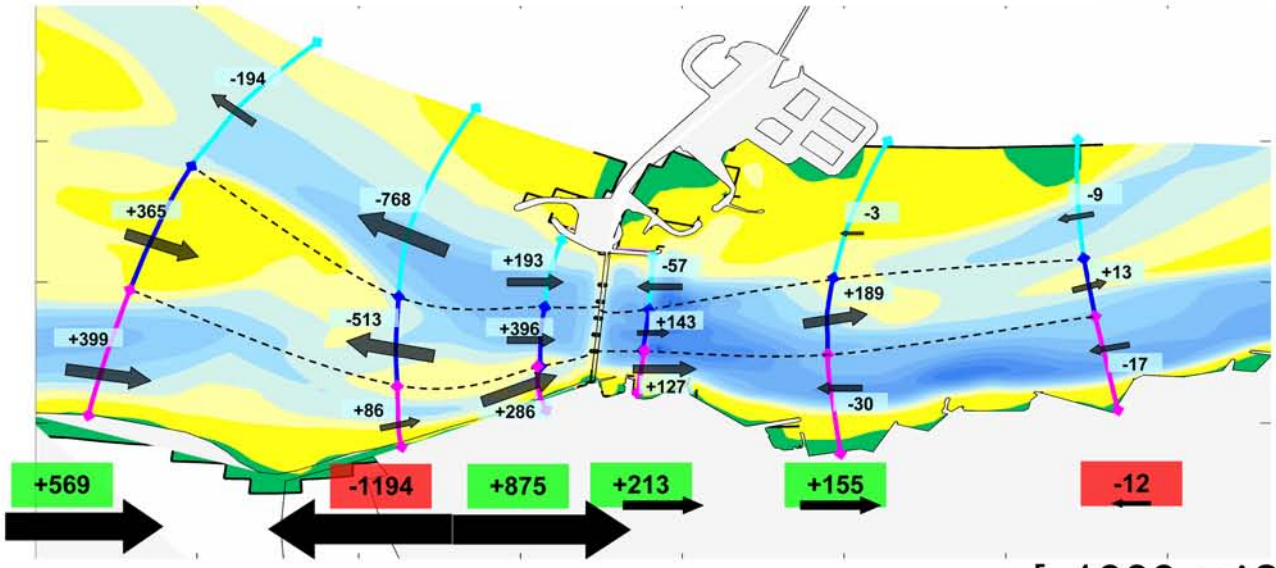

[x1000 m^3 /yr]

Fill to -26m

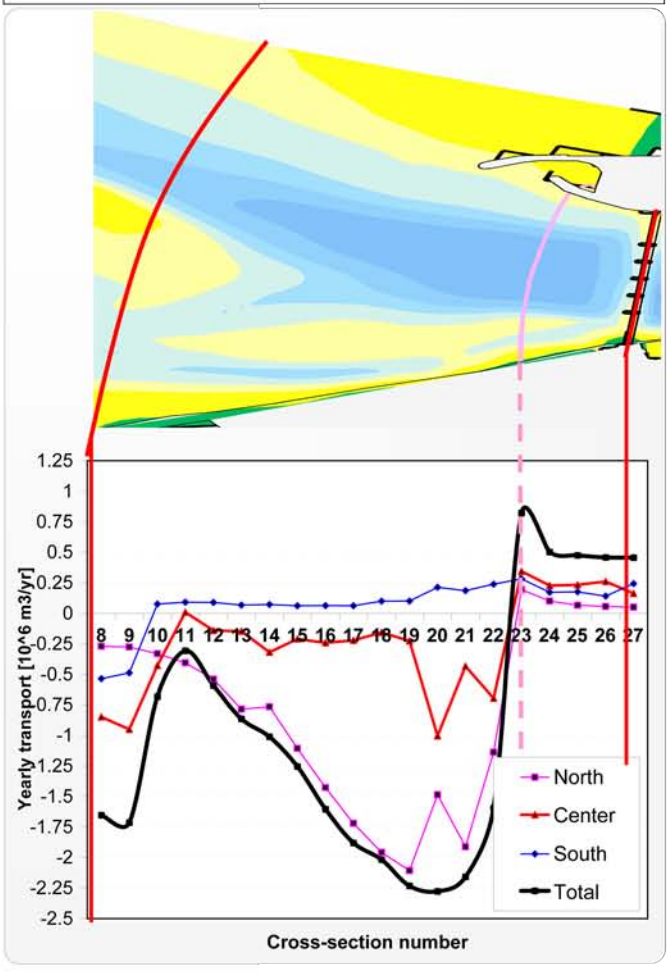

Longidudinal net yearly transports
Scour hole filled, unprotected

TUDelft EcoShape Van Oord Deltares

C.5.2b

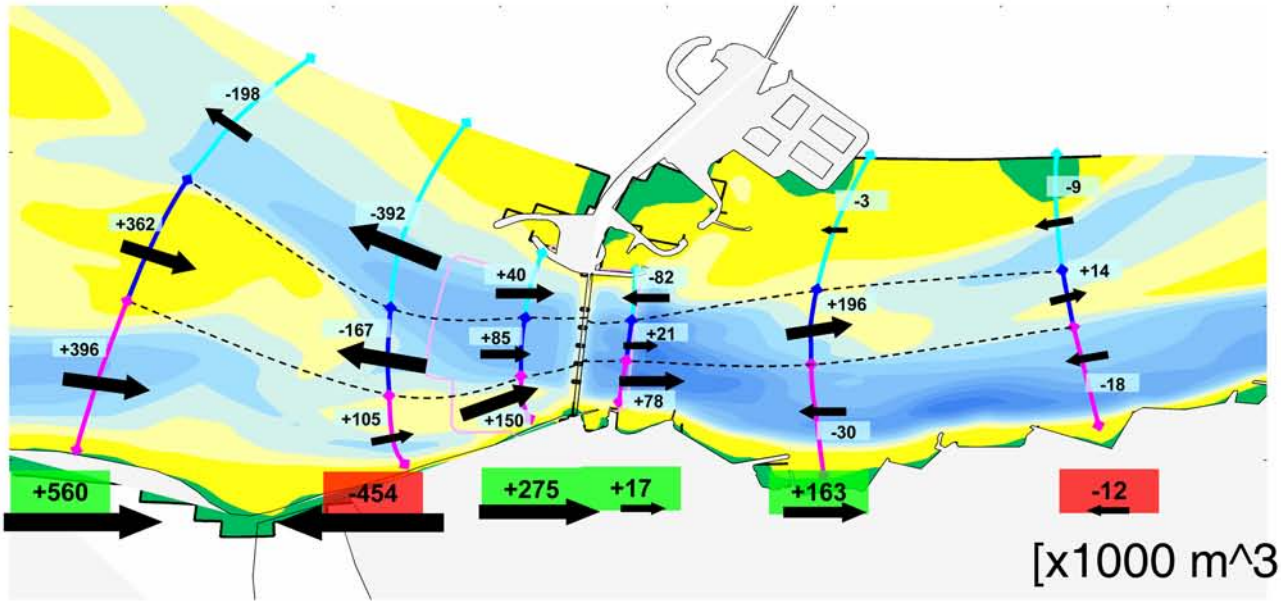

Fill to -26m and extend protection

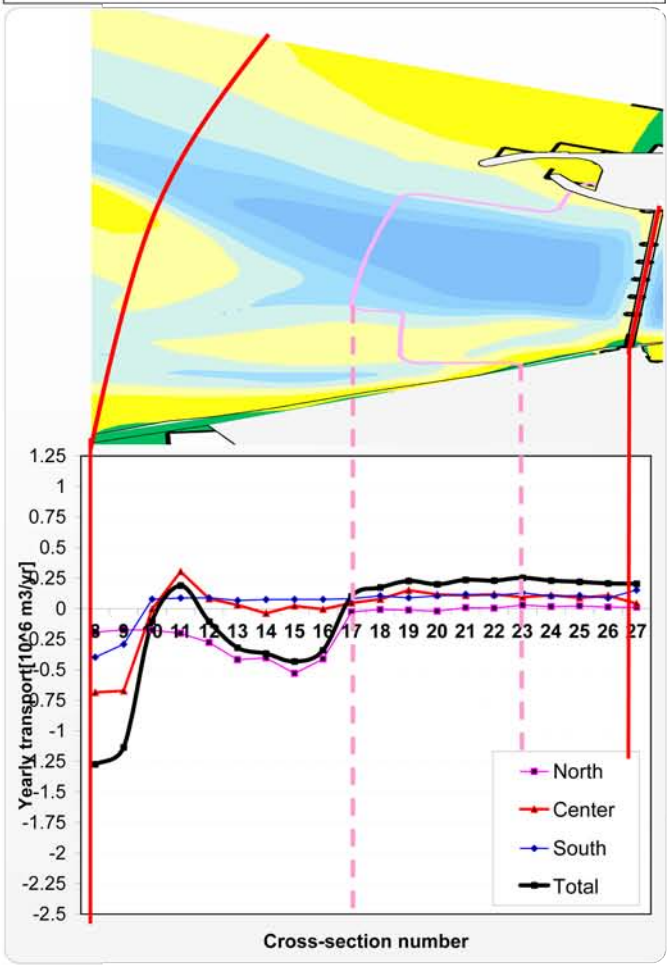

Longidudinal net yearly transports
Scour hole filled, extended bottom protection

TUDelft EcoShape Van Oord Deltares

C.5.2c

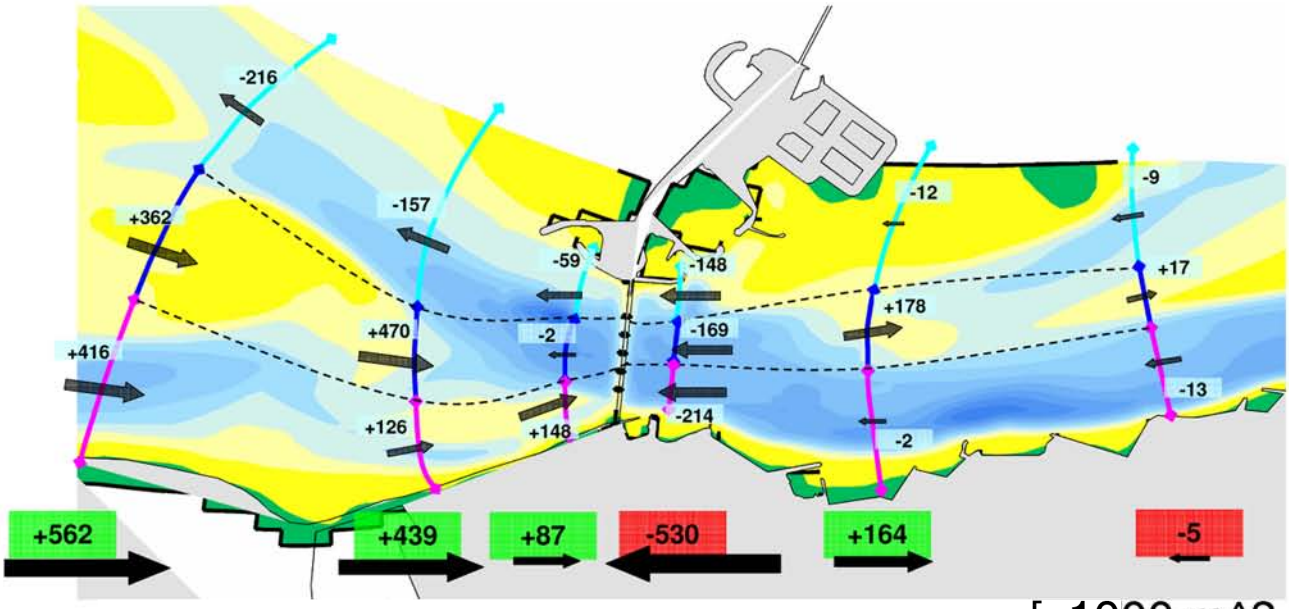

[x1000 m^3 /yr]

Fill to -30m

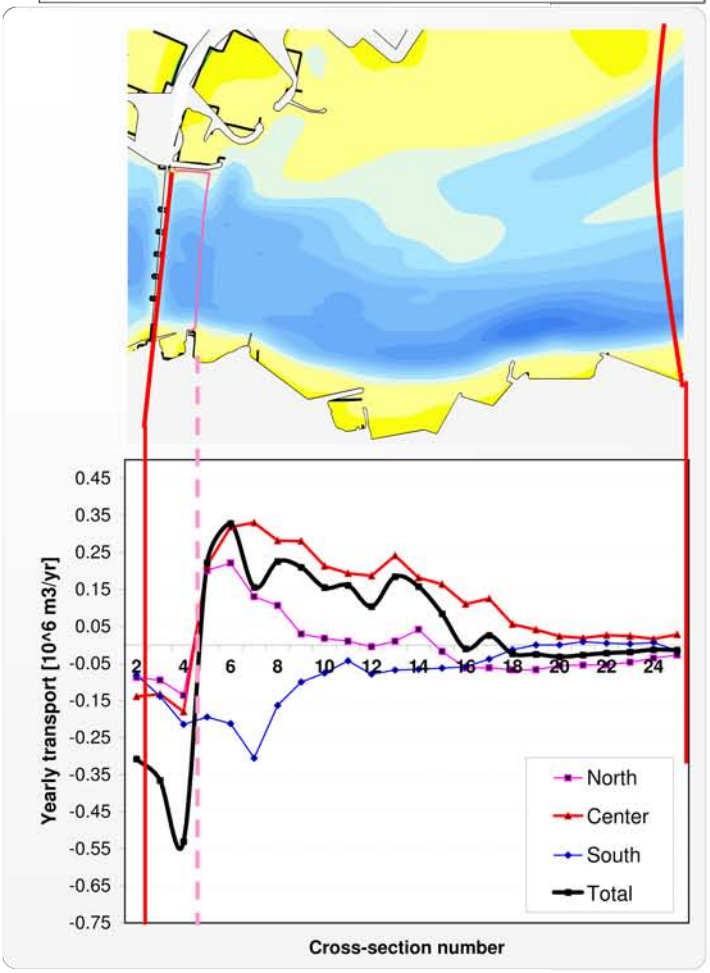

Longidudinal net yearly transports
Landward scour hole filled

TUDelft EcoShape Van Oord Deltares

C.5.2d